MPHIL

Dermatopharmacokinetics as a tool to characterise the performance of testosterone transdermal formulations

Phan, Hilda

Award date:
2017

Awarding institution:
University of Bath

DERMATOPHARMACOKINETICS AS A TOOL TO CHARACTERISE THE PERFORMANCE OF TESTOSTERONE TRANSDERMAL FORMULATIONS

Hilda Phan

2017

UNIVERSITY OF BATH
Department of Pharmacy & Pharmacology

A thesis submitted for the degree for Master of Philosophy

University of Bath

Department of Pharmacy and Pharmacology

May, 2017

Contents

Acknowledgements

I would like to thank my supervisors Dr Begoña Delgado-Charro, Dr Sergey Gordeev and Dr Tim Woodman (University of Bath, Bath, UK) for their full support and guidance. My external supervisor professor Marc Brown (MedPharm, Guildford, UK) is also gratefully acknowledged.

I would like to extend my thanks to Professor Richard Guy (University of Bath, Bath, UK), for useful discussions, Professor Michael Threadgill and Dr Lorenzo Caggiano for the support and guidance with the deuteration process, Dr Phillip Fletcher for his patience with all my Raman questions, and Medpharm (Guildford, UK) for funding this research and kindly providing me with this exciting project.

Lastly, I would like to thank all the research staff, research technicians and my fellow colleagues for all the help and support.

List of abbreviations

ACN acetonitrile

BA benzyl alcohol

COSY correlation spectroscopy

DiPG dipropylene glycol

EtOH ethanol

HCl hydrochloric acid

H_2O_2 hydrogen peroxide

HMBC hetero multiple bond correlation

HSQC hetero nuclear single quantum correlation

IR infrared spectroscopy

IPA isopropyl alcohol

IPM isopropyl myristate

IPP isopropyl palmitate

MS mass spectroscopy

MeOH methanol

NMR nuclear magnetic resonance spectroscopy

NaOH sodium hydroxide

PBS phosphate buffered saline

PEG400 polyethylene glycol 400

PG propylene glycol

SW spectral width

TD time domain

Abstract

The skin is a drug delivery site for local and systemic targets. Testosterone is one of the ~20 drugs approved for transdermal delivery. However, to date there is no formulation which addresses all the relevant considerations: easy to use, small application area, patient friendly, non-irritant to skin and non-transferable between persons.

This work aims to understand the behaviour of testosterone when applied on the skin, using tape stripping and Raman spectroscopy to investigate the kinetics of testosterone skin absorption from various testosterone formulations (two marketed gel formulations, a binary testosterone solution and an *ad hoc* gel formulation.

A series of *in vitro* experiments using Franz cells and dermatomed pig skin investigated the drug delivery from testosterone formulations, after 3, 6 and 24 hours exposure. Regardless of formulation used, the length of exposure did not result in different testosterone recovery from the stratum corneum with no clear time kinetics being apparent from the tape-stripping data. However, more testosterone was quantified in the receptor solution after the 24 hours exposure experiments, suggesting a slow skin absorption process for testosterone from all formulations.

In addition to the diffusion experiments, an initial experiment using Raman micro-spectroscopy was carried out to investigate the physical state of testosterone and its location upon application on the skin. In this experiment line mapping of the drug on the skin surface and, after tape stripping, in deeper layers was performed. Drug crystals were detected in the superficial layers of the skin, but the intensity of the signal dropped below the noise level after a few tape strips. To improve sensitivity of detection, the drug was labelled with deuterium using a novel, one-step method. The deuteration resulted in shifting the strongest Raman peak of testosterone from 1610 cm^{-1} to 1600 cm^{-1} thus significantly reducing its overlap with the skin peak centred at 1654 cm^{-1}.

A second set of Raman experiments investigated the deuterated testosterone in a solution and in a gel. In contrast to the first experiment, crystals were not observed, however, the deuteration improved sensitivity thus allowing smaller concentrations of the drug to be detected.

These results suggest that testosterone formulations work by quickly loading the stratum corneum and skin crevices with drug and residual gel; a fraction of this testosterone skin reservoir is subsequently slowly absorbed. The new deuteration method was fast and simple, resulting in high yield of deuterium incorporated at five positions on testosterone. Raman line maps showed large spatial inhomogeneity of testosterone concentration both on the skin surface and in deeper layers.

Chapter 1

INTRODUCTION

Introduction

The skin is an organ with a far more crucial role than just lining the outside of a body. The first obvious role is to encapsulate the body and keep all the organs and internal content in place, the second important role is to provide the body with a physical barrier and protect it from the harmful external environment, but also to prevent the leakage of body fluids out to the environment. This physical barrier, simple in structure and appearance, is strictly regulated to provide a highly complex and advanced barrier function. (Williams, 2003; Prausnitz *et al.*, 2012)

The skin and its structure

The skin is composed of several layers, as seen in figure 1. The innermost layer, the hypodermis (bottom part of figure 1), is a subcutaneous fatty layer that serves as a border between the skin and the tissue. The main purpose of this layer is to insulate the body and to protect it from physical shock. The layer is a few millimetres thick with variations of thickness seen between different areas of the body, for example it is absent in the eyelids. The next layer of the skin is the dermis. This viable layer, seen as the main component of the skin, locates all the blood vessels, lymphatic vessels, nerve endings, hair follicles and sebaceous glands (pilosebaceous units), and sweat glands. The rich vasculature provides nutrients and oxygen to the tissue, while removing waste products and toxins. The dermis is 3-5 mm thick and is composed of a connective tissue network embedded in a mucopolysaccharide gel. The tissue network mainly consists of collagen fibrils that gives support, and elastic tissue that makes the skin flexible.

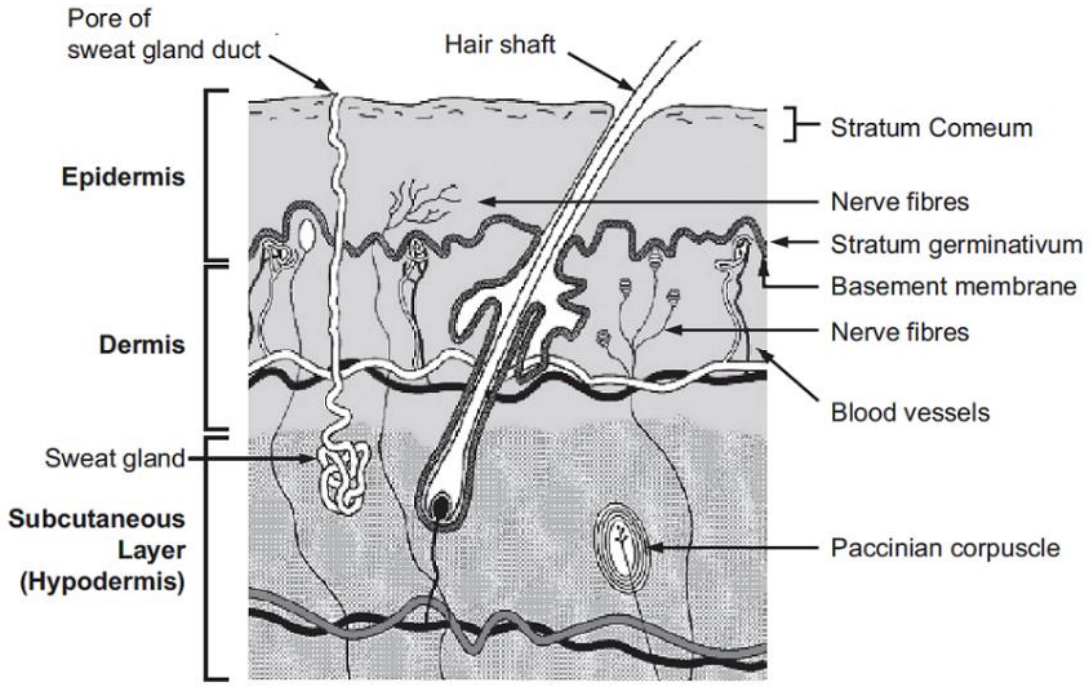

Figure 1. Schematic cross sectional figure of skin and its structure. (World health organization (WHO), 2006)

The last layer of the skin, the epidermis, seen in figure 2, ranges in thickness from 0.06 mm, found for example at the eyelids, to 0.8 mm on soles of the feet and palms of the hands. There are no blood vessels in the epidermis and therefore waste products, nutrients and molecules must permeate across in order to reach the systemic circulation. The epidermis is further divided into four layers – the stratum basale- more commonly known as the basal layer, the stratum spinosum, the stratum granulosum and the stratum corneum- the outermost layer of the skin. (Williams, 2003)

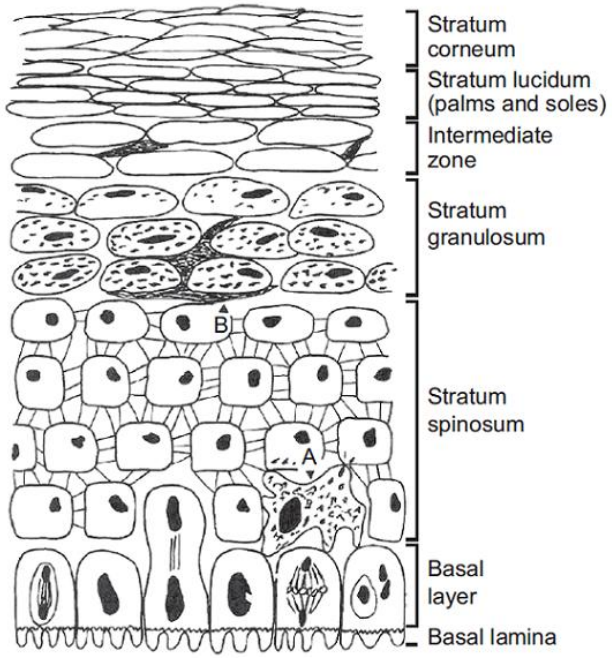

Figure 2. Schematic figure of epidermis and all its layers. (World health organization (WHO), 2006)

The cells of the stratum basale in the epidermis are similar to other tissue cells in that they are metabolically active and contain ribosomes and mitochondria. The keratinocytes found in stratum basale undergo mitosis and migrate further toward the surface. (Williams, 2003; Elias and Feingold, 2005)

There are also other cells found within this layer: Langerhans cells, which play important roles in allergy amongst other skin conditions, the Merkel cells, which are associated with nerve endings and cutaneous sensations and therefore mostly found in touch sensitive areas of the body such as lips and fingertips, and finally melanocytes, which synthesise melanin that protects the skin and body from UV radiation and free radicals.

When the keratinocytes migrate upwards to stratum spinosum, they morph from a more column-like appearance to that of a polygon. The keratinocytes starts to differentiate and synthesise keratin, passing from this layer to the next, the stratum granulosum. This layer is only one to three cell layers thick, and the keratinocytes continue to differentiate and produce keratin, but start to flatten in appearance. Enzymes in this layer degrade organelles within the cell and more granule-like structures arise, giving the layer its name. The now “dead” anucleated, keratinised cells, form the last layer of the epidermis, the stratum corneum. (Williams, 2003)

Although being only around 10-15 cell layers and 10-20 µm thick, this layer provides the main barrier function of the skin. It regulates the outward movement of water, crucial for survival of the

organism, and the inward movement of substances present in the environment (Rougier *et al.*, 1983; Pirot *et al.*, 1997; Wester and Maibach, 1983). It consists of a lipid matrix and dead corneocytes that have differentiated from the basal layer of the epidermis, and is often described as having a "brick and mortar" structure (Bommannan *et al.*, 1990). Because of the dead nature of stratum corneum, diffusion across this layer is passive and is typically modelled using Fick's law of diffusion (Brown *et al.*, 2008).

Topical and transdermal delivery

The skin with an area of 1.7-2 m^2 provides a large and accessible site for both topical and transdermal drug delivery. Local topical treatment is desired when treating cutaneous disorders in the skin itself, as it targets the area of interest and minimises side effects in the rest of the body. (Prausnitz *et al.*, 2012; Rainsford *et al.*, 2008; Heyneman *et al.*, 2000; Goodman, 2012; Mason *et al.*, 2004)

For other conditions where oral drug delivery is not feasible, due to, for example, poor gastrointestinal absorption, transdermal delivery has many advantages compared to oral and intravenous delivery.(Thomas and Finnin, 2004; Prausnitz and Langer, 2008)

Transdermal delivery can offer patient-friendly and non-invasive options in the diverse variety of formulations (gels, creams, patches and spray) that can be used. (Thomas and Finnin, 2004)

The frequency of administration can be reduced to once a day or once a week if for example using a patch, making it easier for the patient. Another advantage with transdermal delivery is the avoidance of first-pass metabolism for drugs with poor oral availability, also, the release of the drug is more controlled and minimises plasma concentration fluctuation (Leichtnam *et al.*, 2006c; Chik *et al.*, 2006; Thomas and Finnin, 2004; Prausnitz and Langer, 2008; Jordan Jr, 1997; Ale *et al.*, 2009). Especially patches have the advantage that depending on the patient's status and whether the drug input needs to be changed or is no longer required, the patch is easily removed (Wiedersberg and Guy, 2014).

The disadvantages with transdermal delivery mainly concern the nature of the skin and stratum corneum. Because the main purpose of the skin is to act like a protective barrier to exogenous compounds, permeability across this layer is very low. Transdermal delivery is not at all suitable for delivering rapid bolus type treatments, and drugs must be very potent in order to exert a physiological effect at the target site after crossing the skin barrier.

To date there are 20~ drugs approved for transdermal administration. A few common traits among these drugs have been identified such as: low molecular weight (under 500 Da) moderate log $P_{o/w}$ between 1-5, ideally between 2-3 and a preference towards lipophilicity rather than hydrophilicity, low dose and high potency. (Wiedersberg and Guy, 2014; Naik *et al.*, 2000; Prausnitz *et al.*, 2012; Prausnitz and Langer, 2008)

The latter means that the drug can be delivered with a patch of reasonable size. If the potency or the skin permeability is too low, a larger area must be used to reach the desired effect (for comparison: a credit card is around 50 cm^2). There are only a few drugs formulated to be delivered transdermally over an area larger than 50 cm^2, the hormone testosterone being one of them. (Wiedersberg and Guy, 2014)

Testosterone and transdermal formulations

Testosterone is the major circulating androgen in man (Lu *et al.*, 2013; Leichtnam *et al.*, 2006c) and is responsible for normal growth and development of male secondary sexual characteristics. In healthy, adult males, the testes produce between 3 to 10 mg of testosterone daily, however the levels of the hormone decline with age (Chik *et al.*, 2006). Men who suffer from hypogonadal disorder may benefit from hormone replacement therapy (Lu *et al.*, 2013). There are several formulations of testosterone products in the market, including oral formulations, subcutaneous implants, intramuscular injections and transdermal products. As previously mentioned, transdermal delivery has some advantages over oral delivery, furthermore, the chemical properties of testosterone itself, listed in table I are very suitable for transdermal delivery (Leichtnam *et al.*, 2006c; Hathout *et al.*, 2010).

Table I. Physicochemical properties of testosterone

Physicochemical properties	
Log $P_{o/w}$	3.3[a]
Molecular weight	288[a,b]
Melting point	155 °C[b]
Solubility in H_2O	0.039 mg/ml at 37 °C[c]

[a] (Moffat *et al.*, 2004)
[b] (The Merck Index Online, 2017)
[c] (Hathout *et al.*, 2010)

Oral testosterone is extensively metabolised in the liver and gastrointestinal tract, another aspect that makes it suitable for transdermal delivery. Beneficially, the approach have evolved from scrotal

patches to a non-scrotal patch (Androderm®) and several transdermal gel formulations (Testim®, Testogel® and Tostran® etc). The latest is a testosterone liquid roll-on type formulation (Axiron®).

The rationale behind a scrotal patch is not farfetched as testosterone is produced by the testes located in the scrotum, and the scrotum was shown in a study to be the site with the highest area normalised skin absorption (Feldmann and Maibach, 1967). Also, the clinical study showed that with the patch on, all hypogonadal patients reached normal testosterone levels in less than four hours (Findlay *et al.*, 1987). The patches were developed by ALZA Corp (Palo Alto, CA), pioneers within transdermal delivery and patch technology. (Prausnitz and Langer, 2008; Wiedersberg and Guy, 2014; Thomas and Finnin, 2004)

Even though there were less frequently reported cases of skin irritation associated with the scrotal patches compared to non-scrotal patches (Jordan Jr *et al.*, 1998; Jordan Jr, 1997; Ale *et al.*, 2009), patients experienced other practical problems such as having a smaller scrotal area than could accommodate the patch, adhesion problems with the patches, and having to regularly shave the genital area (Hadgraft and Lane, 2015; Gooren and Bunck, 2003).

After reports suggested that patients were experiencing difficulties, mentioned in the paragraph before, non-scrotal patches were developed and designed to be used on torso, back or arms (Mazer *et al.*, 1992). Despite the fact that improvements were seen in patients, regarding levels of testosterone and DHT, sexual function etc., the level of skin irritation, erythema and pruritus associated with these patches are a limiting factor for patient satisfaction (Jordan Jr, 1997). The differences between the scrotal and non-scrotal patches regarding skin irritancy lie in the design of the patch, as it was shown in a study that testosterone itself was not the allergen (Jordan Jr, 1997). Because the scrotum has a high permeability, a higher transfer rate of the drug is permitted. The scrotal patch was designed to deliver a controlled amount of the drug continuously whereas the non-scrotal patch delivers the drug following a circadian rhythm. The scrotal patch does not contain permeation enhancers, adhesives or preservatives, all of which are known skin irritants, and clings to the body with body heat. The non-scrotal patches contain both adhesives and permeation enhancers, and furthermore they are applied in areas associated with prolonged pressure for example during sleep or sitting. Other factors affecting the possibility of skin irritation is patch size, patch type (in general, single matrix type patches tend to be less associated with irritation than central drug reservoir patches), irritants, duration of the treatment and application site. (Jordan Jr, 1997; Gooren and Bunck, 2003; Ale *et al.*, 2009)

As previously mentioned, drugs being delivered transdermally need to be potent to give a desired biological effect in order to compensate for low skin permeability and for the development of a

patch of acceptable size. For testosterone preparations, the size criteria was circumvented by making gel preparations. (Wiedersberg and Guy, 2014; Hadgraft and Lane, 2015)

Androgel® (Testogel® in Europe) was the first testosterone gel preparation to be developed and is available since 2000, followed by Testim® available since 2003. The simplicity of use and the lower incidence of skin irritation associated with the gels made them popular within this cohort, and within only a few years after their launch the gels became the testosterone transdermal preparation of choice. The lower incidence of skin irritation is due to the application area. (Hadgraft and Lane, 2015) The gels and the non-scrotal patches contain the same amount of ethanol, a known skin irritant, however as the gels are spread over a larger area (~150 cm^2, compared to 7.5 cm^2 for the patches) the amount of ethanol per unit area is lower. Also the combination of permeation enhancer, ethanol, other excipients in the patch and adhesive have an effect. (Jordan Jr *et al.*, 1998) A few more gel preparations have since been launched, differing in the type and/or number of penetration enhancers or the site of application. (Hadgraft and Lane, 2015)

All the gels are mainly composed in the same way, *i.e*. they have a high content of alcohol (ethanol is the most commonly used) a number of penetration enhancers, such as ethanol and propylene glycol, to aid the penetration of the drug, and a gelling component.

As mentioned previously, gel systems allow delivery over a relatively large skin area, however new complications arise regarding patient-to-patient transfer of the formulation. One study showed that the possibility of interpersonal transfer of testosterone from a gel was low (Rolf *et al.*, 2002), however there have been a number of reports about testosterone adverse effects seen in women and children after secondary transfer. (Lakshman and Basaria, 2009) Although patients are instructed to wash their hands after application, and to cover the treated area with clothing, secondary testosterone transfer remains a problem.

In 2010, Axiron® a new testosterone liquid formulation was approved. This new formulation uses an applicator, instead of hands, to apply the solution to the axillae. The pilot studies showed that the serum concentration of testosterone was higher when applied to the axillae than the inner forearm, and that most of the patients saw improvements in their sexual function and testosterone levels. Despite the measures taken to limit secondary transfer – application to axillae instead of torso and arms, using an applicator instead of the hands, patients are still encouraged to take the same precautionary measures as with gels to reduce exposure to others. Skin irritation is still a common problem, albeit mild. (Hadgraft and Lane, 2015)

New testosterone products to be designed would need to take into account: low transfer risk to other people, small application area and patient friendly aspects such as low irritation, fragrance, feeling on skin, quick drying time, ease of administration.

A formulation which addresses all the above mentioned criteria would be an important progress in the field of testosterone formulation products.

Thesis outline

The work presented in this thesis aims to understand the behaviour of testosterone when applied on the skin in a formulation and to explore the physical state of testosterone in the skin after application. This could inform us about how the drug is distributed over an area and if a correlation to certain anatomical sites (for example hair follicles) could be made, information about the penetration pathway of a drug could be generated. A dermal product has to address a range of challenges such as skin irritancy, transfer risk between patients, ease of use, cosmetic elegance and effectiveness.

Chapter 2 aims to characterise marketed two testosterone transdermal formulations and a binary testosterone solution with tape stripping methodology and passive diffusion skin experiment *in vitro* using Franz cells, to investigate if a kinetic profile is seen over time and if a difference in absorption can be measured.

Chapter 3 involves forced degradation experiments, solubility and stability tests for testosterone in different solvents and storage times, to assess the compatibility of these solvents in a possible future formulation.

In chapter 4, testosterone is deuterated on five positions using a novel method that was developed during this project. The newly synthesised drug was then further characterised with NMR regarding stability in different solvents. The aim was to circumvent problems with low sensitivity seen in preliminary Raman spectroscopy experiments.

Chapter 5 explores the use of Raman spectroscopy in combination with skin diffusion experiments with testosterone in a binary formulation, testosterone marketed formulations and deuterated testosterone in a binary formulation and in *an ad* hoc gel formulation to investigate the lateral distribution of the drug on the skin.

Finally, chapter 6 shows an overview of discussion and conclusions from all chapters.

Chapter 2

DERMATOPHARMACOKINETICS OF TESTOSTERONE FORMULATIONS

Introduction

The skin provides an excellent defence, keeping xenobiotics out, and an equally excellent gate keeper, carefully guarding water transport out. The first contact with the body for exogenous substances, is the stratum corneum. *(Guy and Hadgraft, 2003)*

For a drug to diffuse through the skin, several steps are required. First, the drug must be in a form ready to partition. Then the drug has to partition from the formulation into stratum corneum. (Moser *et al.*, 2001b, c) Within the stratum corneum, structured into ordered bilayer arrays, there are several possible diffusional pathways: intercellular, transcellular, follicular and eccrine, however the intercellular route is predominant. (Guy and Hadgraft, 2003) Secondly the drug has to diffuse through the intercellular lipids in stratum corneum and continue through the epidermis. The flux J of drug through stratum corneum can be described with Fick's first law

$$J = \frac{D_m c_{s,m}}{L} \times \frac{c_v}{c_{s,v}}$$

Where $\mathbf{D_m}$ represents the diffusion coefficient of the drug in the skin, $\mathbf{c_{s,m}}$ the solubility of the drug in the skin**, L** the diffusion path length across the membrane, $\mathbf{c_v}$ the concentration of the drug dissolved in the vehicle and $\mathbf{c_{s,v}}$ the solubility of the drug in the vehicle. (Moser *et al.*, 2001b, c)

The partitioning ability of a drug can be approximated by measuring the octanol-water partition coefficient, expressed as $\mathbf{log\ P_{oct/wat}}$. The generally accepted $\mathbf{log\ P_{oct/wat}}$ value for maximum permeation lies between 1 and 3, whereas lower and higher values indicate low permeability because the drug cannot diffuse in or out from the stratum corneum lipids. (Thomas and Finnin, 2004) The highest rate for passive diffusion is observed when the drug is saturated in the vehicle. There are three ways to enhance the rate further. These are: to increase the diffusion coefficient of the drug**,** $\mathbf{D_m}$, to increase the partitioning of the drug into the skin, $\mathbf{c_{s,m}}$ and to create a supersaturated state of the drug by increasing the ratio $\mathbf{c_v/c_{s,v}}$ (Moser *et al.*, 2001c).

The latter strategy is sometimes a desired effect in pharmaceutical drug delivery science, and is carried out by changing the components in a formulation. The advantage of this thermodynamic approach is an enhanced permeation, without adding penetration enhancers and thus skin irritation is limited. The disadvantage, however, is the instability of the supersaturated state. (Moser *et al.*, 2001a; Leichtnam *et al.*, 2006a) A supersaturated state can be created on the skin by including a volatile agent in the formulation (Leichtnam *et al.*, 2006a; Pellet *et al.*, 1997). Upon application to the skin, the volatile agent, ethanol being the most commonly used, will quickly evaporate leading to

a rapid decrease in the solubility of the drug so that the system reaches a supersaturated state. (Leichtnam *et al.*, 2006a; Moser *et al.*, 2001a)

Tape stripping is a method used in different fields of cutaneous biology and drug delivery (Raney *et al.*, 2015; Navidi *et al.*, 2008; N'Dri-Stempfer *et al.*, 2008, 2009). In dermatopharmacokinetics it is used to monitor the drug levels in the stratum corneum after a topical treatment. The procedure itself is relatively straightforward, and involves sequential removal of layers of the stratum corneum by placing an adhesive tape on the skin, applying a gentle pressure before removing with a sharp upward movement. (Herkenne *et al.*, 2008; Lademann *et al.*, 2009) The drug is then extracted from the tapes and quantified. Additionally, information about the depth of stratum corneum removed can be obtained by weighing the tapes before and after tape stripping. Because the weighing is a time consuming process, other approaches, for example spectrophotometric methods to quantify the molecule of interest have been attempted. (Herkenne *et al.*, 2008; Mohammed *et al.*, 2012).

Testosterone transdermal products usually contain a high ethanol content to ensure drug solubilisation. It is anticipated that solvent evaporation and absorption upon application leads to significant changes in the physical and supersaturation state of the drug with the obvious impact on the kinetics of skin absorption of testosterone.

The aim for the work presented in this chapter was to investigate the time kinetics of testosterone skin absorption from two marketed gel formulations, and testosterone in solution using tape stripping methodology and dermatopharmacokinetics.

Material and methods

Chemicals and solvents were obtained from Sigma-Aldrich

Sigma-Aldrich

Acetonitrile, ethanol, hydrochloric acid, polyethylene glycol 400, potassium chloride, potassium dihydrogen phosphate (KH_2PO_4), disodium hydrogen phosphate (Na_2HPO_4), sodium chloride, sodium hydroxide, testosterone (T1500 -1G, ≥98 %, CAS 58-22-0)
Milli-Q water was used for all experiments.

Skin

Porcine skin from a local abattoir was dermatomed using (Zimmer®, Ohio, US) with a nominal thickness set to 750 µm. The prepared skin was frozen within 24 hours of slaughter, and thawed before use.

Formulations

Testim 50 mg (1 %) gel, Lot GAGL-3, Auxilium Pharmaceuticals, USA, distributor Europe Ferring Pharmaceuticals, Lausanne Schweiz
Testogel 50 mg (1%) gel, Lot 80992, Besins healthcare, Laboratoires Besins international, Bayer, Paris, France

Experimental methodology

Preparation of reagents

Phosphate buffered saline

Phosphate buffered saline (PBS) was prepared by dissolving NaCl (8 g), KCl (0.2 g), Na_2HPO_4 (1.44 g) and KH_2PO_4 (0.24 g) in Milli-Q water (1 L). The pH was adjusted with 0.1 M HCl or 0.1 M NaOH to 7.4.

Testosterone solution for skin experiments

Required amount of testosterone was first dissolved in ethanol (EtOH), followed by polyethylene glycol 400 (PEG400). The final testosterone concentration was 21.1 mg/ml in 75:25 EtOH:PEG400.

Preparation of tapes

Adhesive tape (3M Scotch®, book tape, US) was cut into 2.5 x 2 cm tapes. Before weighing, static electricity was discharged using a R50 discharging bar and ES50 power supply (Eltex Elektrostatik GmbH, Weil am Rhein, Germany) and an ESD wristband set (10 mm 1MEG, Multicomp, Farnell, UK) connected to an earth bonding plug (1x10 mm, 070-0012, Multicomp, Farnell, UK). The tapes were weighed using a microbalance (Sartorius model SE2-F, Sartorius AG, Germany) before and after tape stripping.

Analytical methods

Standard curve preparation

Testosterone was first dissolved in one part acetonitrile (ACN) and then two parts H_2O to make up a standard stock solution with the concentration of 116 µg/ml. From this standard stock, testosterone was further diluted with ACN/H_2O 60:40 or PBS. Typical concentrations prepared was for ACN/H_2O 60:40: 0.058 µg/ml – 23.2 µg/ml, and PBS: 0.058 µg/ml – 11.6 µg/ml respectively. Calibration curves were fitted using least squares linear regression analysis. The limit of quantification was 0.05 µg/ml and the limit of detection was 0.02 µg/ml.

Testosterone was quantified by using a HPLC system (Jasco, Tokyo, Japan) consisting of a Jasco PU-2080 Plus intelligent HPLC pump, a Jasco UV-2075 Plus intelligent UV-Vis detector and a Jasco AS-2051 Plus intelligent sampler and a Jasco ChromNav software. The HPLC method was based on Hathout et al., (2010). A reverse phase C18, 4.6 x 150 mm column (HiQSil, KyaTech, Japan) was used at 25 °C with UV detection at 241 nm. The mobile phase was degassed 60:40 (v/v) mixture of ACN and H_2O, with a flow rate of 1 ml/min. The samples were injected at a volume of 100 µl; the

retention time of testosterone was ~ 4.0 minutes. Standards were injected with every samples batch.

Data analysis

The stratum corneum concentration of testosterone was calculated from the mass of drug found in the tapes, and the mass of stratum corneum on the tapes. The mass of formulation in the stratum corneum on the tapes was considered to be negligible. From the tape stripping template area, the density of the skin (≈1 g/cm^3) (Farvid *et al.*, 2005) and the mass of stratum corneum on the tapes, the depth, $\mathbf{h_{sc}}$, of the stratum corneum was calculated as follows:

$$h_{sc} = \frac{V_{sc}}{\pi r^2} \text{ where } V_{sc} = \frac{mass_{sc}}{\rho_{sc}}$$

Where V_{sc} stands for the volume of stratum corneum and ρ_{sc} means the density of stratum corneum

Statistical analysis used Prism 5 (GraphPad Software, San Diego, CA). Unpaired t-test and one-way analysis of variance (ANOVA) followed by the corresponding Bonferroni test were used to analyse all data. The level of statistical significance was fixed at $p< 0.05$.

Method development and preliminary tests

Dosing methods

Two ways of applying a gel formulation were investigated. First, the inverted vial method, a second, approach used a positive displacement pipette.

Inverted vial method

A 2.0 ml vial was placed bottom up on the scale and the balance was tared. The gel was placed on the end of the vial, the weight of the vial plus gel was recorded, and then the gel was transferred to the pig skin by gentle dabbing on the skin in a circular motion for 30 seconds. The vial was then weighed again to calculate how much of the gel was actually put on the skin membrane.

Positive displacement pipette method

The formulation (10 µl) was applied to the skin with a positive displacement pipette (Pos D, MR-100, Rainin, UK) and the weight was noted. A plastic pipette was used to carefully spread out the gel on the skin, and again the weight was noted. The tip of the plastic pipette was cut with a scissor in to an extraction vial and the residual testosterone was extracted and quantified.

Solubility test

The solubility of testosterone in PBS was determined by adding different amounts (0.14 mg, 0.28 mg and 0.27 mg) of testosterone to one millilitre of PBS, only a fraction was dissolved. The vials were shaken overnight in a waterbath set at 37 °C. The samples were filtered before HPLC analysis. The solubility ± SD for testosterone in PBS was determined to be 30.0 µg/ml ± 0.18.

Evaporation tests

Both Testim® and Testogel® contain ethanol which causes rapid weight loss when they are handled. Simple evaporation tests were carried out to quantify the magnitude of this effect after application on the skin. The first test applied 10 µl of the gel (~6 mg) on an inverted vial, placed on a balance. The weight loss was noted every minute.

The second test simulated inverted vial application on skin and was performed by applying Testim® gel on inverted HPLC vial and then transferring it to a 2.0 cm^2 area marked on the weighing boat. Again the weight loss was noted every minute.

The results from the evaporation tests are shown in figures 3 and 4. In all cases the weight loss seemed to be following an exponential pattern. The mean percentage weight loss ± SD was for the

weighing boat (n=6): 42.8 % ± 14.5, and for the inverted vial (n=3): 57.3 % ± 2.7. The tests indicate that most evaporation occurs within a few minutes after application and then stabilises. This is particularly seen in figure 4, where 2 mg is lost within two minutes compared to figure 3, where the weight loss is continuous. These losses make it difficult to precisely estimate the amount of formulation, and therefore the testosterone applied. For that reason, skin experiments are reported as percentage distribution of testosterone in the various compartments.

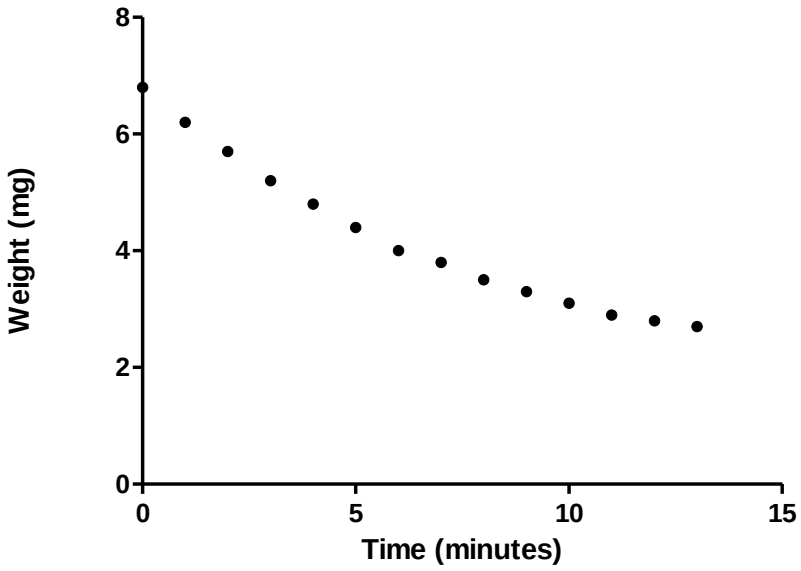

Figure 3. Graph showing one example from the three replicates on the evaporation in form of weight loss of Testim® gel after every minute when applied on an inverted vial.

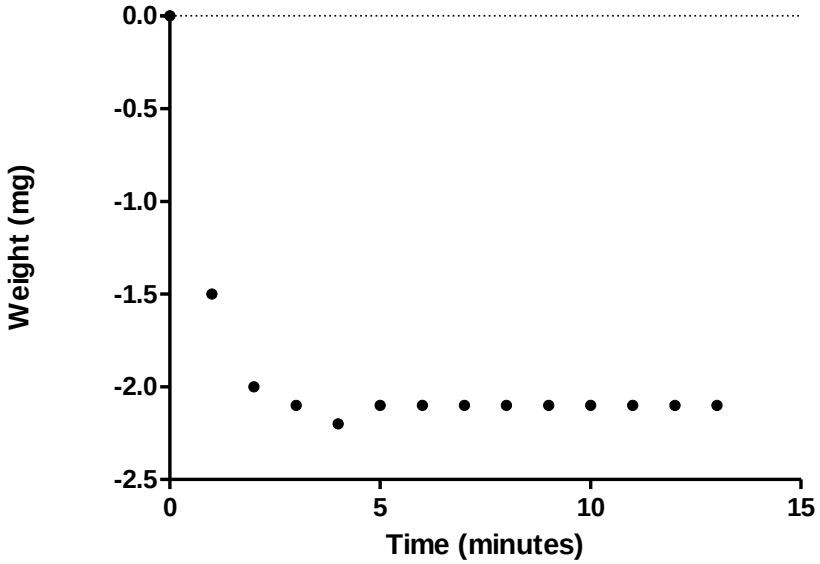

Figure 4. Graph showing the weight loss of Testim® after every minute when applied on a weighing boat (n=6), using the inverted vial application technique.

Skin cleaning formulation removal tests

A series of cleaning tests were carried out with the use of Testim® and Testogel®, to evaluate the cleaning procedure used in the tape stripping experiments. The cleaning tests consisted of diffusion experiments involving short exposure times (10 seconds, 5 minutes and 30 minutes) of the drug formulations. At the end of these experiments, some cells were cleaned with isopropanol wipes (Fast aid® pre injection swabs, 70 % isopropyl alcohol, Robinson Healthcare, UK), and some were not, but all cells were tape stripped as described in the "Diffusion experiment" section and compared.

Another experiment explored the efficacy of using a soap solution instead of the wipes. In this case, the experiment was run for 30 min, at the end of which the cell was disassembled and the skin was cleaned by applying 100 µl of soap solution (0.1% w/v RBS HDS 10 soap, Medline Scientific Ltd, Chalgrove, UK) and then rubbing carefully a few seconds with a cotton bud before carefully soaking up the remaining liquid with another cotton bud. After the cleaning procedure, the tape stripping procedure was performed as described in the "Diffusion experiment" section.

Soap cleaning resulted in a higher amount of testosterone present in the tapes than the isopropanol cleaning. It was assumed that a small amount of testosterone would have been diffusing into the stratum corneum, so the procedure resulting in least testosterone extracted from tapes was preferred.

As expected, the apparent testosterone concentration in the stratum corneum was reduced when the skin was cleaned (mean testosterone in stratum corneum (µg/mg) was 14.7 ± 20.2) with isopropanol wipes, compared to uncleaned skin (mean testosterone in stratum corneum 62.9 ± 80.0 (µg/mg) was), implying that the process removed at least some of the formulation. Note in figure 5 for example that very high values (concentration ≤ 100 µg/mg) only were observed for uncleaned samples

The isopropanol cleaning method was proposed previously, where the authors compared the use of isopropanol wipes to using dry paper towels and found that a more thorough method such as using isopropanol wipes in conjunction with appropriate time of skin contact and was required to remove semi-solid products. (Wiedersberg *et al.*, 2009)

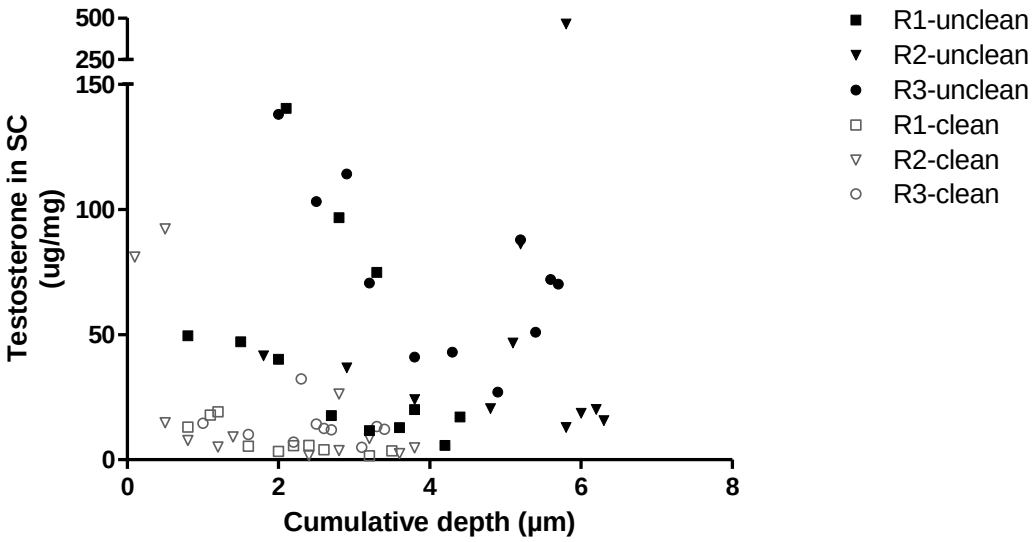

Figure 5. Scatter plot showing the concentration of testosterone found in tape strips as a function of the cumulative depth reached in stratum corneum. The formulation used was Testogel®, the exposure time was 30 minutes. The symbols in black show the three replicates that were not cleaned, whilst open symbols show the three replicates that were cleaned with isopropanol wipes

Testosterone stability in tapes

Another experiment investigated the stability of testosterone on tapes containing stratum corneum samples. A 2 cm^2 area of three skin samples was tape stripped. The tapes were then spiked with 50 µl of testosterone dissolved in mobile phase in different concentrations, shown in table II.

Table II. Concentration and amount of testosterone used to spike tapes containing stratum corneum.

Tape number	Concentration (µg/ml)	Corresponding amount of testosterone (µg)
1-3	116	5.8
4-6	11.6	0.58
7-9	1.16	0.058
10-12	0.58	0.029

Next, the tapes were stored in a cupboard before extraction. One set of tapes were extracted after only five hours storage, whereas the remaining two sets of tapes were stored in the cupboard for extraction later, one week and two weeks respectively. Finally as a control, 50 µl of each concentration was put directly in four HPLC vials (without tape strips). The results for all these experiments were quite similar and considered satisfactory. Typically testosterone was extracted within two weeks.

Diffusion experiment

A vertical, static Franz cell (receptor volume 7.4 ml, area 2 cm^2, PermeGear, Inc., Bethlehem, PA, USA) was assembled. The dermatomed pig skin was clamped between the donor chamber and the receptor chamber. Testim® was applied with either the inverted vial method or the positive displacement method. Testogel® was applied only with the latter method and the testosterone solution was applied with a standard Eppendorf pipette. The exposure time of the experiments was 3, 6 and 24 hours, after which the same procedure was followed in all cases. A sample was taken out from the receptor compartment and filtered (Cronus syringe filter, nylon, 13 mm, 0.45 µm, LabHut, UK) into a HPLC vial. The cell was dismantled, the pig skin was cleaned with an isopropanol wipe (Fast aid® pre injection swabs, 70 % isopropyl alcohol, Robinson Healthcare, UK), five strokes on each side of the wipe. A template with an area of 2 cm^2 was fixed over the skin and then the skin was tape stripped, 12 tapes per piece of skin.

The tapes, the viable skin, the isopropanol wipes, the pipette tips and the glass lids of the Franz cell were extracted in order to report the data as percentage distribution.

The tapes were put in vials together with 1.5 ml extraction solvent (ACN:H_2O 60:40) and then placed on a shaker (IKA HS 260 Basic shaker, IKA1 Werke GmbH & Co., KG, Germany) at ~100 motions per minute overnight. Next, the samples were filtered (Cronus syringe filter, nylon, 4 mm, 0.45 µm) and analysed by HPLC. The same procedure was followed for the extraction of the plastic pipette tip.

The viable skin samples and isopropanol wipes were put into Eppendorf tubes, the lids were put into 25 ml volume beakers. To all samples, 4 ml of extraction solvent (ACN:H_2O 60:40) was added. The beakers were covered with Parafilm® and shaken overnight. Then the samples were filtered (Cronus syringe filter, nylon, 4 mm, 0.45 µm, LabHut, UK) and analysed by HPLC.

Results

Diffusion and tape stripping experiments

Testim® 3, 6 and 24 hours experiments

The results of these experiments are shown in table III, and figures 6, 7, 8 and 9. Both application methods showed similar results regarding total amount absorbed from tapes and skin after 3 and 6 hours, however there was a higher total amount absorbed from tapes and skin after 24 hours with the positive displacement method than the inverted vial method ($p < 0.05$, t-test unpaired). The reason remains unknown, although it can be speculated that the two application methods vary in area of contact, shape of the applicator and time of application. For both methods, the applied doses varied due to the high ethanol content. There was no clear time kinetics seen in Testim® after 3, 6 and 24 hours exposure with either application methods, figures 6 and 7, or difference in total amount recovered ($p > 0.05$, one-way ANOVA). Testosterone was detected in the receptor chamber after 24 hours. This indicates a slow absorption process of testosterone in the skin. The distribution of testosterone in the whole experiment and in tapes, shown in figures 8 and 9, show that tapes 1-2 contained comparable testosterone than tapes 3-12, up to twice as much or sometimes even more.

This could be due to an insufficient cleaning method, formation of a drug reservoir in the stratum corneum or that more stratum corneum was sampled in tapes 1-2 than in 3-12 (Lademann *et al.*, 2009). In some work, drug recovered from tapes 1-2 is not considered to be bioavailable, and therefore these tapes are discarded (FDA Draft Guidance, 1998).

Usually no more than 5 % of testosterone recovered is detected in the receptor solution, even after 24 hours exposure time.

Table III. Summary of results for Testim® 1% gel comparing three exposure times and two application methods.

Exposure (h)	3		6		24	
Application method	**Vial** n=3	**Pipette** n=4	**Vial** n=3	**Pipette** n=4	**Vial** n=3	**Pipette** n=4
Dose testosterone (µg)	49.3 ± 9.5	47.0 ± 15.2	39.2 ± 4.0	46.8 ± 5.9	40.3 ± 6.1	42.8 ± 7.4
Tapes$_{1\text{-}12}$ (µg)	6.3 ± 4.5	8.0 ± 2.8	3.8 ± 1.1	7.5 ± 3.2	7.3 ± 1.4	6.9 ± 1.1
Tapes$_{1\text{-}2}$ (µg)	3.3 ± 2.1	4.1 ± 1.4	1.7 ± 0.3	4.1 ± 1.9	4.7 ± 0.7	3.5 ± 0.9
Tapes$_{3\text{-}12}$ (µg)	3.0 ± 2.6	3.9 ± 1.5	2.1 ± 1.1	3.4 ± 1.5	2.6 ± 0.8	3.4 ± 0.5
Depth stratum corneum (µm)	6.4 ± 2.3	7.1 ± 0.4	4.8 ± 1.2	5.3 ± 1.5	6.4 ± 2.7	6.3 ± 3.8
Viable skin (µg)	1.3 ± 0.1[1]	7.8 ± 1.7	NA-	5.7 ± 1.0	1.7[1] ± 0.7-	7.3 ± 3.1
Receptor (µg)	ND[3]	ND	ND	ND	0.8 ± 0.5	0.8 ± 1.6[2]

[1] These were extracted at a much later opportunity, hence the low value might be due to degradation of the drug.
[2] Detected in only one replicate
[3;] Not detected

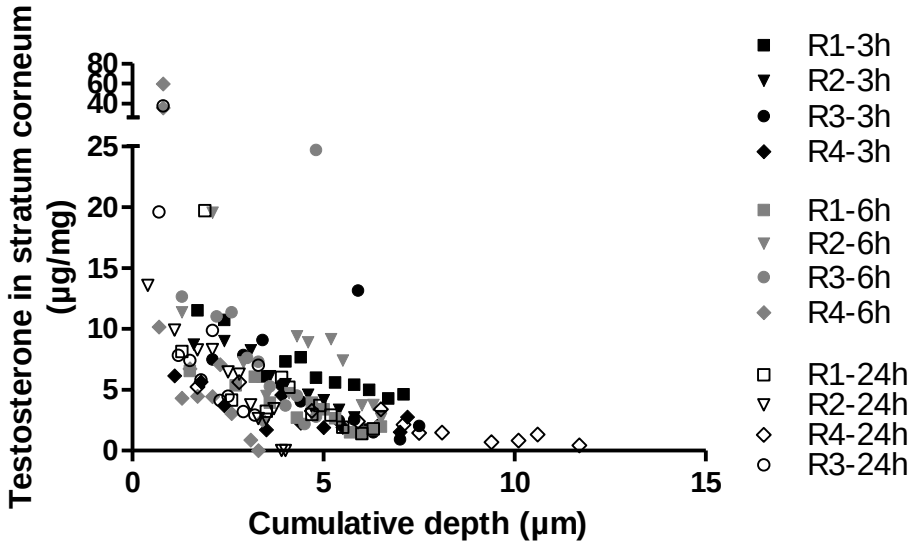

Figure 6. Concentration of testosterone in stratum corneum as a function of the cumulative depth reached in stratum corneum. The formulation used was Testim®, which was applied with the positive displacement method. Very high concentration values are likely due to error in weighing. Black symbols show replicates after 3 hours, grey symbols show replicates after 6 hours exposure time and white symbols show replicates after 24 h exposure time.

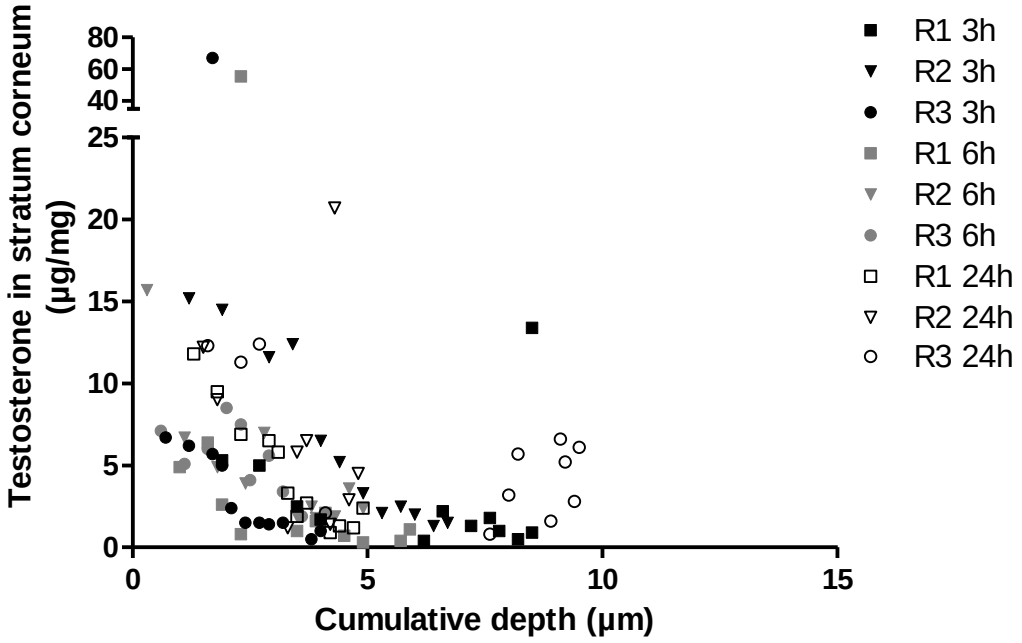

Figure 7. *Concentration of testosterone found in tape strips as a function of the cumulative depth reached in stratum corneum. The formulation used was Testim®, applied with the inverted vial method. Very high concentration values are likely due to errors during weighing. Black symbols show replicates after 3 hours, grey symbols show replicates after 6 hours exposure time and white symbols show replicates after 24 h exposure time.*

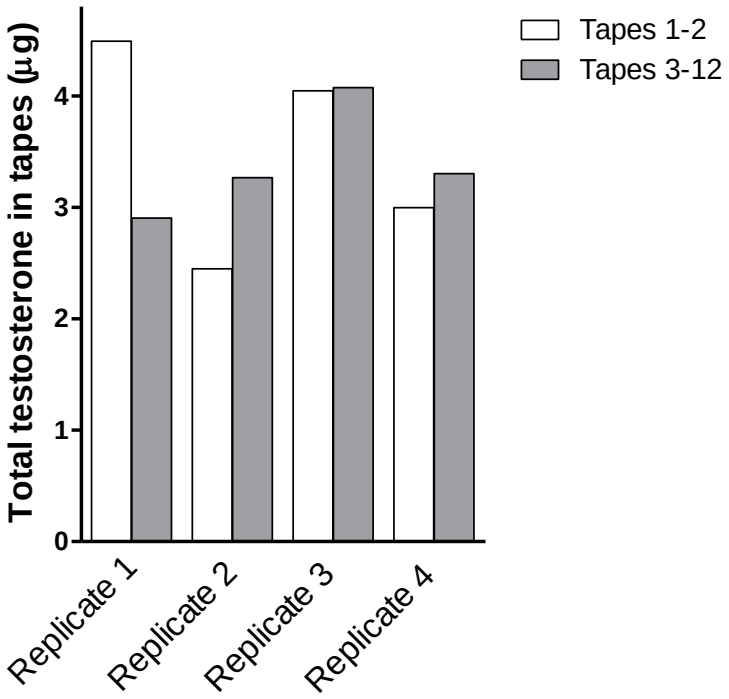

Figure 8. Testosterone recovered in tapes 1-2 (white columns) and tapes 3-12 (grey columns) for four replicates (R1-R4) following 24 hours exposure to Testim®.

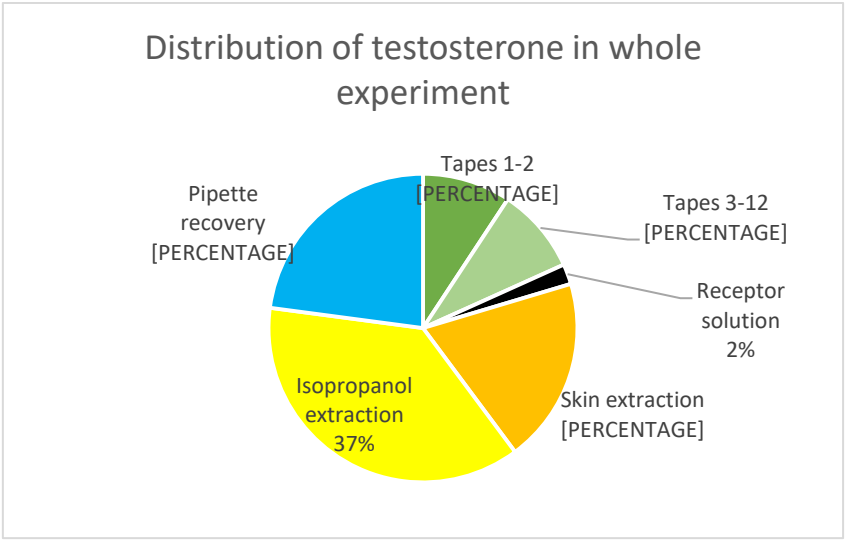

Figure 9. Testosterone mass distribution with respect to the total amount of drug recovered following a 24 hours Testim® experiment. The average values shown for the four replicates.

Testogel® 3, 6 and 24 hours experiments

These experiments were carried out as for Testim®, but applying the formulation with the positive displacement pipette only. The results for these experiments are shown in table IV and figures 10, 11 and 12. As shown in figure 10, no clear time kinetics were seen in experiments with Testogel® experiments, after 3, 6 and 24 hours ($p > 0.05$, one-way ANOVA). There is perhaps a small hint that after 24 hours exposure time, testosterone is detected in the deeper layers of sampled stratum corneum and thus this would indicate that testosterone has penetrated deeper in stratum corneum than after 3 and 6 hours, but between 3 and 6 hours the results were similar.

Comparing Testogel® with Testim® also showed similar result. The formulations are not interchangeable or classified as generics, although they show some similarities regarding testosterone content, composition of the gel and content of alcohol. In contrast to the results of Testim®, testosterone was detected in the receptor solution earliest after 6 hours exposure time, but more testosterone was detected after 24 hours which again indicates a slow absorption process (table IV). The distribution of testosterone in the whole experiment and in tapes, figures 11 and 12, showed similar results to Testim®, *i.e*. tapes 1-2 usually contains comparable testosterone than tapes 3-12 together.

Table IV. Summary of results obtained with Testogel® 1% gel applied with a positive displacement pipette, and three exposure times.

Exposure (h)	**3** **n=4**	**6** **n=4**	**24** **n=4**
Dose testosterone (µg)	48.0 ± 25.9	57.7 ± 6.8[1]	53.0 ± 14.0[1]
Tapes$_{1\text{-}12}$ (µg)	6.5 ± 2.2	7.8 ± 3.8	9.0 ± 5.2
Tapes $_{1\text{-}2}$ (µg)	4.2 ± 1.5	4.8 ± 2.9	4.4 ± 2.0
Tapes$_{3\text{-}12}$ (µg)	2.3 ± 0.8	3.2 ± 1.0	4.6 ± 3.3
Depth stratum corneum (µm)	7.4 ± 1.7	5.2 ± 2.6	7.2 ± 3.7
Viable skin (µg)	6.9 ± 3.9	5.2 ± 0.9	7.5 ± 1.9
Receptor (µg)	ND[3]	0.1 ± 0.2[2]	0.7 ± 0.6

[1] Mean ± SD n=3
[2] Detected in only one replicate
[3.] Not detected

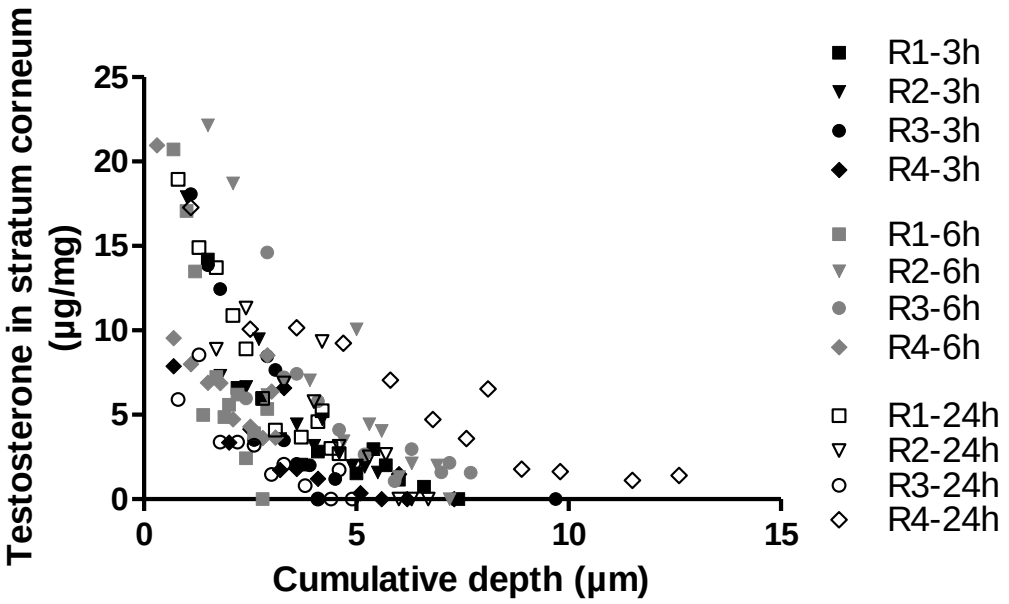

Figure 10. Concentration of testosterone in stratum corneum as a function of the cumulative depth reached in stratum corneum. The formulation used was Testogel®, which was applied with the positive displacement method. Black symbols show replicates after 3 hours, grey symbols show replicates after 6 hours exposure time and white symbols show replicates after 24 h exposure time.

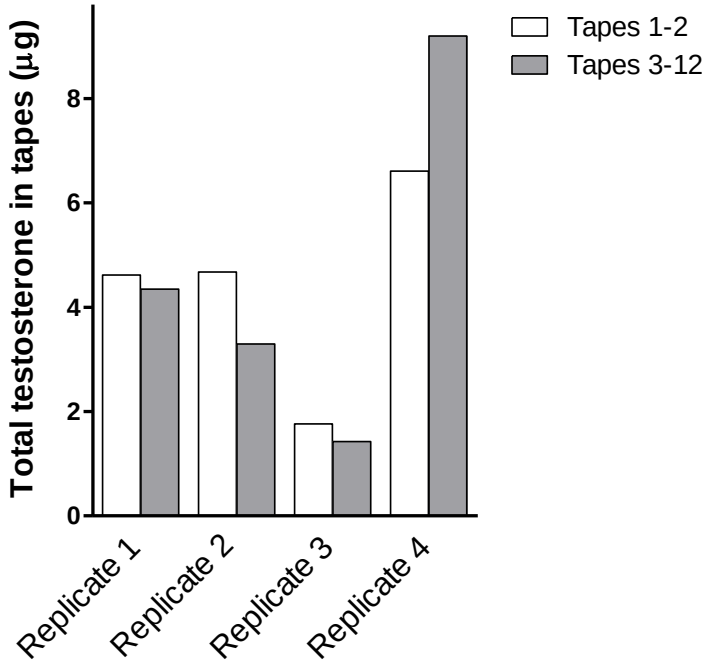

Figure 11. Testosterone recovered in tapes 1-2 (white columns) and tapes 3-12 (grey columns) for four replicates following 24 hours experiment with Testogel®.

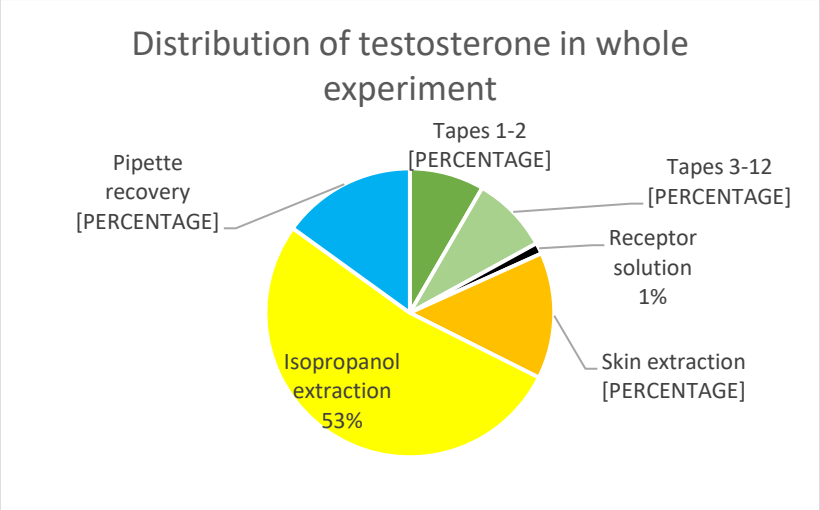

Figure 12. Testosterone mass distribution with respect to the total amount of drug recovered following a 24 hours Testogel® experiment. The average values shown for four replicates.

Testosterone solution, 3, 6 and 24 hours experiments

This experiment was performed to compare the kinetics of testosterone skin absorption from the gel formulations and a control solution. It was expected that a control liquid formulation would be more accurately dosed and also subsequently removed from the skin, the results are shown in table V, and figures 13, 14, and 15. The donor was 200 µl of a 21.1 mg/ml testosterone solution.

There was a significant difference in total amount absorbed from skin and tapes, comparing 3 hours with 6 hours ($p<0.05$ one-way ANOVA), but from figure 13, there is no clear time kinetics seen. Similarly to previously mentioned results, there is a small hint that after 24 hours exposure time, testosterone is detected in the deeper layers of sampled stratum corneum.

Table V. Summary of obtained results with a control testosterone solution (EtOH:PEG400 75:25) .

Exposure (h)	**3 n=4**	**6 n=4**	**24 n=4**
Dose testosterone (µg)	4221	4221	4221
Tapes$_{1\text{-}12}$ (µg)	129.5 ± 57.1	54.0 ± 20.3	146.9 ±89.3
Tapes $_{1\text{-}2}$ (µg)	82.3 ± 40.0	30.4 ± 11.7	110.7 ±86.7
Tapes$_{3\text{-}12}$ (µg)	47.2 ± 18.1	23.7 ± 10.9	36.2 ±9.1
Depth stratum corneum (µm)	9.8 ± 2.3	9.2 ± 2.2	16.9 ±2.6
Viable skin (µg)	581.1 ± 389.3	156.3 ±58.4	167.2 ±8.0
Receptor (µg)	ND	0.3 ±0.5[1]	1.3 ±2.6[1]

[1.] **Detected in only one replicate**

Thus, though the testosterone dose was a 100 times higher than applied with the gel formulations, the absorption of testosterone (figure 15) was lower (10 %) compared to the gel formulations (32 % absorbed for Testogel® and 40 % for Testim®). This formulation contained only two excipients: 75 % EtOH, and 25 % PEG400. Although the drug concentration was lower than saturation in both solvents separately, it can be speculated that the high content of EtOH is causing the drug to crystallise in the superficial layers of stratum corneum instead of being absorbed. Furthermore, it is possible that there is a short-lived supersaturated state of testosterone due to the high ethanol in formulations that will lead to penetration of the drug. However the supersaturated state is very transient, and causing crystallisation of the drug which leads to poor penetration and absorption of the drug.

Figure 14 shows the amount of drug recovered in tapes after 24 hours. In contrast to previous gel formulations, more drug is recovered in tapes 1-2 for all replicates, which after seeing the percentage absorption in figure 15 further builds on the theory that for this particular set of experiment the drug crystallised.

Again, more testosterone was detected in the receptor solution after the 24 hours. These findings, for all formulations, suggest that testosterone in either formulation, gel or solution, quickly loads the stratum corneum and the skin crevices with a reservoir of testosterone and residual formulation (Lakshman and Basaria, 2009). A small fraction of testosterone from this reservoir is slowly absorbed over time.

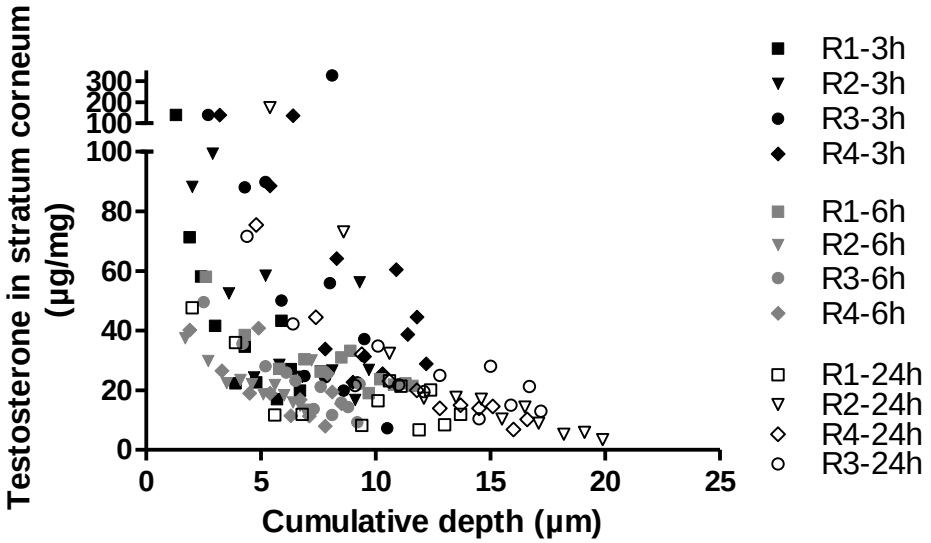

Figure 13. Concentration of testosterone in stratum corneum as a function of the cumulative depth reached in stratum corneum. The formulation used was a simple testosterone solution, which was applied with an Eppendorf pipette. Black symbols show replicates after 3 hours, grey symbols show replicates after 6 hours exposure time and white symbols show replicates after 24 hours exposure time.

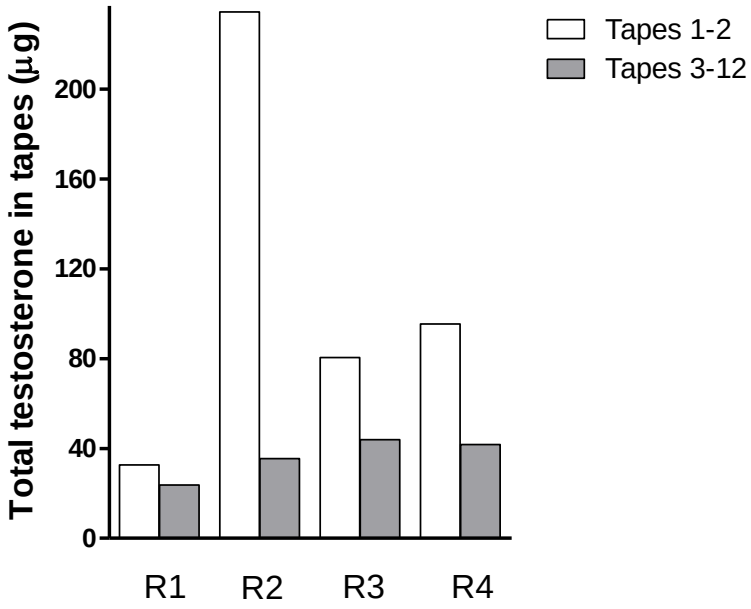

Figure 14. Testosterone recovered in tapes 1-2 (white columns) and tapes 3-12 (grey columns) for four replicates following 24 hours experiment with control testosterone solution. Same as above

.

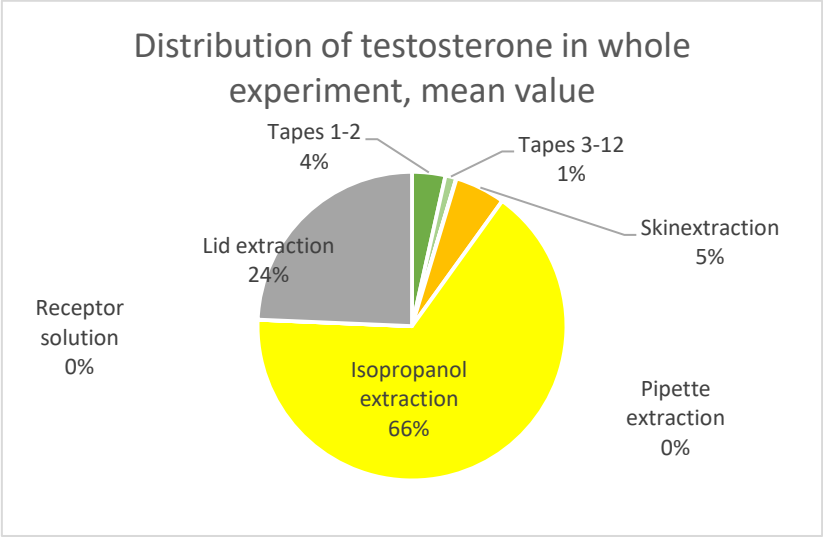

Figure 15. Testosterone mass distribution with respect to the total amount of drug recovered following a 24 hours control testosterone solution experiment. The average values shown for four replicates.

Discussion

Marketed testosterone gel formulations were applied on the skin mounted on Franz cell for different time lengths with the aim of investigating if kinetic profiles could be measured with the tape stripping methodology. Similar stratum corneum depth was sampled with both gel formulations. The percentage recovered from tapes, receptor solution and skin, shown in figures 9 and 12, after applying gel formulations shows the maximal absorption of the drug to be around 30-50 % of the testosterone recovered. The remaining is distributed between isopropanol wipes and pipettes tips.

From the control testosterone solution, figure 15, it seems like the maximum absorption (extraction from tapes, skin and receptor solution) of the drug is only 10 % of the dose recovered. Interestingly the solution results in a lower percentage of testosterone recovered from tapes and viable skin compared to the gels. Despite this, the amount recovered from the receptor is similar to that recovered from Testim® and Testogel® even though the dose applied was in the order of 100 times higher for the solution. The amount recovered from the receptor is not near the solubility of testosterone in PBS, which leads to the conclusion that the receptor solution is not rate limiting for diffusion. Figure 14 show that the amount testosterone recovered from tapes 1-2 are higher than tapes 3-12 in all replicates. This is in contrast to Testim® and Testogel® where the amount recovered from tapes 1-2 were comparable to tapes 3-12. It is speculated that the drug crystallised on the surface, as mentioned earlier.

The variability in extracted drug from tapes and skin could be due to the non-flat appearance of the skin. Formulations can go into crevices and furrows and care must be taken to not push the drug further into the skin during cleaning. A little bit of the formulation might even get pushed further into the skin during tape stripping.

The formulation itself contains ethanol, which helps the drug to penetrate. As the ethanol evaporates, the drug becomes transiently supersaturated as already mentioned. This could explain why there is no change or time kinetics seen in tape strip samples. The sampling from receptor solution indicates however, that the drug is absorbed, albeit slowly. It was suggested that the stratum corneum quickly absorbs the drug formulation and forms a reservoir from which the drug is slowly released (Rougier *et al.*, 1983; Lakshman and Basaria, 2009). The literature also mentions that Testim® has an enhanced absorption, compared to Testogel® (Androgel®), while the reason is not yet understood it is speculated that the effect is due to pentadecalactone, an emollient excipient specific to Testim®. However, this emollient also has a characteristic smell and might also be attributed to a certain stickiness in the formulation, both of which patients find a major drawback. (Gooren and Bunck, 2003; Lakshman and Basaria, 2009).

Previous work (Herkenne *et al.*, 2007) concluded that stratum corneum concentration-depth profiles were valuable in establishing time kinetic and thermodynamic data. Depending on the drug used, different time points may be selected. For example in the same article, ibuprofen was used, and time points between 15 and 180 minutes were chosen. Also they observed the typical flattening of exponential curves to more linear ones at the longer time points. During this work, there was no difference seen between the time points chosen for Testogel® and Testim® in tape strip samples, nor a difference detected between the two formulations. It was however concluded that the stratum corneum quickly loads up with the formulation and then slowly releases to the body. There was no difference observed, when comparing figure 5 (tape stripping after 30 min of application) to the figures 6, 7 and 10 (tape stripping after 24 hours of application) regarding drug concentration in the stratum corneum, which then confirms that the stratum corneum is quickly absorbed with drug within 30 minutes. The differences in the two drugs regarding physicochemical properties partly explain the two different tape stripping time frames. Also, the ibuprofen work was done *in vivo*, while this work was done *in vitro*. It has been shown that the stratum corneum is different, *i.e.* not as uniformly distributed on the tapes when tape stripping in vitro skin compared to in vivo (Lademann *et al.*, 2009).

Care must also be taken in choosing a timeframe after application that is not too short, as the actual tape stripping procedure takes some time to complete, during which the drug is still diffusing. This was quickly realised during shorter cleaning diffusion experiments (similar to the one presented in this work) and also mentioned in (Herkenne *et al.*, 2007).

It has been mentioned that supersaturating a drug in a vehicle is a way to optimise drug delivery (Pellet *et al.*, 1997; Leichtnam *et al.*, 2006b). Although supersaturation is transient it has been characterised using the tape stripping method (Pellet *et al.*, 1997). The authors concluded after using piroxicam in a propylene glycol vehicle saturated at different degrees that the higher degree of saturation the higher amount of penetrated drug in stratum corneum. Another work, evaluating testosterone delivery by supersaturation (Leichtnam *et al.*, 2006a) also found that a higher degree of supersaturation led to a higher flux of testosterone. Although with a higher degree of saturation, crystallisation of testosterone on the skin occurred.

It could be speculated that the reason for the stratum corneum to quickly load with drug and form a reservoir is due to the supersaturation effect, *i.e.* as soon as the formulation is deposited on the skin, the ethanol begins to evaporate, leaving the testosterone in a supersaturated state which will be absorbed into the stratum corneum. However, the ethanol also acts as a penetration enhancer at the same time, which is why a slow absorption also is seen. More work is needed to optimise the

parameters for work with testosterone formulations, it would also be interesting to investigate the physical state of the drug and also the distribution, which will be carried out with Raman spectroscopy. The experiment will be carried out at microscopic level at the same depth of the stratum corneum.

Conclusions

There was no clear time kinetics seen in the two different gel formulations, or in the testosterone control solution. Testosterone was detected in the receptor solution first after a longer exposure time. This indicates that the formulations quickly load the skin and crevices with a reservoir of testosterone, and that testosterone is slowly absorbed from this reservoir over time. The high content of alcohol in formulations could lead to a small degree of crystallisation, in combination with a supersaturated state of testosterone could have an effect on the penetration and absorption. Raman spectroscopy could be used to identify testosterone (crystals) and skin peaks and therefore could be informative about the behaviour of the drug.

Chapter 3

CHARACTERISATION OF TESTOSTERONE

Introduction

The developing stage of a medicinal drug gathers pre-formulation data such as characterising physicochemical properties, characteristic behaviour of the drug in excipients and solvents, solubility, and possible degradation pathways. Forced degradation is carried out to understand the stability of the drug molecule (especially new drugs), and how it changes with different conditions and time.

Previous work concluded that testosterone seems to be very stable in acidic and neutral conditions, but less stable in alkaline conditions. It was also concluded that UV-light could transform testosterone quite rapidly, but if the rate constant would be extrapolated to ambient light conditions, the rate in which testosterone would be transformed would be slower. (Vulliet *et al.*, 2010)

WHO performed accelerated stability studies under simulated tropical conditions (higher temperature and 100% humidity) on a range of pharmaceutical substances, testosterone enantate and testosterone propionate being two of the assessed substances. (World Health Organization (WHO), 1986)

The aims of the work presented in this chapter were to determine the solubility of testosterone in a range of dermally approved solvents/excipients of interest for a transdermal formulation, and then to carry out forced degradation studies of testosterone by varying different conditions regarding: temperature, presence or absence of light, pH and oxidation, before finally assaying the stability of testosterone in the chosen range of solvents/excipients at different temperatures and time points.

Information and recommendations were gathered from various sources (Blessy *et al.*, 2014; Brümmer, 2011; International Council for Harmonisation (ICH), 1996, 2005; World health organization (WHO), 1986). The experimental setup followed a protocol provided by MedPharm.

Material and methods

Chemicals, solvents and excipients

Acros organics

Benzyl alcohol

Croda

SUPER REFINED® ARLASOLVE DMI-LQ-(MH), SR40492

Fisher

Sodium hydroxide

Fluka

Isopropyl myristate, 2-phenoxyethanol

Sigma aldrich

Dipentene (limonene), diethylene glycol monoethyl ether (Transcutol), dipropylene glycol, glycerol, hydrogen peroxide, poly(ethylene)glycol (average Mn 400), propylene glycol, testosterone –CAS 58-22-0

VWR

Acetonitrile, ethanol, hydrochloric acid

Laboratory equipment and material

Cronus syringe filter, nylon, 4 mm and 13 mm, 0.45 µm, LabHut, UK
Whatman™, syringe filter 25 mm GD/X, PVDF filter media with polypropylene housing, pore size 0.45 µm, GE healthcare sciences
Oven / Heraeus, type B6, fabric number 40465233, Kendro 63505 Langensebold, Germany
Centrifuge / Boeco, type 1605-13, ser. No 0003598-02-00, made in Germany

Part I

FORCED DEGRADATION STUDIES

Experimental methodology

Testosterone assay development

Stock solution preparation for forced degradation studies.

A stock solution of the drug was prepared by weighing required amount testosterone into a 50 ml volumetric flask. Sufficient amount of 60 parts ACN and 40 parts H_2O was added to the flask, firstly the ACN was added to dissolve the drug and thereafter the H_2O was added, producing a final concentration of 1000 µg/ml. From this stock solution, flasks with drug concentration of 200 µg/ml and 100 µg/ml was prepared.

Forced degradation studies up to 48 hours

Analytical methodology, evaluating repeatability, accuracy and precision

For evaluation of the analytical method, the HPLC used was from Hewlett Packard Series 1100 with auto sampler, quaternary pump and DAD detector from Agilent Technologies, reverse phase C18, 4.6 x 150 mm column (HiQSil, KyaTech, Japan) was used at 25 °C with UV-DAD detection scanning from 190-400 nm. The standard curve concentrations ranged from 10-225 µg/ml, samples were diluted in ACN:H2O 60:40, but the mobile phase was degassed 50:50 (v/v) mixture of ACN and H_2O, the injection volume was 10 µl and the flow rate was set to 1 ml/min. The acquisition time was 15.0 minutes. With this method the retention time of testosterone was 7.1 minutes. Unknown testosterone concentrations were calculated against known standards. Table VI shows the preliminary results for evaluating repeatability, accuracy and precision where a set of standard was run for three consecutive days and the average of the results were made into a new standard curve to use for evaluating repeatability, accuracy and precision. Only the highest concentration show a higher relative standard deviation % value.

Table VI. Results of a set of standard run for three consecutive days. The average of these were made into a new standard curve later used to evaluate repeatability, accuracy and precision

	Peak area					
Concentration (µg/ml)	Day 1	Day 2	Day 3	**Average peak area**	**Standard deviation**	**Relative standard deviation (%)**
10	308.3	309.7	314.5	310.8	3.3	1.1
25	774.9	780.2	802.3	785.8	14.5	1.8
50	1567.7	1610.1	1624.7	1600.8	29.6	1.9
100	3116.5	3141.3	3167.3	3141.7	25.4	0.8
150	4620.5	4651.9	4733.3	4668.6	58.2	1.2
200	6248.0	6254.3	6292.5	6265.0	24.1	0.4
225	6951.7	6276.8	7068.8	6765.7	427.5	6.3

Three injections each of three concentrations were made to evaluate repeatability, accuracy and precision, shown in table VII. The test did not pass the accuracy criterion (98-102 %), however the precision relative standard deviation % criterion (≤ 2%) was met.

Table VII. Results from three injections each of three concentrations to validate the HPLC method. Calculated according to (Snyder et al., 2011)

Theoretical concentration (µg/ml)	**Recovered concentration (µg/ml)**	**Standard deviation**	**Average concentration (µg/ml)**	**Relative standard deviation (%)**	**Recovery (%)**
25	25.9	0.1	26.0	0.4	103.5
25	26.1				104.2
25	26.0				103.9
100	104.1	0.4	104.4	0.4	104.1
100	104.4				104.4
100	104.9				104.9
225	231.5	0.4	231.1	0.2	102.9
225	230.8				102.6
225	230.8				102.6
	Accuracy mean (n=9)	**Precision relative standard deviation (%)**	**Average n=9**	**Standard deviation**	**Relative standard deviation (%)**
Acceptance criteria	98-102 %	≤ 2 %	103.7	0.8	0.8

Experimental methods

Ambient temperature

The drug solution (100 µg/ml) was transferred to ten amber HPLC vials, four vials were injected immediately – t=0, remaining vials were stored in the lab under ambient temperature condition. Another eight amber HPLC vials were filled with ACN:H_2O 60:40 and served as blank controls at the two analysing time points: t=0 and t=24 h.

Ambient light degradation

The drug solution (100 µg/ml) was transferred to ten clear HPLC vials. Another eight clear HPLC vials were filled with ACN:H_2O 60:40 and served as blank controls at the two analysing time points: t=24 h and t=48 h. All the vials were stored under ambient lab light condition.

70 °C heat degradation

The drug solution (100 µg/ml) was transferred to ten amber HPLC vials, another eight amber HPLC vials were filled with ACN:H_2O 60:40 and served as blank controls at the two analysing time points: t=24 h and t=48 h. The vials were put in an oven set at 70 °C.

Oxidation degradation

A 5 ml aliquot of the 200 µg/ml drug solution was transferred to a borosilicate vial. Hydrogen peroxide (H_2O_2) (5 ml of a 3 % v/v solution) was added to the vial and the vial was mixed by inversion. Another borosilicate vial was filled with ACN:H_2O 60:40 (5 ml) and the 3% v/v H_2O_2 (5 ml) solution. The vials were stored in the lab under ambient lab conditions. The analysing time points were t=3 h, t=6 h and t=24 h, samples were taken from each vial and filtered into eight vials in total

Acid hydrolysis

A 2 ml aliquot of the 200 µg/ml drug solution was transferred to four suitably sized borosilicate glass vials. A 2 ml aliquot from ACN:H_2O 60:40 mix was transferred to four borosilicate vials. 1 M hydrochloric acid (HCl) (1 ml) solution was added to each vial. The vials were stored in the lab under ambient conditions.

The analysis time points were t=3 h and 24 h. At each time point, the pH of the solutions was determined and adjusted to between pH 6 – 8 using 0.1 M sodium hydroxide (NaOH) and the volume of 0.1 M NaOH required to adjust the pH was recorded. At each time point, samples were taken from each blank control and drug solution vial, and filtered into eight HPLC vials in total.

Base hydrolysis

A 2 ml aliquot of the 200 µg/ml drug solution was transferred to four suitably sized borosilicate glass vials. A 2 ml aliquot from ACN:H_2O 60:40 mix was transferred to four borosilicate vials. 1 M NaOH (1 ml) solution was added to each vial. The vials were stored in the lab under ambient conditions.

The analysis time points were t=3 h and 24 h. At each time point, the pH of the solutions were determined and adjusted to between pH 6 – 8 using 0.1 M HCl and the volume of 0.1 M HCl required to adjust the pH was recorded. Samples were taken from each blank control and drug solution vial, and filtered into eight HPLC vials in total.

Forced degradation studies 84 – 108 hours

Because there was no clear decrease or degradation peak detected in the first set of experiments, a second set of experiments with longer exposure time were performed. Also the accuracy criteria was not met in the previous HPLC method setup, some changes were made as follows in the next section.

Analytical methodology, evaluating repeatability, accuracy and precision

For this set of experiment, another HPLC system (Jasco, Tokyo, Japan) consisting of a Jasco PU-2080 Plus intelligent HPLC pump, a Jasco UV-2075 Plus intelligent UV-Vis detector and a Jasco AS-2051 Plus intelligent sampler and a Jasco ChromNav software was used. The samples were injected at a volume of 100 µl; the mobile phase was degassed 50:50 (v/v) mixture of ACN and H_2O, the retention time of testosterone was ~ 7.0 minutes. The concentration range used ranged from 0.058 µg/ml – 23.2 µg/ml,

The method was evaluated by injecting three concentrations three times, results are shown in table VIII. The acceptance criteria: accuracy mean (98-102 %) and precision relative standard deviation % (≤ 2 %) were met.

Table VIII. Results from three injections each of three concentrations to validate the HPLC method. Calculated according to (Snyder et al., 2011)

Theoretical concentration (µg/ml)	Recovered concentration (µg/ml)	Standard deviation	Average concentration (µg/ml)	Relative standard deviation (%)	Recovery (%)
0.058	0.057	0.002	0.1	2.7	98.2
0.058	0.055				95.1
0.058	0.058				100.3
1.16	1.128	0.002	1.1	0.2	97.3
1.16	1.130				97.4
1.16	1.126				97.1
11.6	11.706	0.002	11.7	0.02	100.9
11.6	11.710				100.9
11.6	11.706				100.9
	Accuracy mean (n=9)	**Precision relative standard deviation (%)**	**Average n=9**	**Standard deviation**	**Relative standard deviation (%)**
Acceptance criteria	98-102%	≤2%	98.7	2.1	2.2

Experimental methods

Ambient temperature

The drug solution (100 µg/ml) was transferred to 25 amber HPLC and stored in the lab under normal temperature condition, the analysing time points were: t=24 h, t=36 h, t=48 h, t=60 h, t=72 h and t=84 h.

Another 12 amber HPLC vials were filled with ACN:H_2O 60:40 and served as blank controls at the time points t=24 h, t=48 h and t=72 h.

Ambient light degradation

The drug solution (100 µg/ml) was transferred to 25 clear HPLC vials and stored in the lab under normal light condition, the analysing time points were: t=24 h, t=36 h, t=48 h, t=60 h and t=72 h.

Another set clear amber HPLC vials were filled with ACN:H_2O 60:40 and served as blank controls at the time points t=24 h, t=48 h and t=72 h.

70 °C heat degradation

The drug solution (100 µg/ml) was transferred to 25 amber HPLC vials and stored in an oven set at 70 °C, the analysing time points were: t=24 h, t=36 h, t=48 h, t=60 h, t=72 h, and t=84 h.

Another 12 amber HPLC vials were filled with ACN:H_2O 60:40 and served as blank controls at the time points t=24 h, t=48 h and t=72 h.

Oxidation degradation

A 16 ml aliquot of the 200 µg/ml drug solution was transferred to one borosilicate vial. H_2O_2 (16 ml of a 3 % v/v solution) was added to the vial and the vial was mixed by inversion. Another borosilicate vial was filled with ACN:H_2O 60:40 (16 ml) and the 3% v/v H_2O_2 (16 ml) solution. 30 HPLC vials were filled with the drug-peroxide solution (1 ml), 12 vials were filled with the blank solution (1 ml). These vials were stored under normal lab conditions and put in the -80 °C freezer for later analysis at each time point t=12 h, t=24 h, t=36 h, t=48 h, t=60 h, t=72 h and 84 h.

Acid hydrolysis

A 2 ml aliquot of the 200 µg/ml drug solution was transferred to eight suitably sized borosilicate glass vials. A 2 ml aliquot from ACN:H_2O 60:40 mix was transferred to three borosilicate vials. To all vials, 1 M HCl solution (1 ml) was added, and these vials were stored in the lab under normal conditions.

The analysis time points were t=3 h, t=12 h, t=24 h, t=36 h, t=48 h, t=60 h, t=72 h, t=84 h, t=96 h and t=108 h, (only t=24 h, t=48 h, t=72 h for blank). The samples were stored at 25 °C. At each time point, the pH of the solutions was determined and adjusted to between pH 6 – 8 using 0.1 M NaOH, and the volume of 0.1 M NaOH required to adjust the pH was recorded. After neutralising the samples, the samples were filtered before analysis.

Base hydrolysis

A 2 ml aliquot of the 200 µg/ml drug solution was transferred to eight suitably sized borosilicate glass vials. A 2 ml aliquot from ACN:H_2O 60:40 mix was transferred to three borosilicate vials. 1 M NaOH solution (1 ml) was added to all vials, and these vials were stored in the lab under normal conditions.

The analysis time points were t=12 h, t=24 h, t=36 h, t=48 h, t=60 h, t=72 h, t=84 h, t=96 h and t=108 h, (only t=24 h, t=48 h and t=72 h for blank). The samples were stored at 25 °C. At each time point, the pH of the solutions was determined and adjusted to between pH 6 – 8 using 0.1 M HCl and the volume of 0.1 M HCl required to adjust the pH was recorded. After neutralising the samples, the samples were filtered before analysis.

Theoretical concentration refers to calculated concentration of how much testosterone there should be in the vial based on the volume used to neutralise the sample together with what was in the vial from the beginning.

Part II

SOLUBILITY STUDIES

HPLC method for solubility studies

Testosterone was quantified by using a HPLC system (Jasco, Tokyo, Japan) consisting of a Jasco PU-2080 Plus intelligent HPLC pump, a Jasco UV-2075 Plus intelligent UV-Vis detector and a Jasco AS-2051 Plus intelligent sampler and a Jasco ChromNav software. For the mobile phase, a 60:40 (v/v) mixture of ACN and H_2O was used, the injection volume was 100 µl and the flow rate was set to 1 ml/min. The acquisition time was 8.0 minutes. With this method the retention time of testosterone was 4.5 minutes. Unknown testosterone concentrations were calculated against known standards.

Depending of the results, *i.e.* double peaks or overlapping shouldering peaks, the samples could be re-injected with mobile phase 50:50 (v/v) mixture of ACN:H_2O, and acquisition time 15 minutes, to separate the double peaks. With this method, the retention time of testosterone was 7.1 minutes. A new standard curve was run in the same mobile phase.

Solubility: measurement at 24 hours

Solubility of testosterone in different solvents/excipients was investigated by adding excess testosterone to a vial together with required amount of solvent (see table IX below). A magnet was added, the vial was sealed with a lid and with Parafilm® and placed on a submersible stirrer. This stirrer was placed in a waterbath with circulation set at 25 °C. The experiment was run for 24 hours, after which the content was filtered to remove excess undissolved drug and suitably diluted with mobile phase before analysing with HPLC.

Table IX. Table showing the solvents and excipients used in solubility and stability studies.

Arlasolve DMI	Glycerol	Phenoxyethanol
Benzyl alcohol (BA)	Isopropyl alcohol (IPA)	Polyethylene glycol 400 (PEG400)
Dipropylene glycol (DiPG)	Isopropyl myristate (IPM)	Propylene glycol (PG)
Ethanol (EtOH)	Isopropyl palmitate (IPP)	Transcutol
Eucalyptus oil	Limonene	Water

Solubility: measurement at 72 hours

The solubility of testosterone in dipropylene glycol (DiPG), propylene glycerol (PG), glycerol, benzyl alcohol (BA), phenoxyethanol and limonene was re-tested (at a later opportunity) due to high variability between replicates for one solvent. The procedure was the same, as above mentioned, however the experiment was run for 72 hours and a wider but shorter vial was used for solvents:

DiPG, PG and glycerol, allowing a larger magnet to be used. All samples were vortexed and then ultra-sonicated, before covering the lid with Parafilm® and placing on a submersible stirrer.

Because the solubility concentration of these six solvents increased in all cases and the variability decreased (except for propylene glycol) it was decided to re-do all solubility measurements and increase the incubation time to 72 hours.

Grubb's outlier test and unpaired t-test were used to analyse all data. The level of statistical significance was fixed at $p < 0.05$.

Where the difference in solubility data for 24 hours and 72 hours did not show a significant difference according to t-test, $p>0.05$, these are grouped together. If there was a significant difference between the two data sets, the data from 72 hours data are reported.

Part III

STABILITY STUDIES

HPLC method

Testosterone was quantified by using the above mentioned Jasco HPLC system. For the mobile phase, a 50:50 (v/v) mixture of ACN and H_2O was used, the injection volume was 100 µl and the flow rate was set to 1 ml/min. The acquisition time was 15.0 minutes. With this method the retention time of testosterone was 7.0 minutes. Unknown testosterone concentrations were calculated against known standards.

Sample preparation

Testosterone (40 mg ± 0.1 mg) was weighed into glass bottles, followed by 39.96 ± 0.2 g of solvent/excipient. A magnet was added, and the solution was left to mix until the drug was dissolved. For each of the 15 solvents/excipients, a control bottle was prepared in the same way. Glass bottles with drug were prepared in triplicate, whereas only one replicate with control was prepared.

In those solvents (H_2O and glycerol) where the solubility was lower than 1 mg/g, the bottles were left to mix overnight, prior to centrifuging. The supernatant was transferred to a new bottle and ~4g of the relevant solvent was added to ensure physical stability of the system. All solvents and controls were then transferred to 4 ml borosilicate vials. Where possible, the vials were filled up to full capacity. These vials were placed in a room heated to 25 °C, a waterbath set at 40 °C and an oven set at 50 °C, for 2-4 weeks before assaying.

The assaying procedure was carried out as follows: ~500 mg of solvent-drug mixture and control solvent was weighed into four individual 10 ml volumetric flasks. After adding mobile phase ACN:H_2O 50:50, the flasks were vortexed and inverted. Those solvents/excipients volumetric flasks that were determined (visually) to be immiscible with the mobile phase were put on a magnet stirrer for two hours prior to centrifuging (8000 rpm for ten minutes) before continuing. All the samples were filtered and diluted 1:2 with mobile phase before analysing with HPLC.

Results

Part I. Forced degradation studies

Forced degradation studies up to 48 hours

Ambient temperature

No obvious decrease of testosterone concentration was measured after 24 hours, as shown in table X.

Table X. Average testosterone concentration recovered after ambient temperature exposure.

Time (h)	Average concentration (µg/ml)	Standard deviation	Relative standard deviation %	Replicates
0	98.5	0.2	0.2	n=4
24	99.1	0.2	0.2	n=4

Ambient light degradation

No obvious decrease of testosterone concentration was measured after 48 h, as shown in table XI.

Table XI. Average testosterone concentration recovered after ambient light exposure.

Time (h)	Average concentration (µg/ml)	Standard deviation	Relative standard deviation %	Replicates
0	98.5	0.2	0.2	n=4
24	99.2	0.4	0.4	n=4
48	98.5	0.5	0.5	n=4

70 °C heat degradation

No obvious decrease of testosterone concentration was measured after 48 h, as shown in table XII.

Table XII. Average testosterone concentration recovered after 70 °C heat exposure.

Time (h)	Average concentration (µg/ml)	Standard deviation	Relative standard deviation %	Replicates
0	98.5	0.2	0.2	n=4
24	101.9	4.2	4.1	n=4
48	100.1	1.8	1.8	n=4

Oxidation degradation

No obvious decrease in testosterone concentration was measured after 24 hours, as can be seen in table XIII, however some changes in the testosterone peak shape was observed. Figure 16 shows a chromatogram of testosterone at time zero, before addition of oxidation product, whereas figure 17 shows a chromatogram of testosterone after 24 hours of oxidation. To the right in the figure is an

expansion of the peak, and it is clearly seen that the peak shape has changed. The peak area however, corresponded well with theoretical concentration (100 µg/ml) value and was determined to be pure according to peak purity scan, shown in figure 18.

Table XIII. Average testosterone concentration recovered after oxidation exposure.

Time (h)	Average concentration (µg/ml	Standard deviation	Relative standard deviation %	Replicates
0	98.5	0.2	0.2	n=4
3	101.3	0.6	0.6	n=4
6	101.5	0.4	0.4	n=4
24	100.3	0.8	0.8	n=4

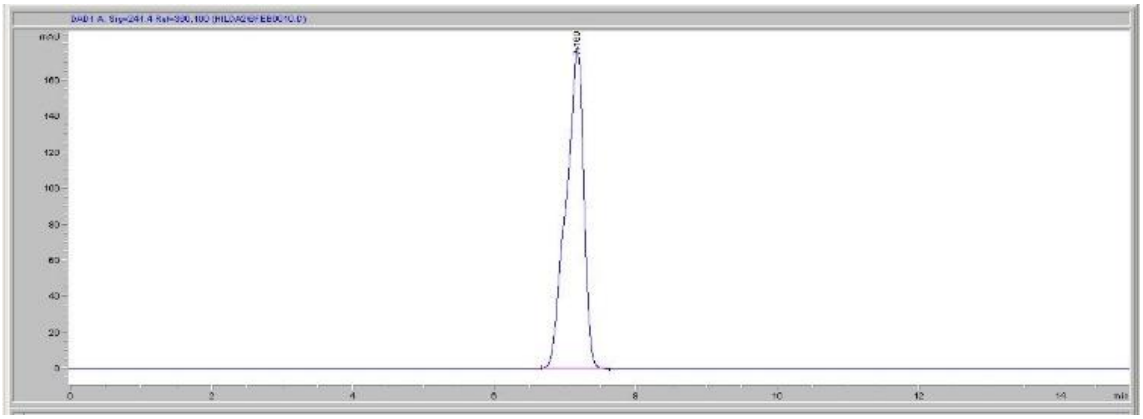

Figure 16. Chromatogram of testosterone at t=0.

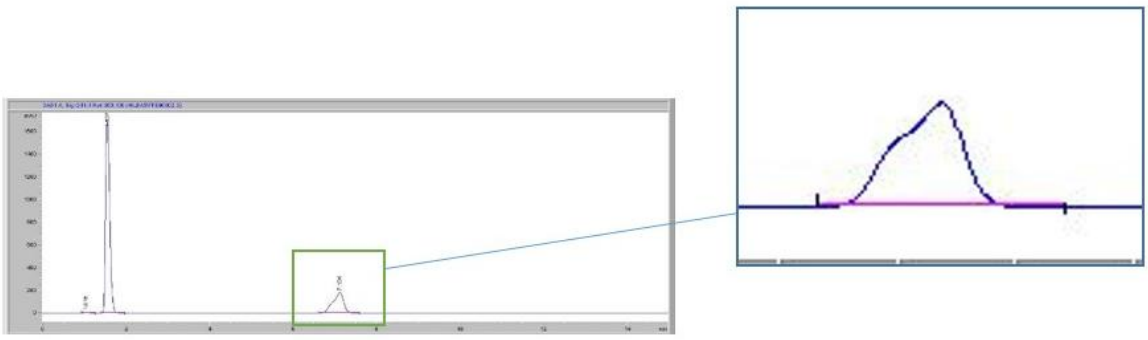

Figure 17. Chromatogram of testosterone after exposure to oxidation for 24 hours. An expansion of the testosterone peak is shown to the right in the figure. The left hand side of the chromatogram shows a peak of oxidation product.

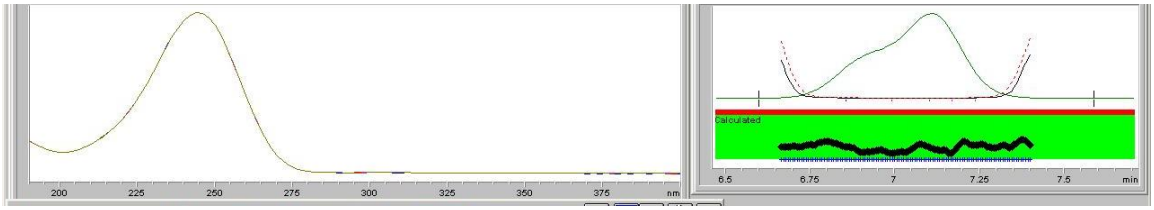

Figure 18. Peak purity scan of testosterone after 24 hours oxidation

Acid hydrolysis

No difference in drug peak concentration was measured, as shown in table XIV. Although, as seen in figure 19, the right hand side peak, which is the drug peak, the peak appearance changed to that of a shouldering peak.

Table XIV. Average testosterone concentration recovered after acid hydrolysis

Time (h)	Average concentration (µg/ml)	Standard deviation	Relative standard deviation %	Theoretical concentration (µg/ml)	Replicates
3	26.6	0.2	0.6	28.8	n=4
24	26.5	0.1	0.2	27.0	n=4

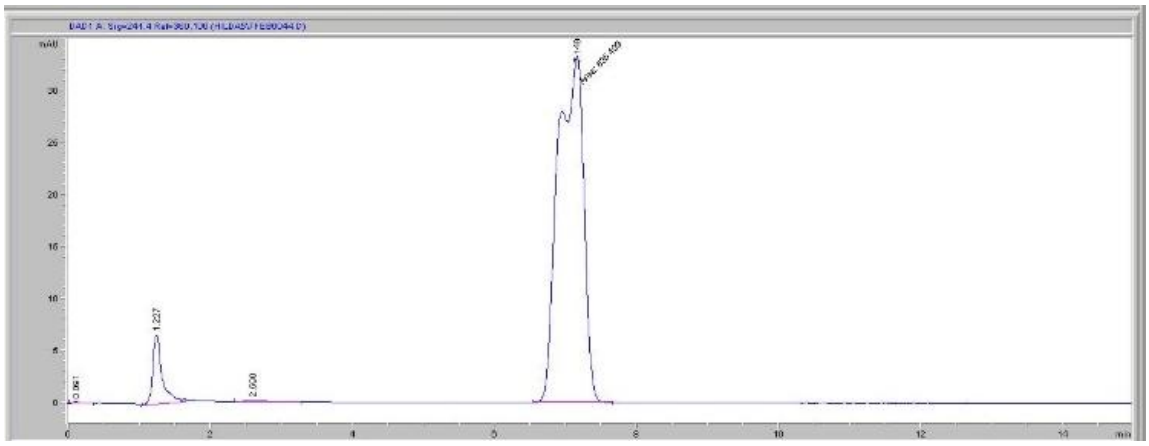

Figure 19. Chromatogram of testosterone (major peak) after acid hydrolysis treatment for 24 hours. The peak to the left is assigned to the acid.

Base hydrolysis

The results showed a slight decrease in drug peak concentration compared to the theoretical concentration, as displayed in table XV, however not distinguishable enough to draw a conclusion. The drug peak was distorted, as can be seen in figure 20, but again seemed to be pure according to peak purity scan (figure 21) which looks identical to figure 18.

Table XV. Average concentration recovered after base hydrolysis

Time (h)	Average concentration (µg/ml)	Standard deviation	Relative standard deviation %	Theoretical concentration (µg/ml)	Replicates
3	28.2	0.2	0.7	32.0	n=4
24	29.0	0.2	0.5	32.8	n=4

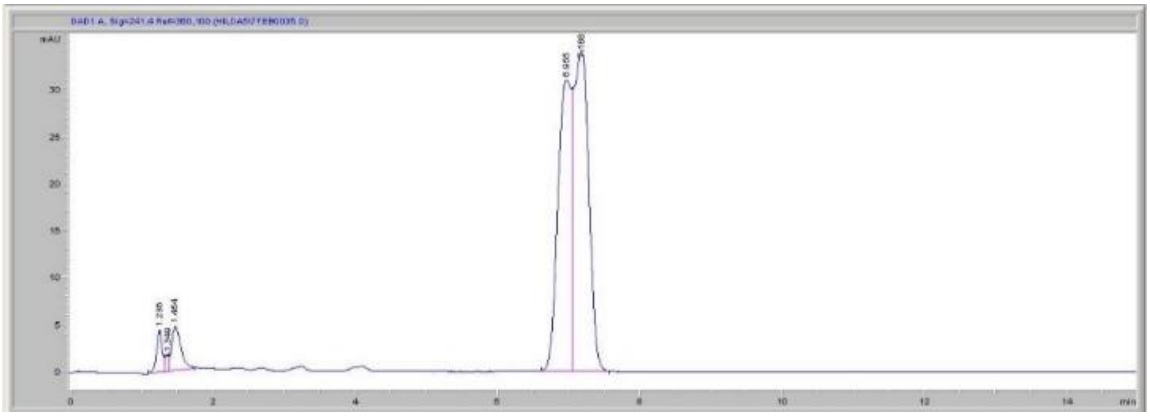

Figure 20. Chromatogram of testosterone drug peak (major peak) after 24 hours of base hydrolysis treatment. The double peak in the beginning of the spectra is assigned to the base.

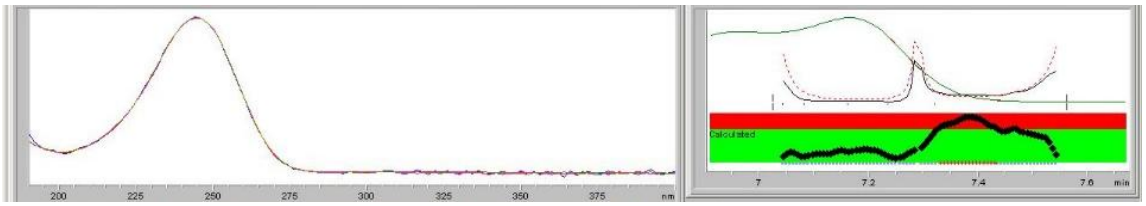

Figure 21. Purity scan of testosterone peak after exposure in alkaline conditions.

Forced degradation studies 84 – 108 hours

Because there was no clear decrease or degradation peak detected in the first set of experiments, a second set of experiments with longer exposure time were performed.

Ambient temperature control

No significant decrease was measured after 84 hours, as shown in table XVI.

Table XVI. Average testosterone concentration recovered after ambient lab temperature exposure

Time (h)	Average concentration (µg/ml)	Standard deviation	Relative standard deviation %	Replicates
24	96.5	1.6	1.6	n=4
36	95.7	1.9	2.0	n=4
48	98.8	2.8	2.8	n=4
60	97.5	1.4	1.4	n=4
84	100.7	3.5	3.5	n=5

Ambient light degradation

No significant decrease was measured after 72 hours, as seen in table XVII.

Table XVII. Average concentration recovered after ambient light exposure

Time (h)	Average concentration (µg/ml)	Standard deviation	Relative standard deviation %	Replicates
24	99.9	3.2	3.2	n=4
36	99.3	2.2	2.3	n=4
48	100.1	3.8	3.8	n=4
60	102.0	1.9	1.9	n=4
72	100.2	4.6	4.6	n=4

70 °C heat degradation

No significant decrease in concentration was measured after 84 hours exposure to heat, as seen in table XVIII.

Table XVIII. Average concentration recovered after 70 °C heat

Time (h)	Average concentration (µg/ml)	Standard deviation	Relative standard deviation %	Replicates
24	98.9	5.4	5.5	n=4
36	103.8	8.0	7.7	n=4
48	99.7	4.1	4.1	n=4
60	108.8	12.7	11.6	n=4
72	105.8	10.9	10.3	n=4
84	103.6	4.7	4.6	n=5

Oxidation degradation

Even after 84 hours exposure of testosterone to oxidation product, no significant decrease in the drug concentration recovered was measured, as shown in table XIX. Similarly to the previous experiment, the drug peak was distorted, but the peak area corresponded well to expected concentration.

Table XIX. Average concentration recovered after oxidation

Time (h)	Average concentration (µg/ml)	Standard deviation	Relative standard deviation %	Replicates
12	94.7	0.9	0.9	n=4
24	95.9	1.7	1.8	n=4
36	96.1	1.1	1.1	n=4
48	95.2	1.4	1.4	n=4
60	97.3	1.2	1.2	n=4
72	96.0	1.0	1.0	n=4
84	96.1	1.2	1.2	n=6

Acid hydrolysis

After exposure of testosterone to acidic treatment for 108 hours, no clear decrease was measured in the drug concentration. Further, no additional peaks were detected. As seen in table XX, the average concentration recovered was lower than what the theoretical concentration was calculated to be, however, the average concentration recovered was consistent during the whole experiment.

Table XX. Average testosterone concentration recovered after acid hydrolysis

Time (h)	Average concentration (µg/ml)	Standard deviation	Relative standard deviation %	Theoretical concentration (µg/ml)	Replicates
12	24.2	0.7	2.8	27.2	n=4
24	24.9	0.6	2.4	28.4	n=4
48	25.0	0.4	1.6	27.6	n=4
60	24.7	0.5	2.0	27.6	n=4
72	25.4	1.1	4.3	27.6	n=4
84	24.6	1.7	6.8	27.4	n=4
96	25.0	0.4	1.8	27.6	n=4
108	24.2	0.2	0.7	27.6	n=4

*36 h is not shown in the table because at time point t=36 h, 1M NaOH was mistaken for 0.1M NaOH, thus less was required to neutralise the sample. The average concentration recovered was 63.32 µg/ml and the theoretical concentration was 66.67 µg/ml.

Base hydrolysis

Small peaks were detected at the beginning of the chromatogram, the area of the solvent double peak did increase after a longer exposure time, and the smaller peaks increased as well, albeit not very much. This is shown in figures 22, 23 and 24, where comparing figures 22 and 23 it is seen that the solvent front peak is increasing. Figure 24 shows an expansion of figure 23, to denote more clearly the rise of smaller peaks detected before the testosterone peak. The average concentration recovered of the drug peak was seen to decrease with time, as shown in table XXI. This is more clearly seen in figure 25 which shows the decrease of the drug concentration over time.

Table XXI. Average testosterone concentration recovered after base hydrolysis

Time (h)	Average concentration (µg/ml)	Standard deviation	Relative standard deviation %	Theoretical concentration (µg/ml)	Replicates
24	28.3	0.8	2.7	33.3	n=4
36	27.5	0.6	2.2	33.3	n=4
48	26.0	0.3	1.2	33.3	n=4
60	26.1	1.0	4.0	33.3	n=4
72	25.4	0.9	3.7	33.3	n=4
84	23.9	0.4	1.6	33.3	n=4
96	23.0	0.3	1.3	33.3	n=4
108	21.6	0.1	0.5	33.3	n=4

*At 12 h, the average concentration was 23.66 µg/ml (theoretical concentration 28.37 µg/ml)

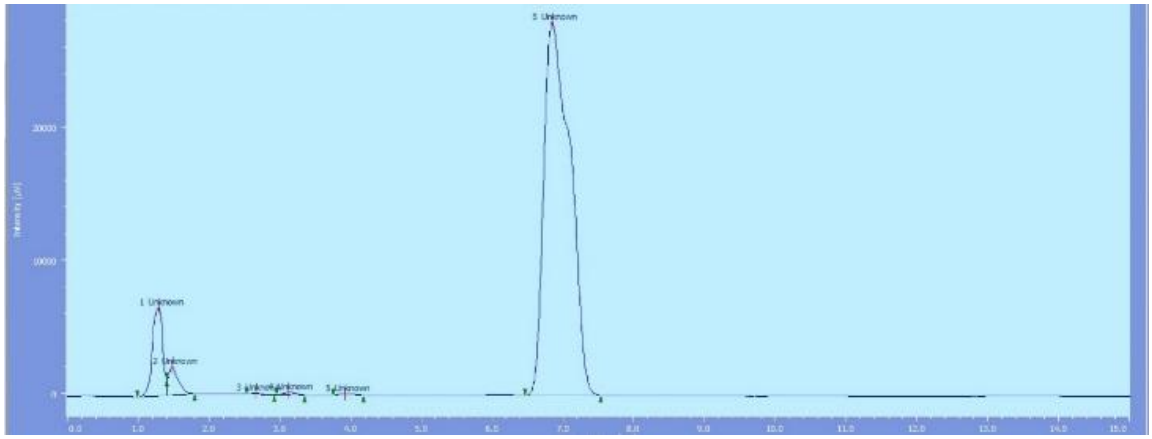

Figure 22. Chromatogram of testosterone in 1 M NaOH after 12 h. Solvent front has a double peak and the minor peaks detected are not seen in blank. The sample was diluted ten times.

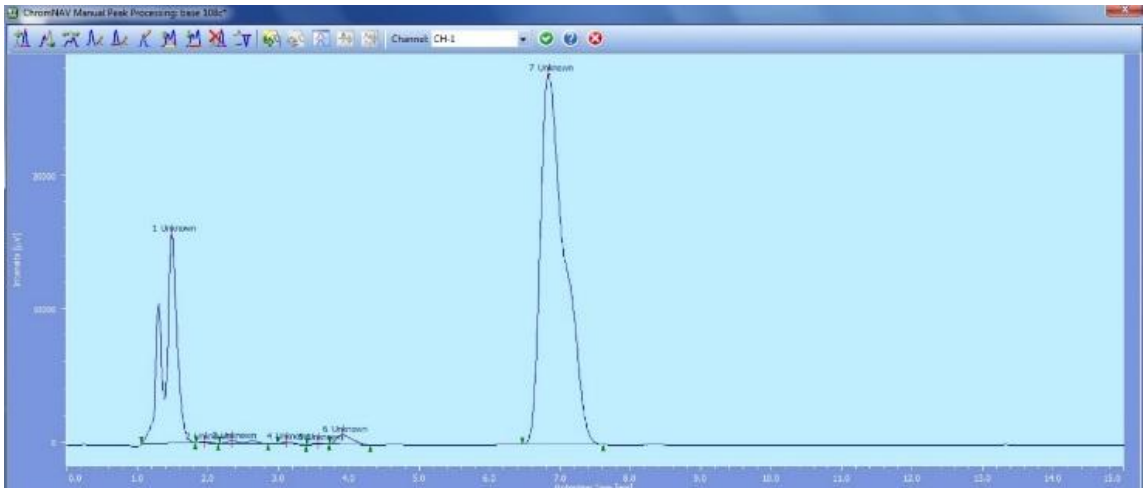

Figure 23. Chromatogram of testosterone in 1 M NaOH after 108 h. The area of solvent front (especially peak to the right) and minor peaks are increasing, the drug peak area is decreasing

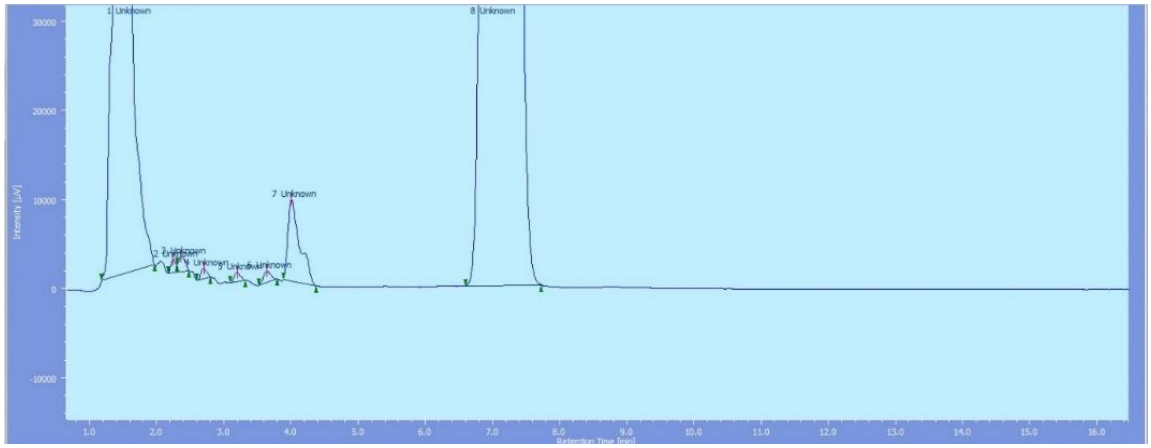

Figure 24. Expansion of figure 23, showing solvent front to the far left and the testosterone peak to the far right.

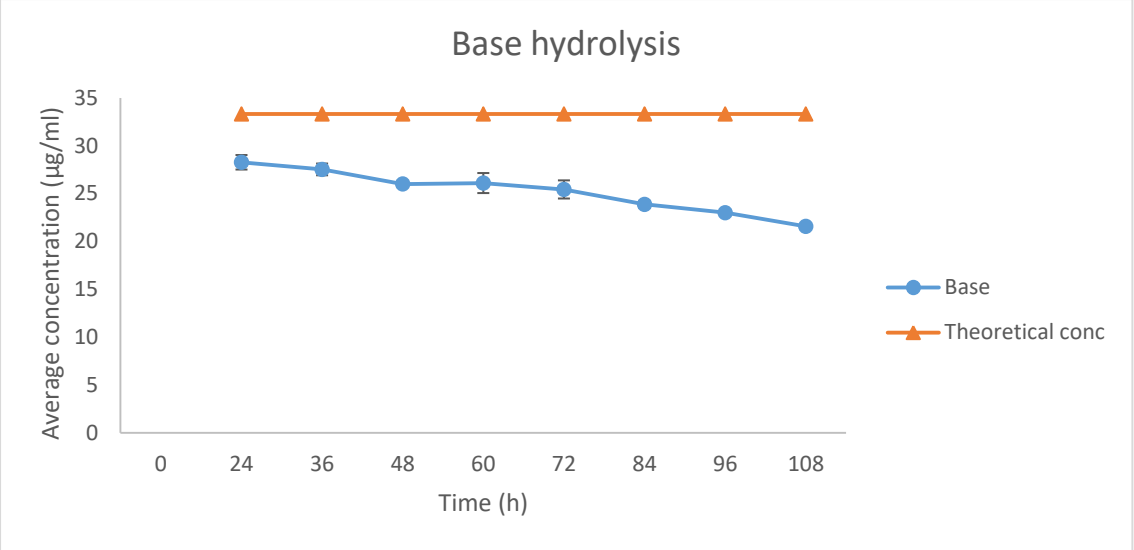

Figure 25. A graph depicting average testosterone concentration recovered as a function of with time after alkaline hydrolysis.

Part II. Solubility studies

The solubility of testosterone was measured in a range of different solvents and excipients, shown previously in table IX. Initially the solubility was measured after 24 hours incubation however due to high variability for several solvents, it was decided to repeat the experiments at 72 hours exposure time.

For some solvents, as indicated earlier, where the difference in solubility data for 24 hours and 72 hours did not show a significant difference according to t-test, $p>0.05$, these are grouped together (A) If there was a significant difference between the two data sets, the data from 72 hours data are reported (B). The data are reported ranked from lowest to the highest average solubility, as shown in table XXII.

Table XXII. Table overview of the average solubility of testosterone in all solvents used, ranked from lowest to highest.

Solvent	Average solubility (mg/ml)	Standard deviation	Relative standard deviation %	Replicates
Water[b]	0.0153	0.0019	12.4	4
Glycerol[b]	1.6	0.37	23	8
Limonene[b]	5.44	0.32	5.9	4
Isopropyl palmitate [a]	*6.38_c*[*] 6.57	*0.72* 0.38	*11.3* 5.8	*9* 8
Isopropyl myristate [a]	7.46	0.67	9	9
Eucalyptus[a]	26.1	2.1	8	9
Polyethylene glycol 400[a]	29.4	1.4	4.9	4
Propylene glycol [b]	78.3	19	24.2	8
Transcutol[b]	94.3	1.0	1.1	4
Arlasolve DMI[a]	93.5	5.8	6.2	9
Dipropylene glycol[b]	110.3	16.1	14.6	11
Isopropyl alcohol [a]	109.8	11.5	10.5	9
Ethanol [a]	161.9	11.3	7.0	9
Phenoxyethanol[a]	414.7	102.7	24.8	9
Benzyl alcohol[b]	595.5	30.2	5.1	4

A. 24-72 hours grouped together
B. 72 hours
$_c$ = Significant outlier found

Part III. Stability test

Stability of testosterone in 15 solvents/excipients (see full list in solubility experiments) stored in temperatures 25 °C, 40 °C and 50 °C for 2-4 weeks was measured

Even after four weeks of different temperature treatments, testosterone showed no sign of degradation in all the solvents. Table XXIII, shows the average concentration recovered for each solvent at different time points and temperatures.

Figures 26 and 27 show the mean concentration recovered for all solvents at the different time points and at the different temperatures. Graphs for water, glycerol and eucalyptus are shown separately in figures 28 and 31 due to the case that it was not possible to fully extract testosterone from these solvents (probably due to low solubility of the drug in the first two solvents, and possibly due to immiscibility in the latter). However the concentration recovered, did not change for either of the three solvents during the time points.

The reason for the high error bars regarding testosterone stability in PEG400 in figure 27 is probably due to a weighing error already at t=0, because the size of the error bars did not change, noticeably between the time points.

The weight error was taken into account in figures 29 and 30, which shows the percentage recovery, instead of only concentration recovered, with respect to percentage recovered of t=0 control *i.e.* (concentration recovered/theoretical concentration divided by concentration$_{t=0}$ recovered/theoretical concentration$_{t=0}$). Drug measured in limonene and glycerol fall below 90 % recovery after four weeks, while in all other solvents the concentration recovered did not change noticeably.

Table XXIII. Table over average testosterone concentration (n=3, however each replicate represents a mean value of three dilutions) for different temperatures and time points for each solvent.

		Time 2 weeks	Time 4 weeks
Solvent **Time 0 weeks**	**Temperature**	**Average concentration** ± SD (RSD%) (mg/ml)	**Average concentration** ± SD (RSD%) (mg/ml)
Arlasolve DMI **Time$_{0\ weeks}$** *47.3 ± 1.4 (3.0%)*	25 °C	44.5 ± 1.9 (4.3%)	45.8 ± 2.0 (4.5%)
	40 °C	46.1 ± 1.7 (3.7%)	45.4 ± 1.5 (3.2%)
	50 °C	46.7 ± 2.1 (4.6%)	45.2 ± 2.5 (5.5%)
Benzyl alcohol (BA) **Time$_{0\ weeks}$** *44.0 ± 1.7 (4.0%)*	25 °C	43.6 ± 1.5 (3.4%)	42.7 ± 2.0 (4.8%)
	40 °C	43.4 ± 1.2 (2.8%)	43.1 ± 1.8 (4.2%)
	50 °C	43.8 ± 1.9 (4.3%)	43.5 ± 1.9 (4.3%)
Dipropylene glycol (DiPG) **Time$_{0\ weeks}$** *46.3 ± 0.5 (1.1%)*	25 °C	46.6 ± 0.5 (1.2%)	44.4 ± 0.5 (1.2%)
	40 °C	46.4 ± 0.2 (0.5%)	45.6 ± 1.0 (2.3%)
	50 °C	46.5 ± 1.2 (2.5%)	44.8 ± 0.2 (0.5%)
Ethanol (EtOH) **Time$_{0\ weeks}$** *47.0 ± 1.9 (4.0%)*	25 °C	46.9 ± 2.4 (5.2%)	45.0 ± 1.2 (2.6%)
	40 °C	45.6 ± 1.8 (3.9%)	43.8 ± 0.2 (0.5%)
	50 °C	45.2 ± 1.5 (3.3%)	46.6 ± 1.3 (2.7%)
Eucalyptus **Time$_{0\ weeks}$** *24.3 ± 1.3 (5.3%)*	25 °C	24.9 ± 1.3 (5.4%)	24.9 ± 1.9 (7.8%)
	40 °C	25.2 ± 1.2 (4.8%)	26.7 ± 0.6 (2.4%)
	50 °C	24.7 ± 1.0 (4.2%)	27.3 ± 0.1 (0.3%)
Glycerol **Time$_{0\ weeks}$** *22.8 ± 0.5 (2.2%)*	25 °C	21.2 ± 1.1 (5.1%)	20.6 ± 1.2 (5.8%)
	40 °C	18.3 ± 2.5 (13.5%)	20.2 ± 2.2 (10.8%)
	50 °C	20.1 ± 2.9 (14.4%)	18.3 ± 2.4 (13.1%)
Isopropyl alcohol (IPA) **Time$_{0\ weeks}$** *47.2 ± 0.6 (1.3%)*	25 °C	46.7 ± 1.1 (2.4%)	46.0 ± 1.2 (2.5%)
	40 °C	48.1 ± 0.9 (1.8%)	47.1 ± 2.6 (5.6%)
	50 °C	45.2 ± 1.5 (3.3%)	46.6 ± 1.3 (2.7%)
Isopropyl myristate (IPM) **Time$_{0\ weeks}$** *47.3 ± 2.4 (5.0%)*	25 °C	44.2 ± 2.2 (4.9%)	44.5 ± 3.7 (8.4%)
	40 °C	44.5 ± 2.8 (6.4%)	44.6 ± 2.7 (6.1%)
	50 °C	44.6 ± 2.8 (6.3%)	43.2 ± 2.6 (6.0%)
Isopropyl palmitate (IPP) **Time$_{0\ weeks}$** *43.0 ± 5.1 (12.0%)*	25 °C	42.6 ± 6.0 (14.1%)	41.6 ± 4.9 (11.9%)
	40 °C	41.9 ± 5.1 (12.2%)	41.8 ± 5.0 (12.0%)
	50 °C	40.8 ± 5.2 (12.8%)	41.1 ± 4.7 (11.4%)
Limonene **Time$_{0\ weeks}$** *49.8 ± 1.3 (2.5%)*	25 °C	46.9 ± 1.6 (3.4%)	44.2 ± 1.5 (3.5%)
	40 °C	48.1 ± 0.4 (0.8%)	43.6 ± 0.3 (0.6%)
	50 °C	44.6 ± 0.4 (0.9%)	44.3 ± 1.2 (2.8%)
Phenoxyethanol **Time$_{0\ weeks}$** *46.7 ± 1.3 (2.8%)*	25 °C	43.7 ± 0.4 (1.0%)	45.3 ± 0.6 (1.4%)
	40 °C	44.5 ± 1.1 (2.4%)	45.9 ± 0.6 (1.3%)
	50 °C	44.3 ± 0.6 (1.5%)	45.1 ± 0.7 (1.7%)
Polyethylene glycol 400 (PEG400) **Time$_{0\ weeks}$** *47.5 ± 10.9 (23.0%)*	25 °C	45.9 ± 10.8 (23.6%)	45.2 ± 10.5 (23.2%)
	40 °C	46.6 ± 9.9 (21.2%)	45.2 ± 9.7 (21.5%)
	50 °C	45.9 ± 9.8 (21.3%)	44.7 ± 9.7 (21.7%)
Propylene glycol (PG) **Time$_{0\ weeks}$** *45.3 ± 0.9 (1.9%)*	25 °C	43.0 ± 0.5 (1.2%)	44.3 ± 1.7 (3.9%)
	40 °C	43.4 ± 0.5 (1.2%)	44.1 ± 0.5 (1.0%)
	50 °C	43.2 ± 0.6 (1.4%)	44.6 ± 0.1 (0.2%)
Transcutol **Time$_{0\ weeks}$** *45.1 ± 0.8 (1.8%)*	25 °C	44.3 ± 2.1 (4.8%)	43.5 ± 1.3 (2.9%)
	40 °C	44.2 ± 1.0 (2.2%)	44.3 ± 1.1 (2.5%)
	50 °C	44.0 ± 0.9 (2.1%)	43.5 ± 1.1 (2.4%)
Water **Time$_{0\ weeks}$** *1.02 ± 0.01 (1.09%)*	25 °C	1.11 ± 0.05 (4.6%)	1.11 ± 0.05 (4.5%)
	40 °C	1.14 ± 0.11 (9.6%)	1.17 ± 0.11 (9.2%)
	50 °C	1.13 ± 0.09 (7.8%)	1.11 ± 0.08 (7.2%)

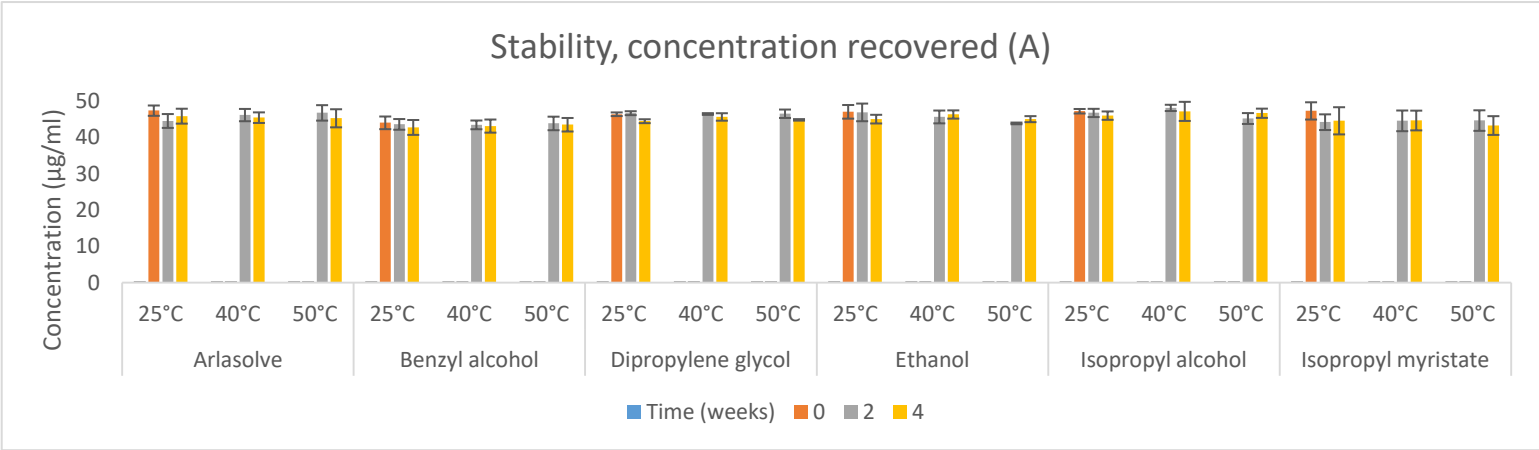

Figure 26. Stability of testosterone in assessed solvents, showing how the concentration at each temperature change over time (two and four weeks).

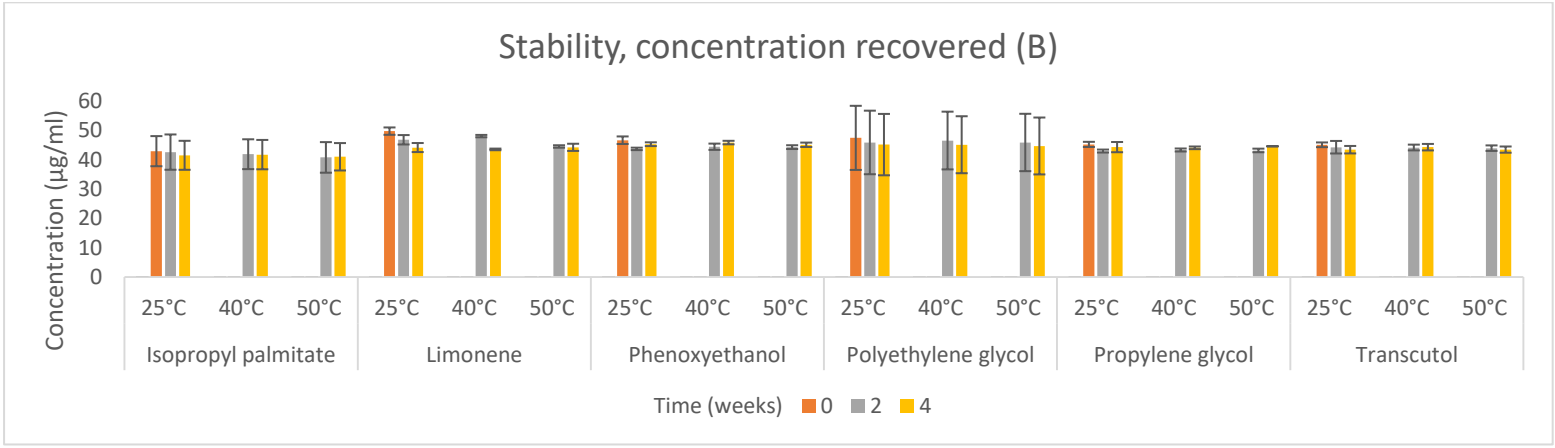

Figure 27. Stability of testosterone in assessed solvents, showing how the concentration at each temperature change over time (two and four weeks).

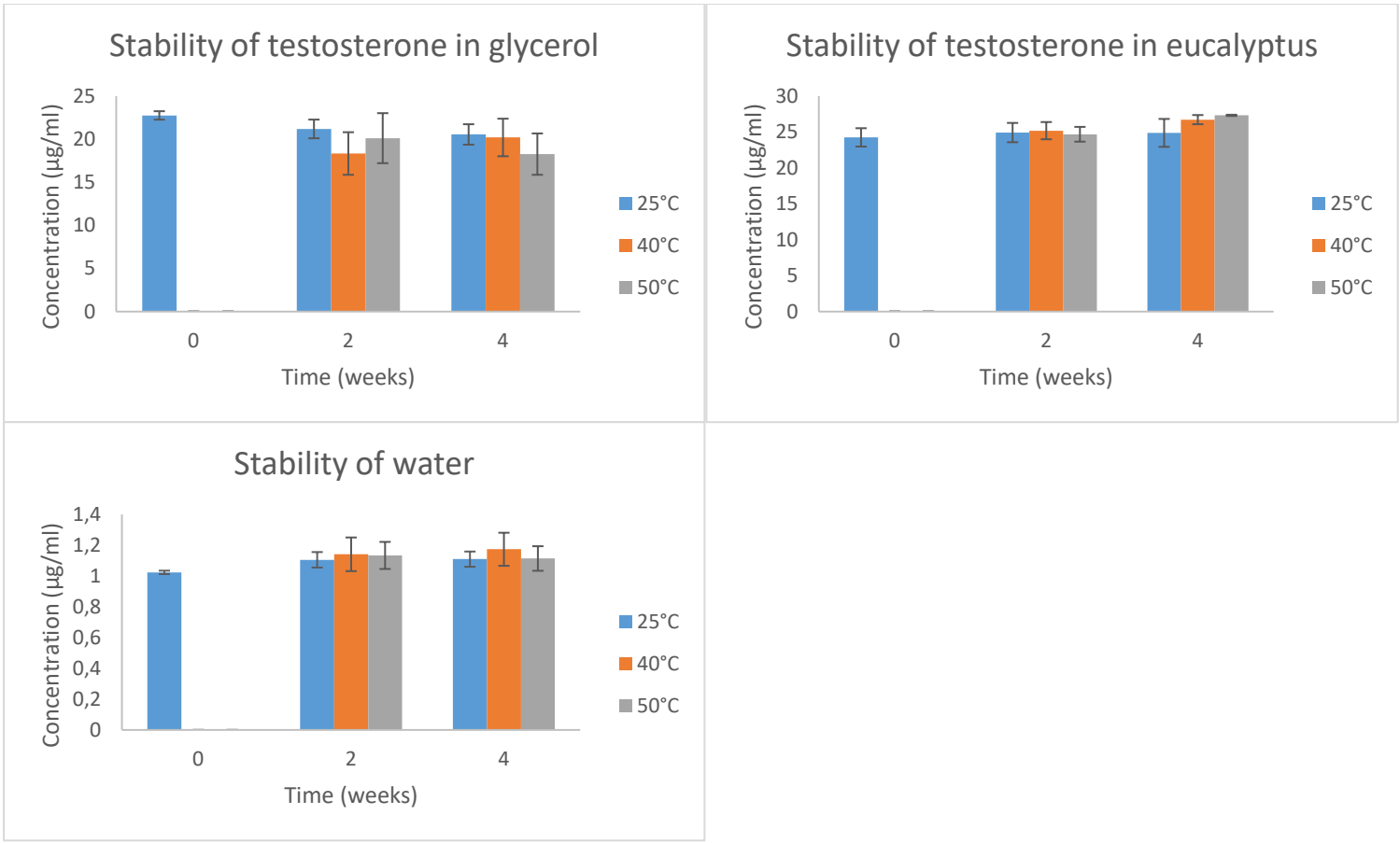

Figure 28. Testosterone stability in glycerol, eucalyptus and water at 25 °C, 40 °C and 50 °C after four weeks' time.

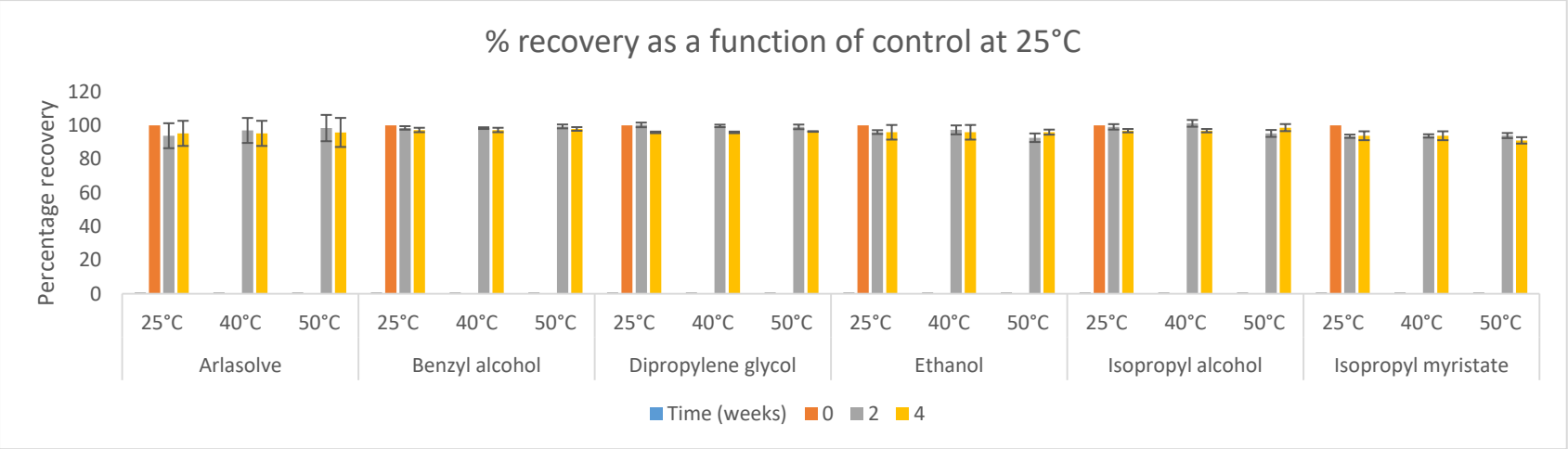

Figure 29. Stability of testosterone in assessed solvents, with % recovery (concentration recovered/theoretical concentration) shown as percentage recovery with respect to t=0.

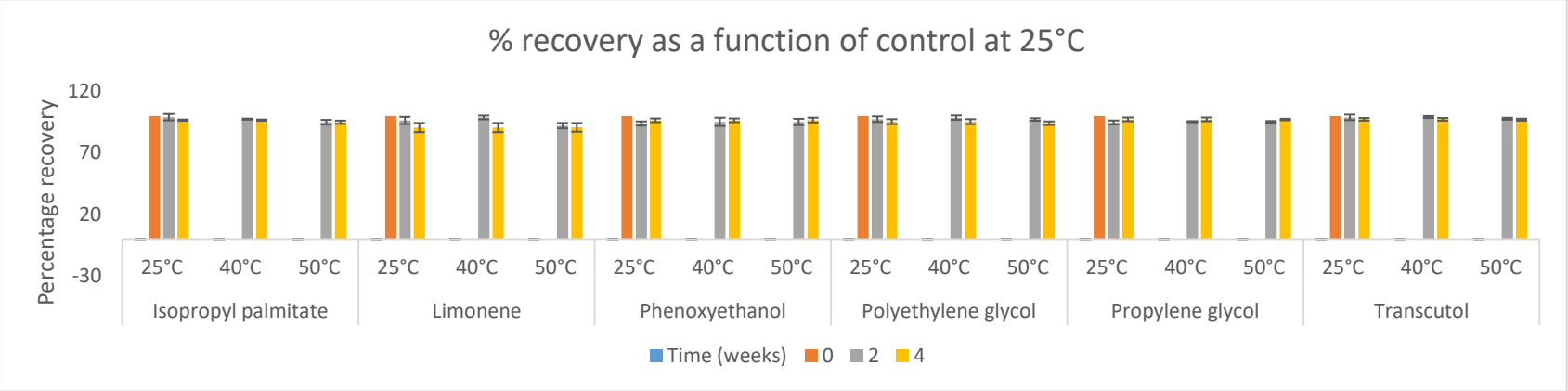

Figure 30. Stability of testosterone in assessed solvents, with % recovery (from concentration/theoretical concentration) shown as percentage recovery with respect to t=0.

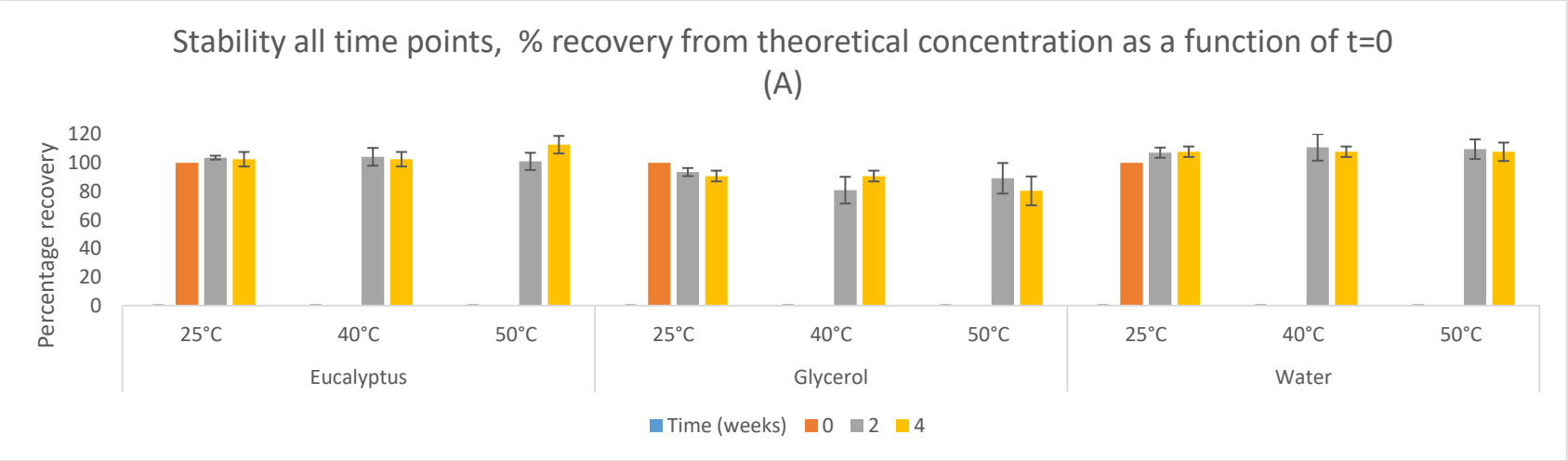

Figure 31. Stability of testosterone in solvents eucalyptus, glycerol and water, with % recovery (from concentration/theoretical concentration) shown with respect to t=0.

Discussion

The two testosterone formulations used during skin diffusion experiments had a fairly long (minimum one and a half year) shelf life, which suggest a reasonably high stability. The solubility of the drug has been measured in a few solvents, the most common are water and ethanol. While testosterone is soluble in ethanol (161.9 ± 11.3 mg/ml), the solubility in water is low (0.0153 ± 0.0019 mg/ml). Water is a commonly used solvent in pharmaceutical formulations (Chang *et al.*, 2013). For hydrophobic drugs, such as testosterone, water is more of a problem as the high solubility of testosterone in for example ethanol rapidly decreases when water is added. Drug formulation must be able to hold a sufficient amount of drug while still be able to deliver the drug. Additionally, the excipients and solvents must not interact with each other, the drug or alter the skin permanently, but nonetheless give a satisfactory drug delivery while remaining cosmetically acceptable and elegant.

It was expected that testosterone would be fairly stable during all conditions, which is also why the stability study was carried out for a longer period of time rather than say, 24 hours.

During these experiments testosterone showed no remarkable change under stressed conditions, although there were changes observed in the shape of the drug peak, no degradation products were detected, except under alkaline conditions. This is in agreement with previous work (Vulliet *et al.*, 2010) who concluded that testosterone seems to be very stable in acidic and neutral conditions, less stable in alkaline conditions. There has also been work undertaken on accelerated stability studies under simulated tropical conditions (higher temperature and 100% humidity) on testosterone enantate and testosterone propionate amongst other drugs, where it was concluded that these two were resistant to degradation under these conditions (World Health Organization (WHO), 1986).

There are not many articles about testosterone and stability/degradation. Those that exist are about biodegradation and microbial transformation. There has also been some work in assessing the stability of testosterone in freeze-thaw cycles. It was concluded that micronutrients and hormone (testosterone being one of the tested substances) serum concentration in plasma were not affected by freezing to -70 °C and thawing cycles (Comstock *et al.*, 2001).

The peak area of minor peaks and solvent front in base hydrolysis increases with time, if there are degradation peaks, they elute earlier than testosterone.

Leaving samples for solubility studies for a longer time (72 hours) did increase the solubility and decreased relative standard deviation data. This has also been mentioned in previous work where the authors were examining the effect of vehicles on estradiol permeation through skin (Møllgaard and Hoelgaard, 1983). Although it was mentioned in the article that 72 hours should be sufficient for

equilibrium to be reached even in viscous samples, there was, in this set of data, a larger variability seen in the solubility of testosterone in viscous samples such as PG and glycerol.

Stability data indicates no significant change of testosterone after four weeks, in the temperature range investigated for all solvents assayed. Testosterone in limonene, and glycerol showed a recovery below 90 % after four weeks.

Conclusions

After 84 and 108 hours, there was no clear decrease in the drug concentration, change in peak shape or any changes elsewhere in the chromatograms seen for ambient temperature, light and 70 °C heat experiments.

Under oxidation, acid hydrolysis and base hydrolysis, changes in the peak shape were observed. Despite these changes, there were no evidence for testosterone degradation except under alkaline conditions.

For all solubility studies, and especially those that are performed in more viscous solvents such as PG and glycerol, measuring solubility for a longer time (72 hours) is more beneficial as it is sufficient for equilibrium to be reached.

Testosterone is, regardless of time and temperature, chemically stable in the fifteen solvents assayed.

Chapter 4

CHARACTERISATION OF TESTOSTERONE USING NMR SPECTROSCOPY

Background

Testosterone has physicochemical properties that are suitable for transdermal delivery. A range of experiments attempted to characterise the lateral distribution and the main diffusion route of testosterone on skin with the help of Raman spectroscopy, a technique that is complementary to IR but has the advantage that it is insensitive to water and that it is possible to investigate drug distribution over a surface.

Even though testosterone on a glass slide was easily detected by Raman, this was not the case when applied on the skin, as skin's complex composition of lipids and amides obscured the testosterone peaks. To circumvent this problem it was decided to try to label testosterone with deuterium.

Labelling testosterone with deuterium has been undertaken in studies of testosterone metabolism, and CYP3A4 metabolising activity (Atzrodt *et al.*, 2012; Furuta *et al.*, 2003). Hydrogen to deuterium exchange can be a long and expensive procedure; however methods have evolved over time, going from low yielding multi-step synthesis to making the exchange directly on the target molecule. Some problems remain such as low incorporation yield or decomposition of the compound due to extreme reaction conditions. (Atzrodt *et al.*, 2012)

As testosterone can undergo keto-enol tautomerism it was hoped that under the right conditions it would be more reactive to the deuterium incorporation, resulting in a straightforward and simple one step synthesis. The proposed overall synthesis pathway of deuterium incorporation of testosterone is shown in figure 32.

Previous reports have shown deuterium incorporation of testosterone at positions 2, 4 and 6 (Wähälä *et al.*, 1995; Atzrodt *et al.*, 2012; Furuta *et al.*, 2003). The opposite reaction, where hydrogen exchanges back into testosterone that has been deuterated at positions 2,4 and 6 has also been described (Furuta *et al.*, 2003). In one example epi-testosterone is used for the starting material (and the product is also epi-testosterone) (Wähälä *et al.*, 1995). The method of Atzrodt *et al., 2012* simplifies the deuterium exchange route, but still requires multiple steps.

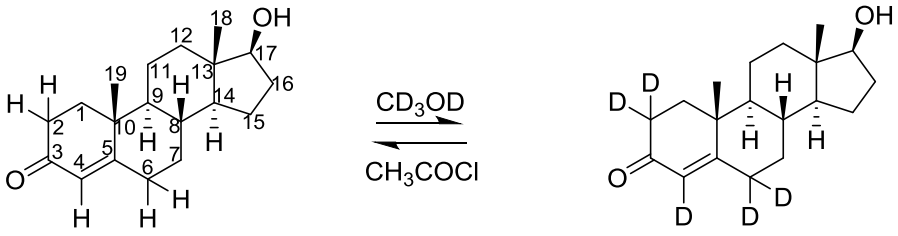

Figure 32. Overall synthesis of [2,2,4,6,6-D_5] testosterone.

Material and method

Chemicals and reagents

Chemicals were obtained from Sigma-Aldrich, Goss scientific and VWR and used without further purification, unless otherwise indicated

Goss scientific

Methanol-D4 (D99.8%) + 0.05% V/V TMS, methanol-D (D99%)

Sigma-Aldrich

Acetyl chloride 98 %, chloroform-d, ethyl acetate, poly(ethylene)glycol (average Mn 400), testosterone

VWR

Ethanol, methanol, n-hexane

Part I

SYNTHESIS AND CHARACTERISATION OF [2,2,4,6,6-D_5] TESTOSTERONE

A one step reaction

Synthesis reaction mechanism

Figures 33 and 36 show the full reaction mechanism for deuterium incorporation on positions 2 and 6 during acidic conditions. The reaction mechanism for deuterium incorporation on position 4 is not entirely straightforward, and thus two possible reaction pathways are possible, shown by figures 34 and 35.

Deuterium incorporation on position 2

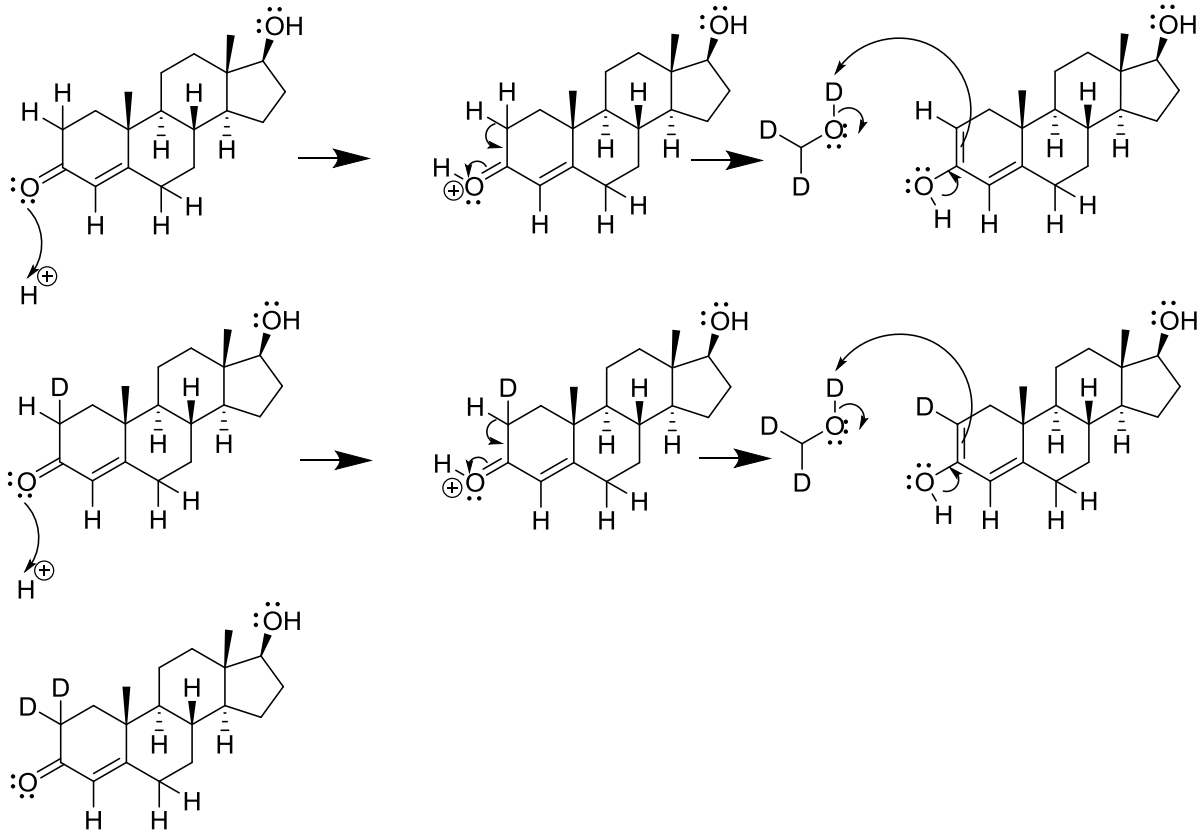

Figure 33. Reaction mechanism for deuterium incorporation on position 2.

Deuterium incorporation on position 4

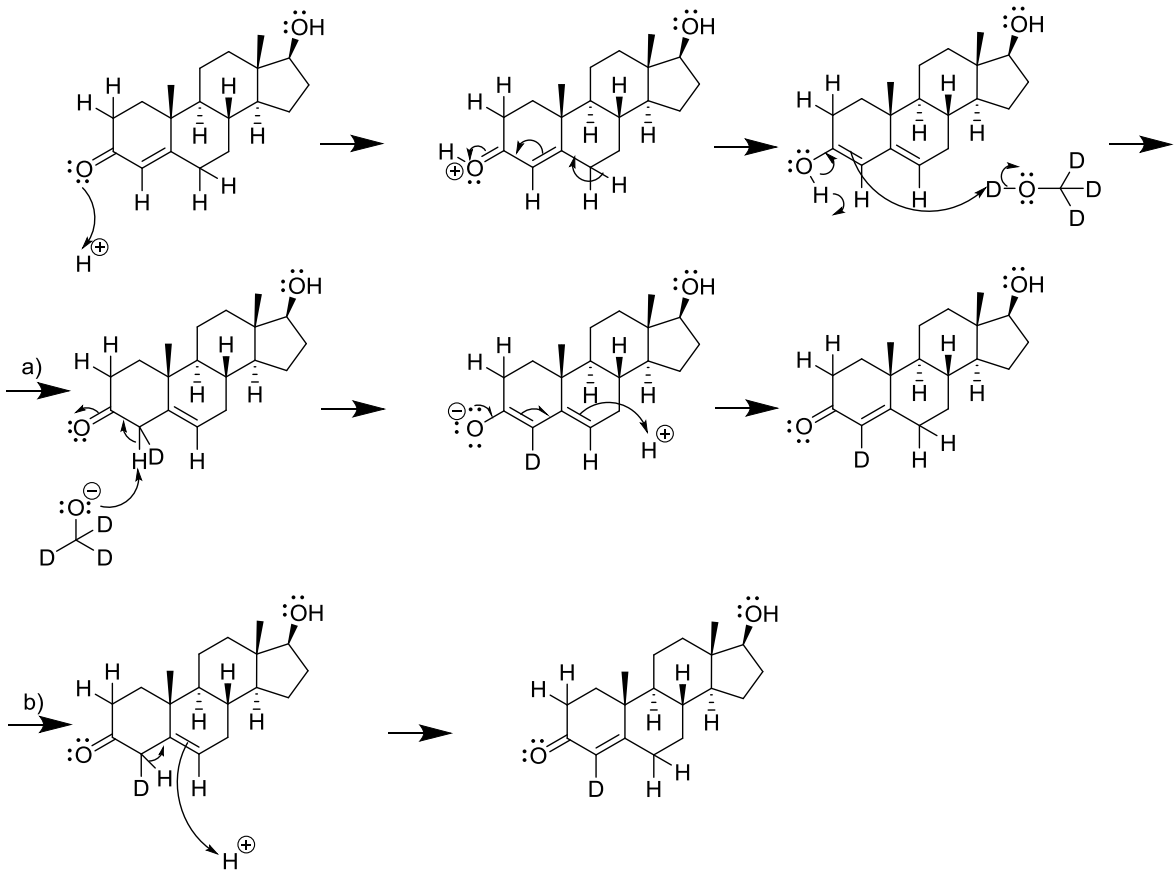

Figure 34. First theory about reaction mechanism for deuterium incorporation on position 4 on testosterone with two possible finishing pathways (a and b).

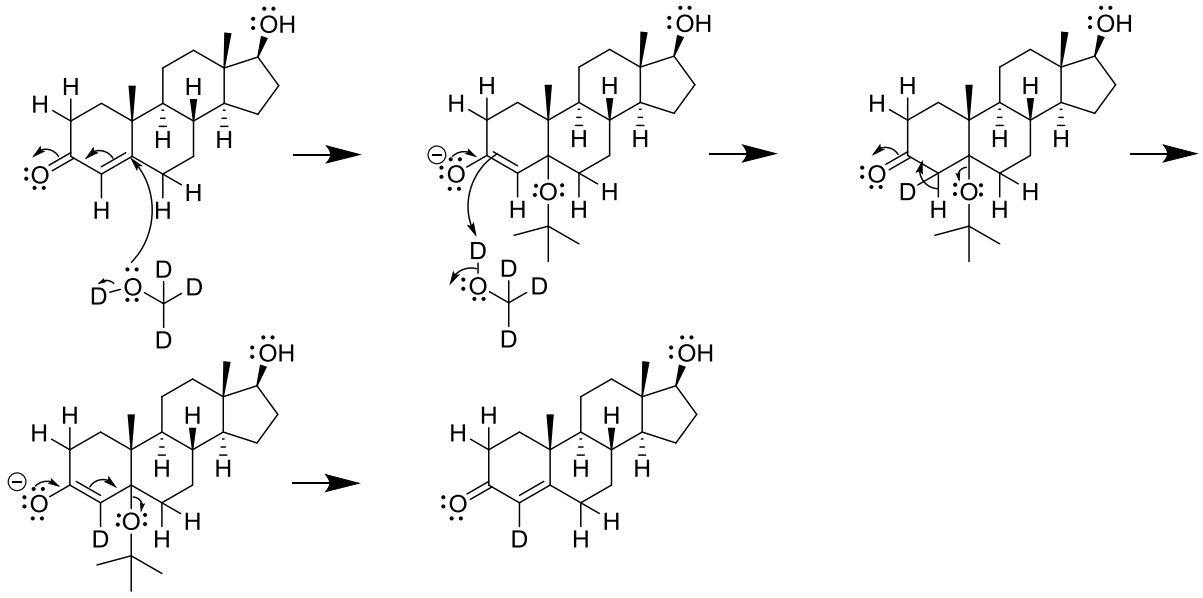

Figure 35. Second theory about reaction mechanism for deuterium incorporation position 4 on testosterone.

Deuterium incorporation on position 6

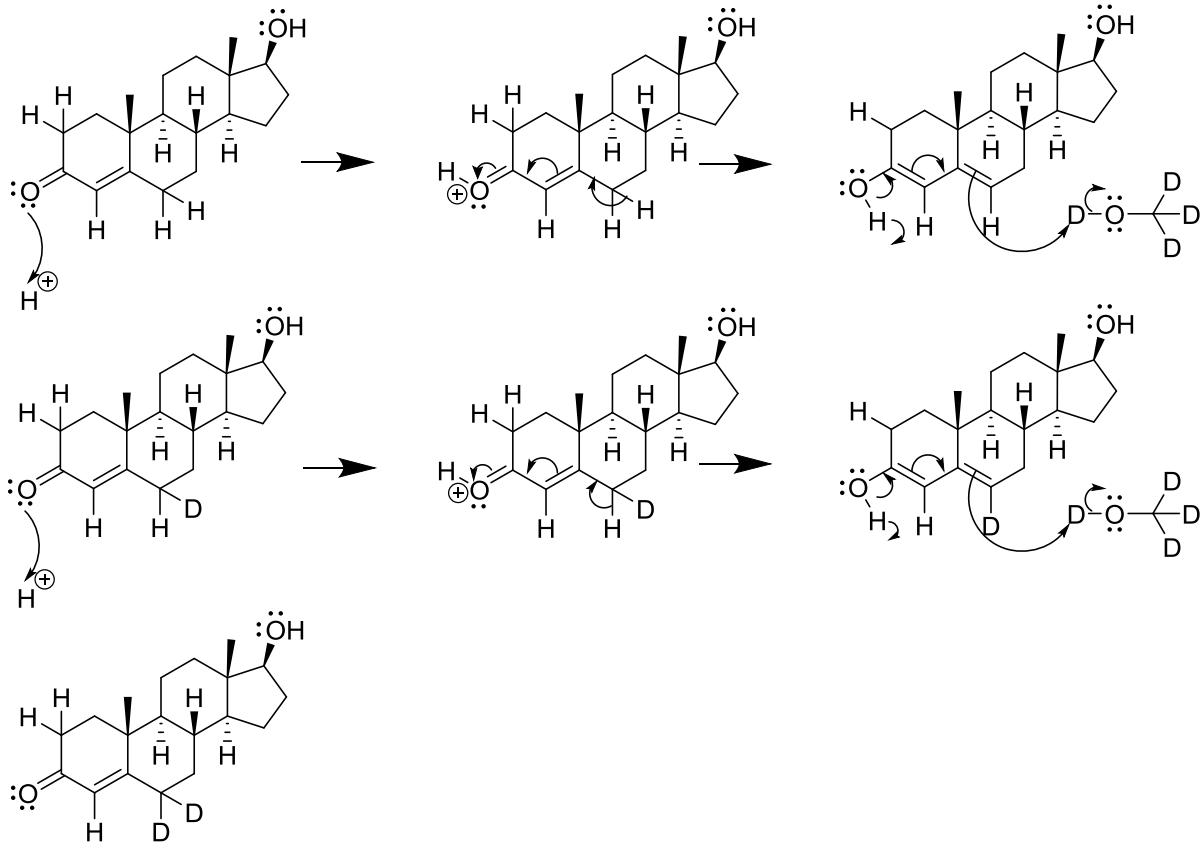

Figure 36. Reaction mechanism for deuterium incorporation on position 6 on testosterone.

Experimental methodology

Preliminary synthesis reaction

Deuterium incorporation and NMR

Testosterone (~10 mg, 0.035 mmol,) was weighed into each of two vials. Deuterated methanol (CD_3OD) (0.6 ml) was added to both vials. One vial served as a control, the other vial had an acid catalyst (acetyl chloride (~25 µl)) added to it. The contents were analysed by ^{1}H NMR and then heated to 37 °C in a waterbath for 21 hours.

The volatiles were evaporated *in vacuo* and CD_3OD (~1 ml) was added. The samples was analysed by ^{1}H and ^{13}C, including 2D experiments (HSQC, COSY, HMBC). For the deuterated product, an additional ^{2}H NMR spectrum was recorded.

The solvent was again evaporated *in vacuo* and MeOH (~1 ml) was added to the round bottom flasks before another analysis with ^{2}H NMR.

NMR analysis was provided by the Chemical Characterisation and Analysis Facility (CCAF) at the University of Bath. NMR spectra were recorded using a Bruker Avance III NMR spectrometer operating at 500.13 MHz for ^{1}H. Unless otherwise specified samples were analysed using CD_3OD at 25 °C using standard Bruker pulse sequences (Topspin 2.1), parameter settings (pulse sequence zg30, time domain (TD) 65536 points, 16 transients, spectral width (SW) 20.66 ppm and acquisition time 3.17 s).

Spectra were referenced using the residual solvent signal, at 3.31 ppm for ^{1}H and 49.00 ppm for ^{13}C. ^{2}H spectra were acquired in proteo-methanol, with a residue of CD_3OD (following evaporation of the sample from CD_3OD).

Further characterisation of the product was performed using IR-spectroscopy and MS-spectrometry.

Infrared spectroscopy

The content, less than 0.5 ml, of each sample that was left in the NMR tubes (after the overnight experiment) were transferred to two vials (10 ml). The vials were left open to let the solvent evaporate and the remaining content was dissolved in dichloromethane (~ 0.5 ml) the solution was transferred to a NaCl disc and left to dry before analysis. IR spectra were obtained on a Perkin-Elmer 782 infra- red spectrometer.

Mass spectrometry

Mass spectrometry was carried out on an ESI-MS, micrOTOF from Bruker Daltronics, the samples were then run in both positive and negative ion mode.

Raman spectroscopy

A drop of the deuterated testosterone solution was placed on a silica wafer and left to evaporate in ambient lab conditions. Raman experiments were performed with an inVia Raman Microscope (Renishaw) and a 50x short objective. The laser at excitation wavelength at 532nm gave strong fluorescing peaks and therefore it was decided to mainly use an excitation wavelength of 785 nm instead. A few milligrams of pure testosterone was put on the glass slide, the spectra from this served as a reference. A drop of the control solution was also placed on a glass slide and allowed to evaporate before analysis.

Large scale synthesis

Testosterone (230.2 mg, 0.80 mmol) was transferred to a round bottom flask (50 ml). Deuterated methanol (CH_3OD) (15 ml) and acetyl chloride (0.5 ml) were added to the flask. A colour change to pale yellow was seen immediately. Over several hours, the colour changed to bright orange and finally to deep red. The reaction was left to stir overnight.

The reaction was monitored by evaporating one millilitre of the solution *in vacuo* and subsequent NMR analysis in CD_3OD (1 ml). Based on the level of deuteration observed in the ^1H spectrum, it was decided to leave the reaction stirring for a further ~3 hours, after which the volatiles were evaporated *in vacuo*. The product was obtained as a pale yellow crystalline compound

Recrystallisation

Several co-solvent systems were assessed for the purification of testosterone, where the combination of ethyl acetate and hexane gave the best results. Ethyl acetate (~ few ml) was heated to 40 °C and minimal amount of this solvent required to dissolve the solid was used. Then slowly, hexane was added dropwise until needle-like crystals started to form, after which the solvent system was left for about an hour to cool, 15 minutes on ice cooling, before pipetting the excess solvent and vacuum filtering the solution. The recovery was ~75 %

The above mentioned procedure was followed for the deuterated compound, however after several non-successful attempts at crystallising the product (no needle crystals were seen, but small micro

crystals instead), it was decided to vacuum filter the solution without pipetting the excess solvent beforehand. The recovery yield was ~5 %.

Raman spectroscopy

Raman measurements were performed by placing a few grains of the recrystallisation product, the deuterated compound left in the reaction flask and the recrystallised testosterone on a glass slide. Both the green (532 nm) and the red (785 nm) lasers were used together with a 50x long objective, between 1-10 % of laser power was used with between 5-10 accumulation scans.

Part II

IN-EXCHANGE AND BACK-EXCHANGE OF [2,2,4,6,6-D_5] TESTOSTERONE

Background

The preliminary synthetic reaction was monitored with NMR and showed that deuterium was incorporated within 20 minutes. In order to determine how fast and at which positions the deuterium was incorporated a series of NMR spectra were acquired during the incorporation reaction.

As the deuterated testosterone was destined to be used in skin diffusion experiments assessed with Raman spectroscopy, it was necessary to determine the stability of the product in appropriate conditions. The difference in this deuterated product and normal testosterone was not of such a magnitude that HPLC could distinguish between them, hence NMR was used to monitor back-exchange of deuterium to hydrogen.

NMR customarily uses deuterated solvents to avoid the presence of large solvent peaks. However biological studies of protein and DNA tend to use aqueous solutions on a regular basis with up to 90% H_2O, and consequently a considerable effort has been made by the NMR community to overcome the problem of large solvent peaks that can shield the peaks of interest. There are many methods available for this, all with strengths and weaknesses. In this study two methods were employed – presaturation of the solvent signal and secondly, use of a diffusion step in the pulse sequence to reduce the size of the (faster moving) solvent signals.

The two application methods are different in that, where presaturation experiments aim to diminish the solvent peak by applying a weak irradiation at the solvent frequency before the acquisition scan, diffusion uses the difference in diffusion properties of species in solution. For diffusion the faster moving solvent signals becomes attenuated, while the peaks for the slower moving (larger) compound of interest becomes less attenuated and thus remains in the spectra. (Price, 2006; Brand *et al.*, 2006) Standard presaturation is very good where only one signal needs to be supressed. By contrast diffusion experiments have the advantage that a solvent with several peaks can be suppressed (Claridge, 2016).

Experimental methodology

In-exchange experiment

Approximately 10 mg testosterone was placed in an NMR tube together with ~ 1 ml CD_3OD. Spectra were recorded after adding the solvent, and again after six days. After six days, acetyl chloride (25 µl) was added to the NMR tube, and a series of spectra were recorded using preset parameters: pulse sequence zg30, TD 206610 points, 8 transients, SW 20.66 ppm and acquisition time 10 s, D1 10, spectra were referenced using the residual solvent signal, at 3.31 ppm for ^1H.

Spectra were acquired at intervals during the course of an hour.

Back-exchange and stability experiment

Overall method

In each of ten vials (25 ml), ~40 mg of deuterated testosterone were added followed by six millilitres of solvent. Table XXIV details the solvent used and the different conditions (ambient, acidic and heat) for each of the ten vials. Those vials that were exposed to heat were placed in a temperature controlled room set to 37 °C. The vials that were exposed to acidic conditions had 0.1 N HCl (1 ml) added to them, with the pH confirmed to be lower than 5.5 using pH indicator paper. The remaining vials were stored under ambient lab conditions. The stability of the product was assessed in two ways, described by Method 1 and 2 in the following sections.

Method 1. Evaporating solvents and adding deuterated chloroform

From each of the ten vials, a sample (0.6 ml) was taken out to a round bottom flask (25 ml). The solvent from each of the round bottom flasks were evaporated off and then deuterated chloroform (0.7 ml) was added to each of the flasks. The content was then transferred to NMR tubes and analysed. During a time course of two weeks, NMR samples were prepared as mentioned and analysed at t= 1, 2, 6, 10 and 16 days by ^1H NMR. Spectra were referenced using the residual solvent signal, at 7.26 ppm for ^1H)

Method 2. Analysing the tube directly without external interference

A sample (0.6 ml) was taken out from each of the vials and put into NMR tubes and analysed. The samples were then stored under appropriate conditions (for example those exposed to heat were stored in the temperature controlled room) for the duration of the stability experiment serving as a double control for stability. During a time course of two weeks, the already prepared NMR tube samples were analysed at time points: t=0, 1, 6, 9 and 15 days, using presaturation or diffusion

applications where applicable. On all MeOH and MeOD samples, presaturation were carried out (pulse sequence noesygppr1d, TD 65536 points, 64 transients, SW 20.66 ppm and acquisition time 3.17 s, D1 2, spectra were referenced using the residual solvent signal, at 3.31 ppm). Diffusion suppression was used for EtOH samples and samples in the binary formulation (PEG400 and EtOH). The standard Bruker pulse sequence ledbpgp2s1d was used (TD 103304 points, 16 transients, SW 20.66 ppm and acquisition time 5.00 s, D1 4). MeOH and MeOD spectra were referenced using the residual solvent signal, at 3.31 ppm), whilst residual solvent signal at 1.25 ppm was used for EtOH and EtOH/PEG400 samples.

Table XXIV. Table of the solvents and conditions, marked with x, used for deuterated testosterone stability experiment

Solvent	Neutral condition	pH (acidic)	Heat 37 °C
Methanol	x	x	x
Ethanol	x	x	x
Ethanol/PEG400	x	x	x
MeOD (CH_3OD)			x

Results

Part I. Synthesis and characterisation of [2,2,4,6,6-D_5] testosterone

Preliminary synthesis reaction

The preliminary synthesis was successful and the process was monitored by NMR which confirmed incorporation of deuterium at positions 2, 4 and 6. When a proton is replaced by a deuterium, the signal in the ^{1}H spectrum is lost, as ^{2}H resonates at a very different frequency. This effect is often used to probe for exchangeable protons in samples with a 'D_2O shake', where samples in organic solvents are treated with a small amount of D_2O. In this case the range of exchangeable protons in testosterone is extended by the effects discussed above.

Comparing the ^{1}H NMR spectrum of the control sample with the deuterated compound showed loss of peaks, as shown in the stacked plot depicted in figure 37. Deuterium NMR is commonly used to follow the addition of deuterium to compounds (Martin and Martin, 1981; Hayashi *et al.*, 2004; Garson and Staunton, 1979; Thurmond *et al.*, 1991). In effect whereas deuterium incorporation can be seen in the ^{1}H by a reduction in the size of peaks, for ^{2}H NMR new peaks arise at almost identical chemical shifts. This is indeed the case here, as shown in figure 38. The top spectrum shows the ^{2}H NMR for deuterated testosterone in CD_3OD and shows peak for the methyl and alcohol signals, and new peaks arising at 5.7 ppm and ~2.3 ppm. The middle spectrum shows a ^{1}H spectrum for deuterated testosterone in CD_3OD. The two peaks mentioned are absent in this spectra. The lower spectrum show spectrum of testosterone in CD_3OD, peaks at 5.7 ppm and ~2.3 ppm are clearly seen.

After a full assignment of the new compound and testosterone, it was confirmed that the disappearing peaks belonged to protons at position 2 and 6. The singlet found at 5.71 ppm (H4) had decreased significantly.

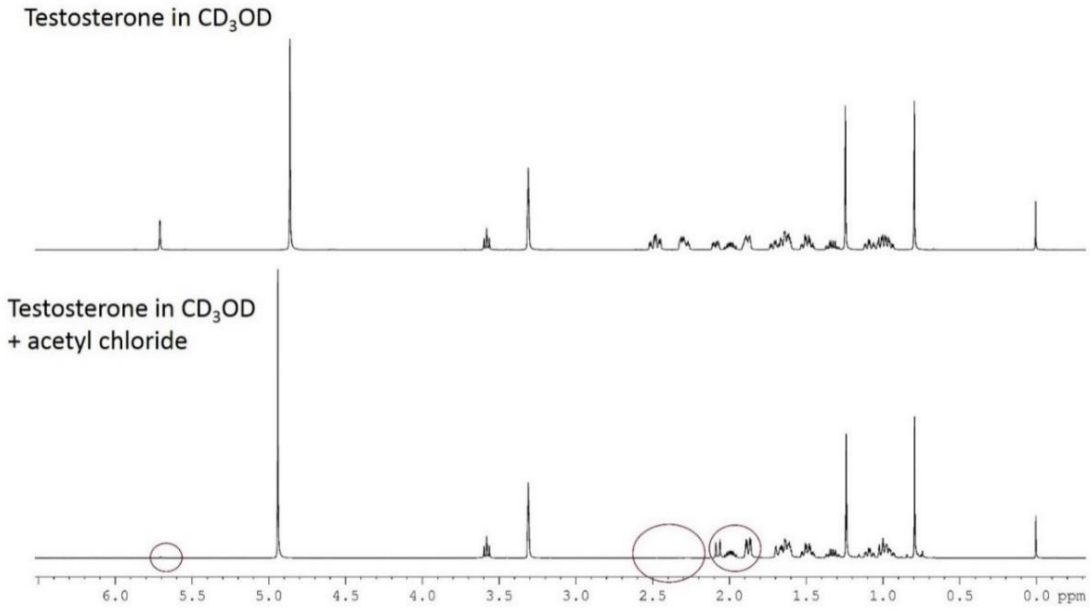

Figure 37. Stacked plot of ^{1}H-NMR spectra. The upper spectrum shows testosterone in CD_3OD, while the lower spectrum shows testosterone in CD_3OD, with the addition of acetyl chloride. Encircled in the lower spectra are the changes seen in the spectra upon addition of acid.

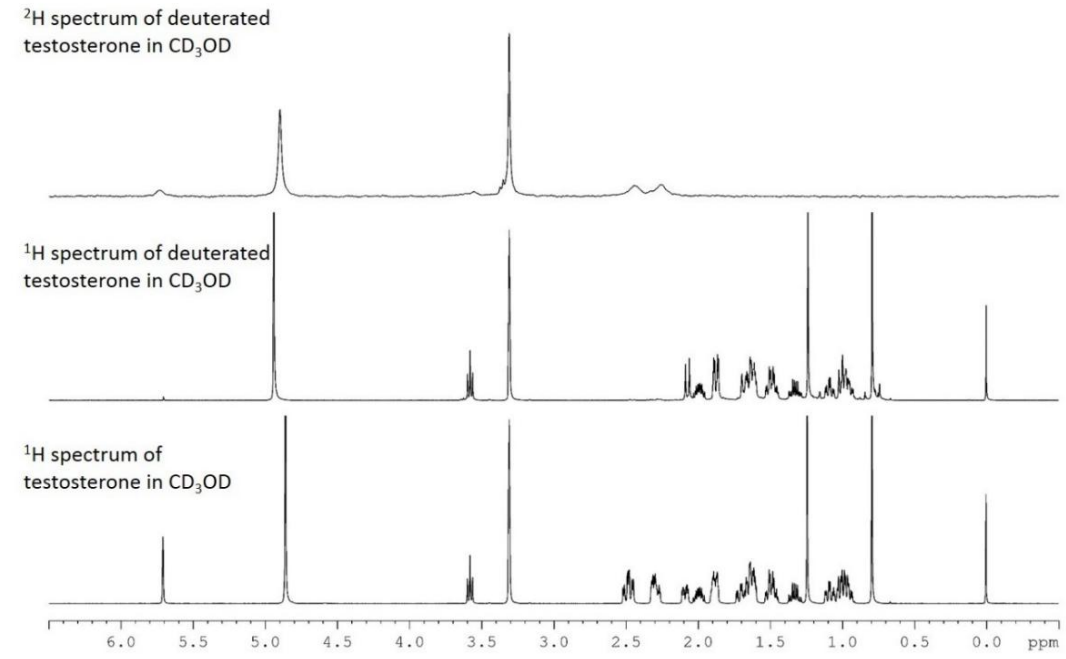

Figure 38. Stacked plot of NMR spectra. The upper spectrum is a deuterium spectrum of testosterone in CD_3OD, the middle spectrum is a proton spectrum of deuterated testosterone in CD_3OD, while the lower spectrum is a proton spectrum of testosterone in CD_3OD.

Characterisation of testosterone and deuterated testosterone

Assignment of testosterone and deuterated testosterone

^{1}H NMR of testosterone t=0 control (CD_3OD) (500 Hz) δ

The ^{1}H spectrum of testosterone t=0 control was assigned, going downfield to upfield, as follows in table XXV.

Table XXV. Proton-1 chemical shifts for testosterone in CD_3OD as obtained experimentally at 500.13 MHz.

Shift (ppm)	Integral	Split pattern[1]	Coupling constant J (Hz)	Proton
5.71	1H	s		4
3.58	1H	t	8.7	17
2.48	2H	m		2_{β}, 6_{β} $-H_2$
2.30	2H	m		2_{α}, 6_{α} $-H_2$
2.09	1H	ddd	13.5, 5.0, 3.2	1_{β}-H
2.00	1H	ddt	5.8, 15.1, 9.4	16_{α}-H
1.88	2H	m		7, 12_{β} $-H_2$
1.65	4H	m		1_{α}, 8, 11 and 15_{α}-H (in this order, 1 α is more downfield than 15 α))
1.49	2H	m		11, 16_{α}-H
1.33	1H	dq	5.8, 12.1	15_{β}-H
1.24	3H	s		19
1.09	1H	dt	4.1, 12.8	12_{α}-H
1.08	1H	m		7
1.01	1H	m		14
0.95	1H	m		9
0.79	3H	s		18

[1] s = singlet, t= triplet, m= multiplet, ddd = double double doublet, ddt = double double triplet, dq = double quartet, dt = double triplet

C-NMR of testosterone t=0 control (CD_3OD) (125 Hz) δ

The ^{13}C spectrum of testosterone t=0 control was assigned, going downfield to upfield, as follows in table XXVI.

Table XXVI. Carbon-13 chemical shifts for testosterone in CD_3OD as obtained experimentally at 500.13 MHz.

Shift (ppm)	Carbon
202.4	3
175.2	5
124.1	4
82.3	17
55.5	9
51.8	14
44.0	13
40.1	10
37.7	12
36.9	8
36.8	1
34.7	2
33.9	6
32.9	7
30.6	16
24.2	15
21.7	11
17.7	19
11.6	18

^{1}H NMR of deuterated testosterone (CD_3OD) (500 Hz) δ

The ^{1}H spectrum of deuterated testosterone was assigned, going downfield to upfield, as follows in table XXVII

Table XXVII. Proton-1 chemical shifts for deuterated testosterone in CD_3OD as obtained experimentally at 500.13 MHz.

Shift (ppm)	Integral	Split pattern[1]	Coupling constant J (Hz)	Proton
3.58	1H	t	8.7	17
2.09	1H	d	13.5	1_β-H
2.00	1H	ddt	5.8, 15.1, 9.4	16_α-H
1.88	2H	m		7, 12 $_\beta$ $-H_2$
1.67	1H	d	13.5	1_α-H
1.63	3H	m		8, 11,15_α-H
1.50	2H	m		11, 16_α-H
1.33	1H	dq	5.9, 12.2	15_β-H
1.23	3H	s		19
1.09	1H	dt	4.2, 12.8	12
1.08	1H	dt	11.9	, 7_α-H
0.98	2H	m		, 14, 9-H
0.77	3H	s		18

[1] t= triplet, d = doublet, ddt = double double triplet , m= multiplet, dq = double quartet, s = singlet, dt = double triplet

IR and MS spectra

The IR spectrum of testosterone showed three large peaks at roughly 3400 cm^{-1}, 2940 cm^{-1} and at 1660 cm^{-1} belonging to a OH-stretch, C=C stretch and a C=O stretch. There is a small indication of a beginning of a peak in the deuterated compound spectrum at around 2300 cm^{-1}.

The incorporation of deuterium into testosterone was also observed with mass spectrometry. Using the positive ion mode both the control sample and the deuterated compound showed both [M+H] and [M+Na] peaks. For the deuterated product a peak at 293 corresponded to testosterone with four deuterium atoms, so $C_{19}H_{25}D_4O_2$ as the [M+H]. Although deuteration was seen at carbons 2,4 and 6, it was clear from the ^{1}H NMR that the level of incorporation was not 100 % at these sites. Closer inspection of the region around 293 shows the presence of other peaks, which will correspond to more or less deuterium in the molecule. This is also seen in the [M+Na] peaks: 315 corresponds to four and 316 to five deuterium atoms in the molecule.

Raman spectra

Raman experiments were carried out to characterise the new compound, to obtain a spectrum of testosterone to use as a control and to compare how the deuterated compound would be different from the control. Figure 39 shows a Raman spectrum of pure testosterone. The peaks at around

1600 cm^{-1} and 3000 cm^{-1} were used as references. Raman analysis was more easily performed when the deuterated compound was in a crystalline form than in a solution, however strong fluorescence caused interference when using 532 nm excitation wavelength. When analysing the residual crystals in the reaction flask however, a clear spectrum that lined up well with testosterone was seen, as shown in figure 40. This shows both recrystallised testosterone and deuterated testosterone, with a clear indication of a group of peaks arising in the 2000 cm^{-1} area in the deuterated compound spectrum, corresponding to carbon-deuterium bonds. In the expanded area shown in figure 41, the deuterated compound peaks show shifts compared to the original testosterone peaks. Software analysis showed that the shift spanned around 10-12 wavelengths. There is a slight shoulder seen on the left peak. This shoulder lines up with the left of the two clear testosterone peaks, and therefore indicates that there is a small amount of non-deuterated product left. However comparing the signal contribution with the overall signal from the deuterated compound shows that it is around 3% that seems to be non-deuterated.

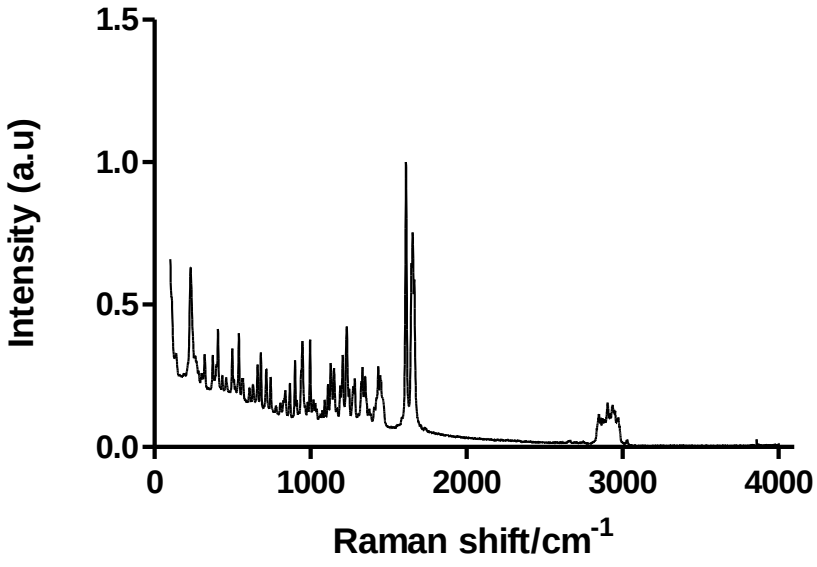

Figure 39. Raman spectrum of pure testosterone taken with 785nm excitation wavelength.

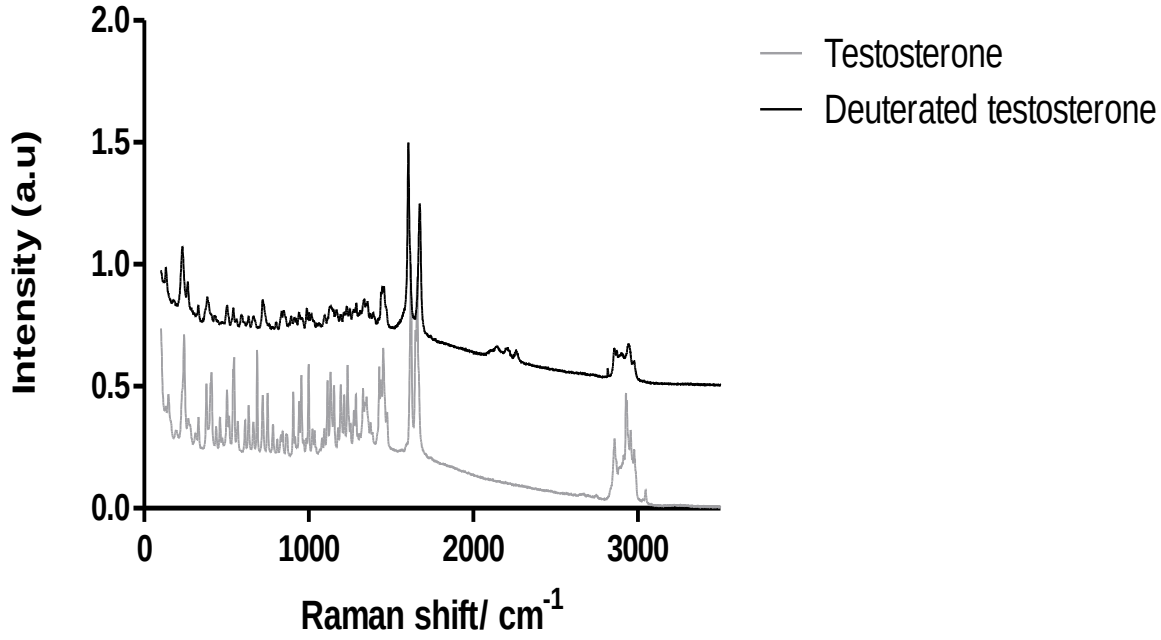

Figure 40. Normalised spectra of recrystallised testosterone and deuterated testosterone at excitation wavelength 785 nm presented together as a stack plot.

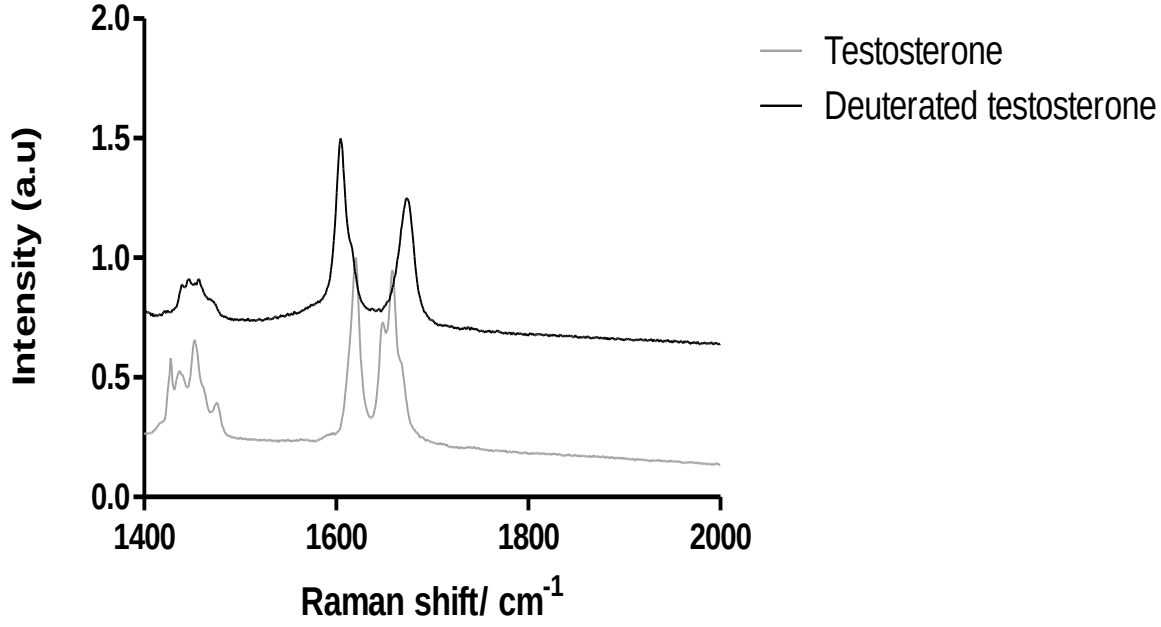

Figure 41. Expansion of figure 40, the spectra are showing peaks in the range 1400-2000 cm^{-1}.

Synthesis on larger scale

Recrystallisation

Despite successful attempt to recrystallise testosterone, deuterated testosterone was not so easily recrystallised with the same method.

When the hexane was added, the crystals did not form needle-like crystals, but rather micro crystals. Despite leaving the solution to set for a certain time, and after cooling under ice, the crystallisation process was not successful (~5% yield). Most of the product were still left in the filtrate, which was later confirmed by Raman analysis.

Part II. In-exchange and back-exchange of [2,2,4,6,6-D_5] testosterone

In-exchange experiment

After six days of exposing testosterone to CD_3OD, no change was seen in the spectra, but upon addition of acetyl chloride, deuterium incorporation was seen within four minutes. Table XXVIII shows the integrals for assigned peaks 5.7 ppm and 2.2-2.4 ppm in the testosterone spectrum, and the speed of the in-exchange is depicted in figure 42. The methyl hydrogens at position H19, 1.24 ppm, were used as calibration point.

Table XXVIII. Table of integrals for assigned hydrogen positions in 5.7 ppm and 2.2-2.4 ppm in testosterone

	Integral	
Time (min)	5.7 ppm (H4)	2.4-2.2 ppm (H2,6)
0	1.03	4.07
4	0.42	0.03
8	0.27	0.05
12	0.17	0.16
32	0.04	0.01
39	0.02	0.07
48	0.01	0.04
54	0.02	0.01

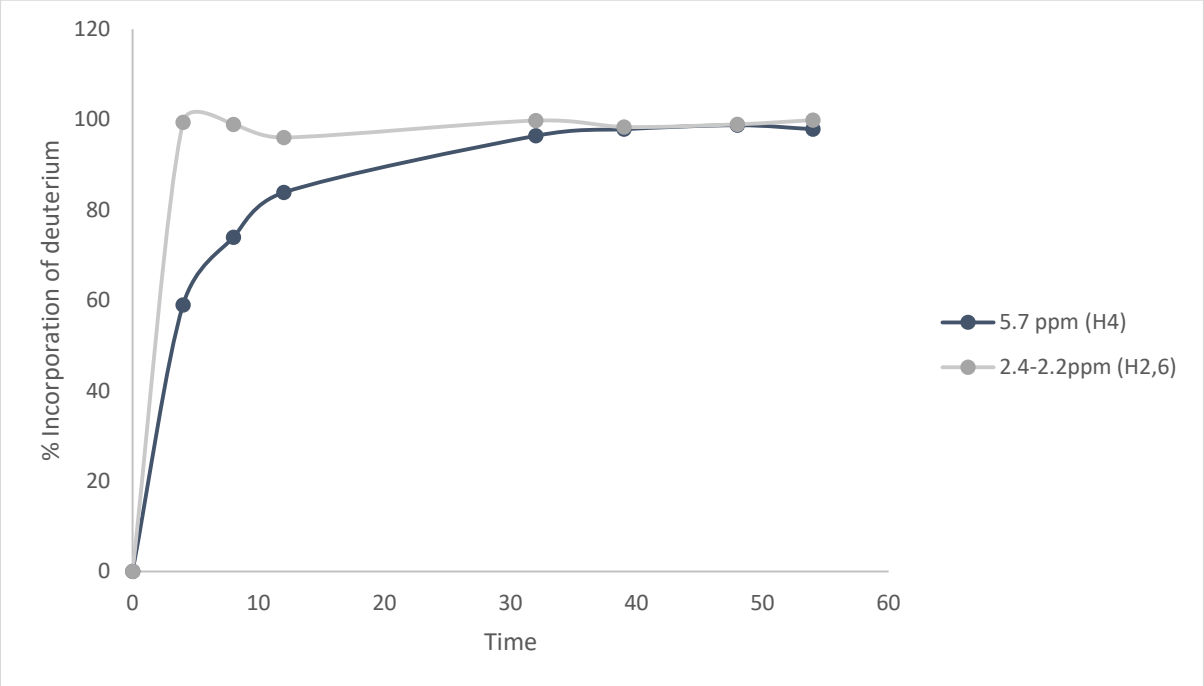

Figure 42. Graph depicting the speed of in-exchange of deuterium in testosterone peaks at 5.7 ppm and 2.2-2.4 ppm during one hour.

Back-exchange and stability experiment

Method 1. Evaporating solvents and adding deuterated chloroform

For the duration of the experiment, the peak at 5.7 ppm showed no clear sign of back-exchange in either conditions, as can be seen in figure 43. Shown in figure 44, is the stability of the two peaks at 2.2 and 2.4 ppm, due to the environment in which the spectra are taken, the two peaks' integrals are combined. Again no clear sign of back-exchange occurred.

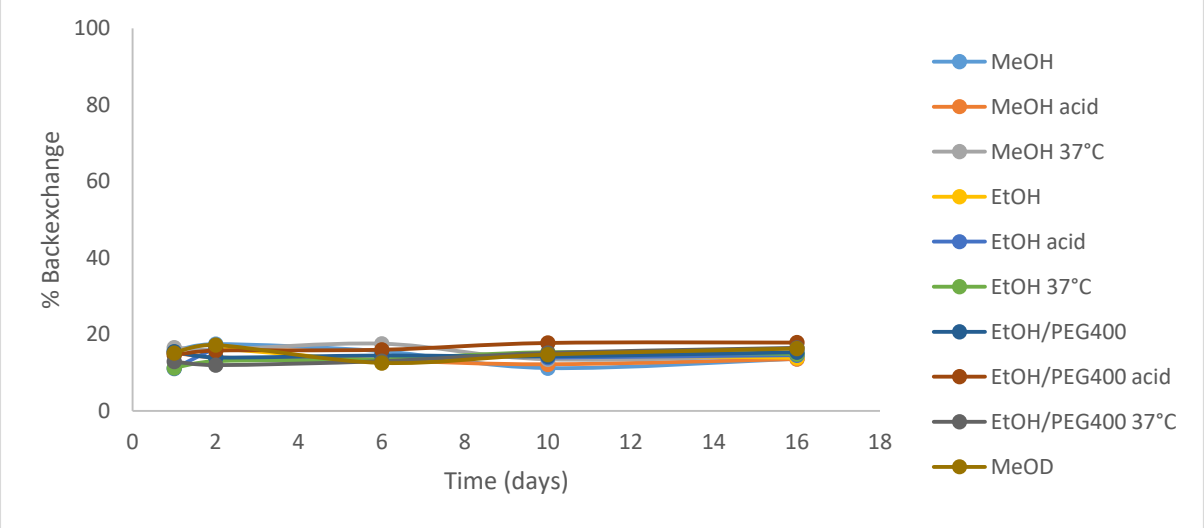

Figure 43. Time line stability of H4 (5.7 ppm) in testosterone in different solvents and conditions, analysed and assessed using Method 1, i.e. evaporating the solvent and adding deuterated chloroform before NMR analysis.

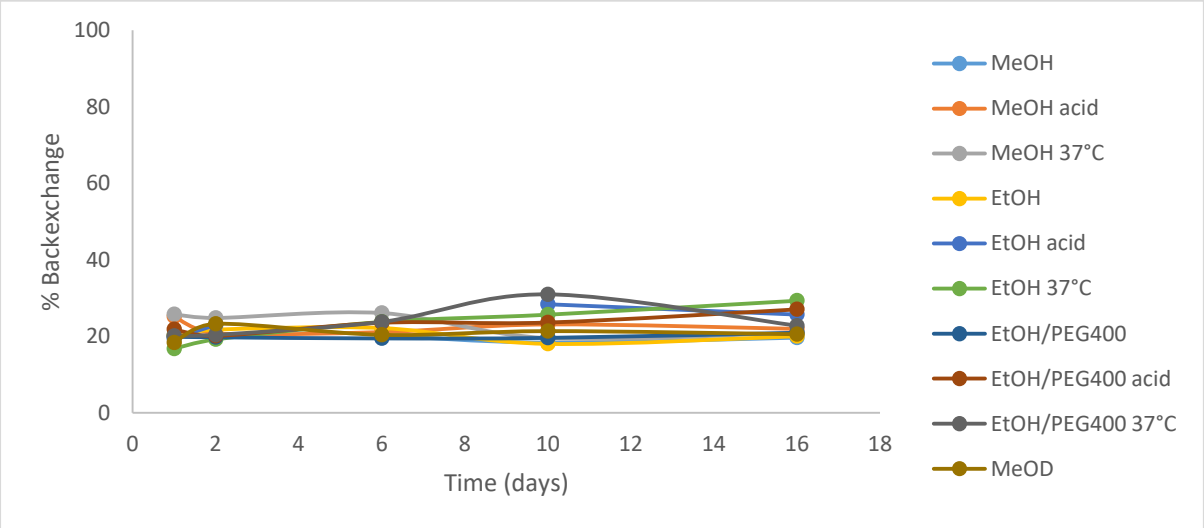

Figure 44. Time line stability of $H2_{\alpha,\beta}$ and $H6_{\alpha,\beta}$ (2.4-2.2 ppm) in testosterone in different solvents and conditions, analysed and assessed using Method 1, i.e. evaporating the solvent and adding deuterated chloroform before NMR analysis.

Method 2. Analysing the tube directly without external interference

Figures 45 and 46 show the stability at the same peaks mentioned above, but assessed with method 2, *i.e.* NMR diffusion and presaturation experiments. Again, the results are stable and show small tendency for back-exchange.

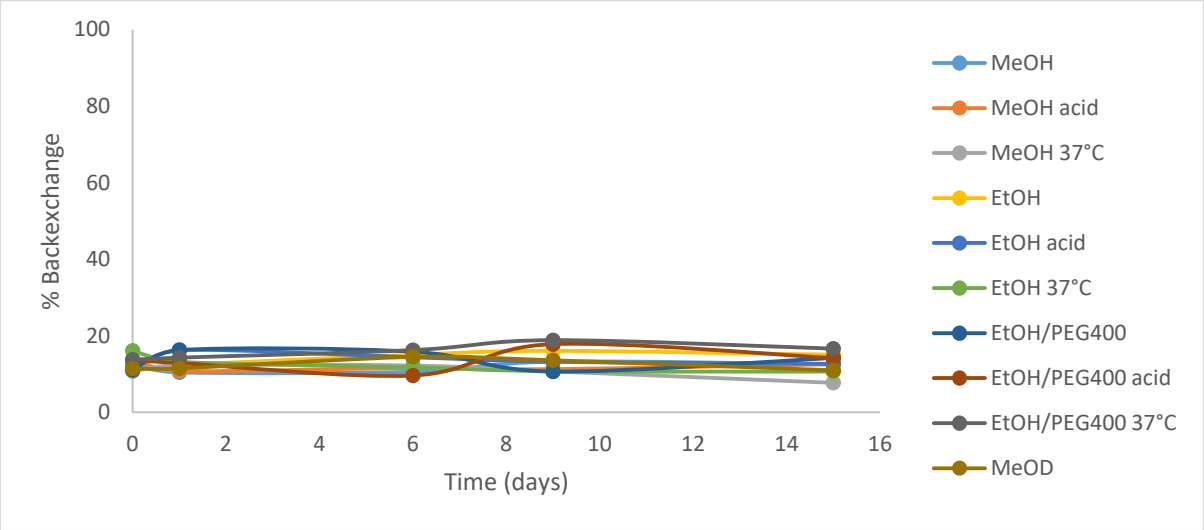

Figure 45. Time line stability of H4 (5.7 ppm) in testosterone in different solvents and conditions, analysed and assessed using Method 2, i.e. NMR analysis was carried out directly on the NMR tube without interfering with the sample.

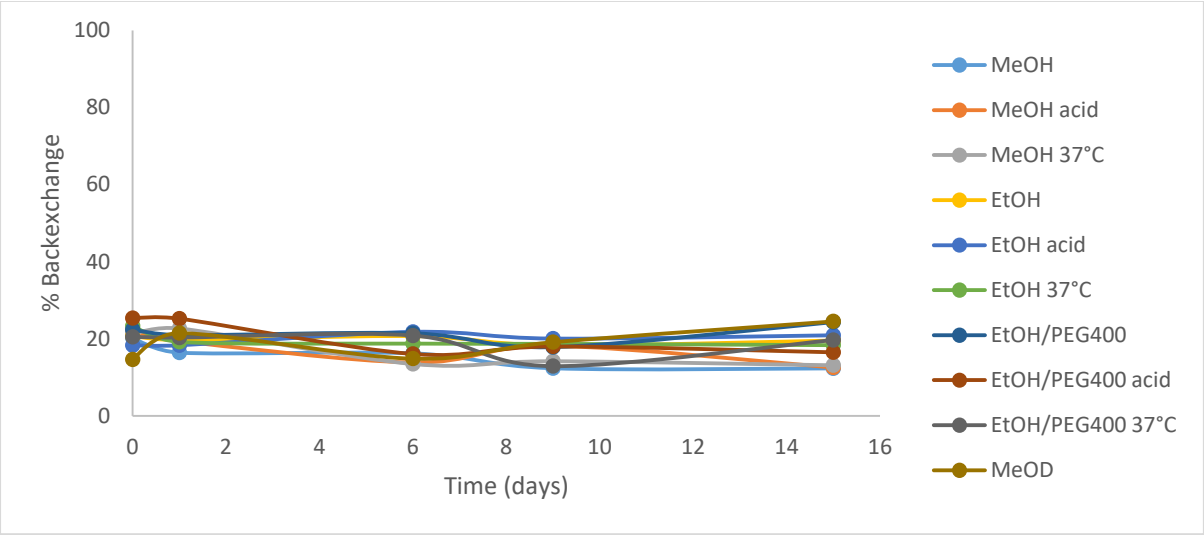

Figure 46. Time line stability of $H2_{\alpha,\beta}$ and $H6_{\alpha,\beta}$ (2.4-2.2 ppm) in testosterone in different solvents and conditions, analysed and assessed using Method 2, i.e. NMR analysis was carried out directly on the NMR tube without interfering with the sample.

Discussion

Although the deuteration process and subsequent NMR assignment and monitoring were not part of the original project the use of these two have added valuable impact to the project. It has been possible to develop a novel simple deuteration method, assign all the hydrogen and carbon peaks for testosterone in various solvents, monitor in-exchange and back-exchange of the deuteration process and assess the stability of the deuterated compound in various solvents and conditions.

Part I. Synthesis and characterisation of [2,2,4,6,6-D_5] testosterone

Preliminary synthesis reaction

The deuterated compound was successfully synthesised on a small scale using CD_3OD and acetyl chloride with ^1H used to monitor the reaction progress. The use of a control (no acetyl chloride) confirmed that a catalyst is needed for the reaction. This was confirmed with NMR analysis carried out after exposure of the pure testosterone in solvent, without acetyl chloride, to 37 °C for 21 hours, *i.e.* neutral conditions, where the NMR spectra still looked identical to those taken at t=0. The deuterated sample was also investigated in proteo-methanol, following solvent evaporation. No change in the integrals for the peaks that had been reduced was seen, showing that the deuterated testosterone did not back-exchange in these conditions. It should be noted that a previous synthesis of deuterated testosterone has been reported using an alkaline catalyst (Atzrodt *et al.*, 2012). This is surprising as testosterone is not stabile under alkaline conditions (Vulliet *et al.*, 2010). However the synthesis makes use of microwave heating and consequently the time under alkaline conditions was kept to just a minute.

NMR assignment

The NMR spectra of testosterone in deuterated chloroform have been reported multiple times, however there is only one report in deuterated methanol. This work tabulates selected proton resonances along with a full assignment of the ^{13}C spectrum (Kolet *et al.*, 2013). As there are obvious shifts in the ^1H spectra when recorded in chloroform and methanol a full assignment of the testosterone spectrum was undertaken. Using both 1D and 2D NMR spectra (^1H, ^{13}C, HSQC , COSY and HMBC, figures 47- 54) allowed full assignment of all the peaks in both the deuterated testosterone and testosterone samples. The loss of some of the peaks following deuteration was a key step in identifying which protons had exchanged.

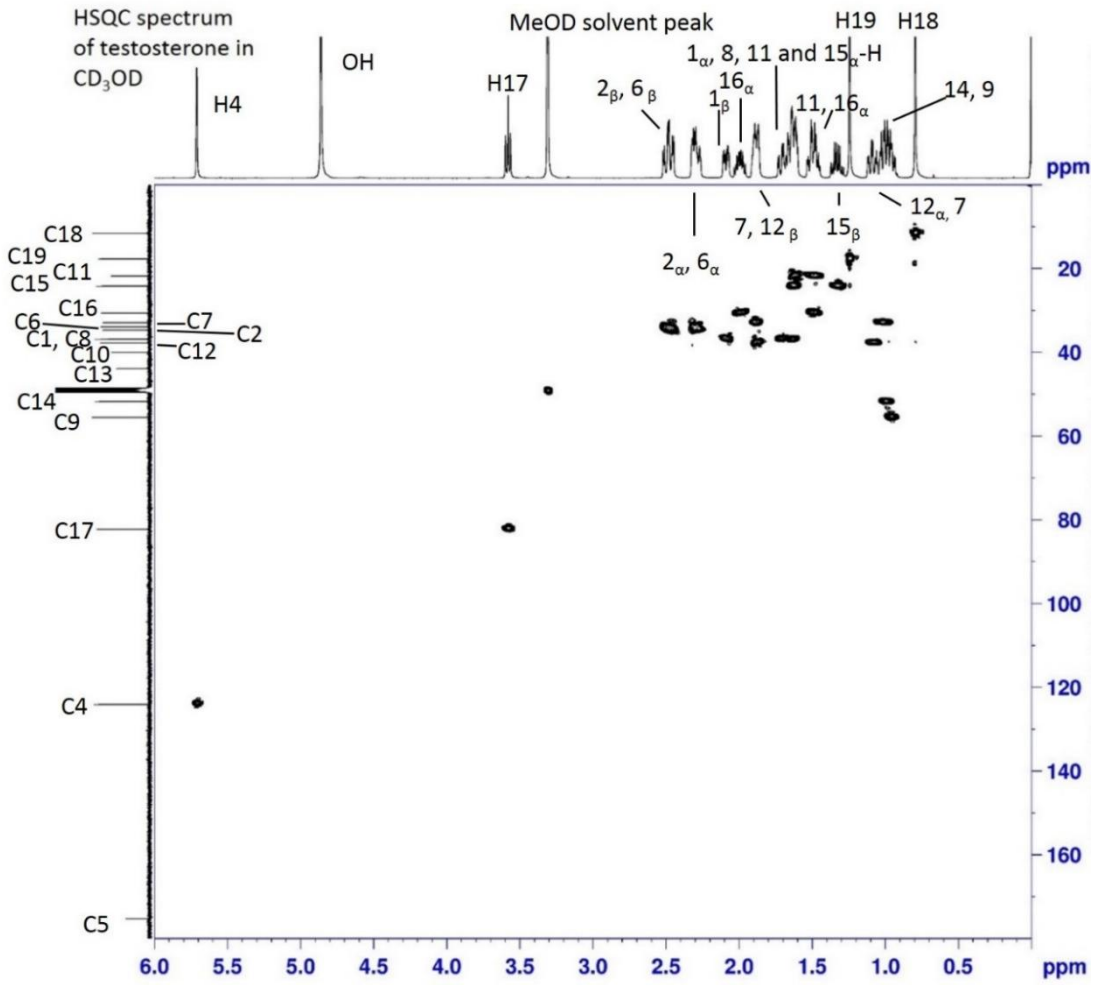

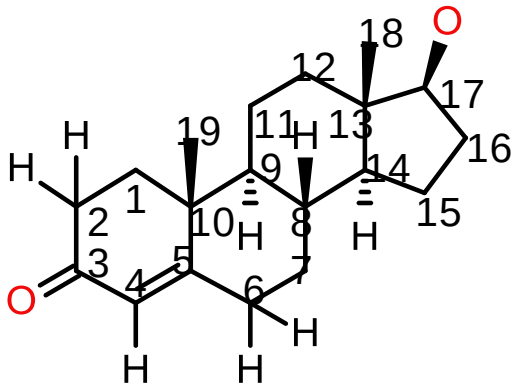

Figure 47. HSQC spectrum of testosterone in CD_3OD, with assigned peaks for protons and carbons. C3 carbon has a chemical shift of 202.4 ppm and is not shown in the figure. HSQC spectrum shows the correlation between a proton coupling to the specific heteronucleus (in this work carbon) it is attached to (one bond).

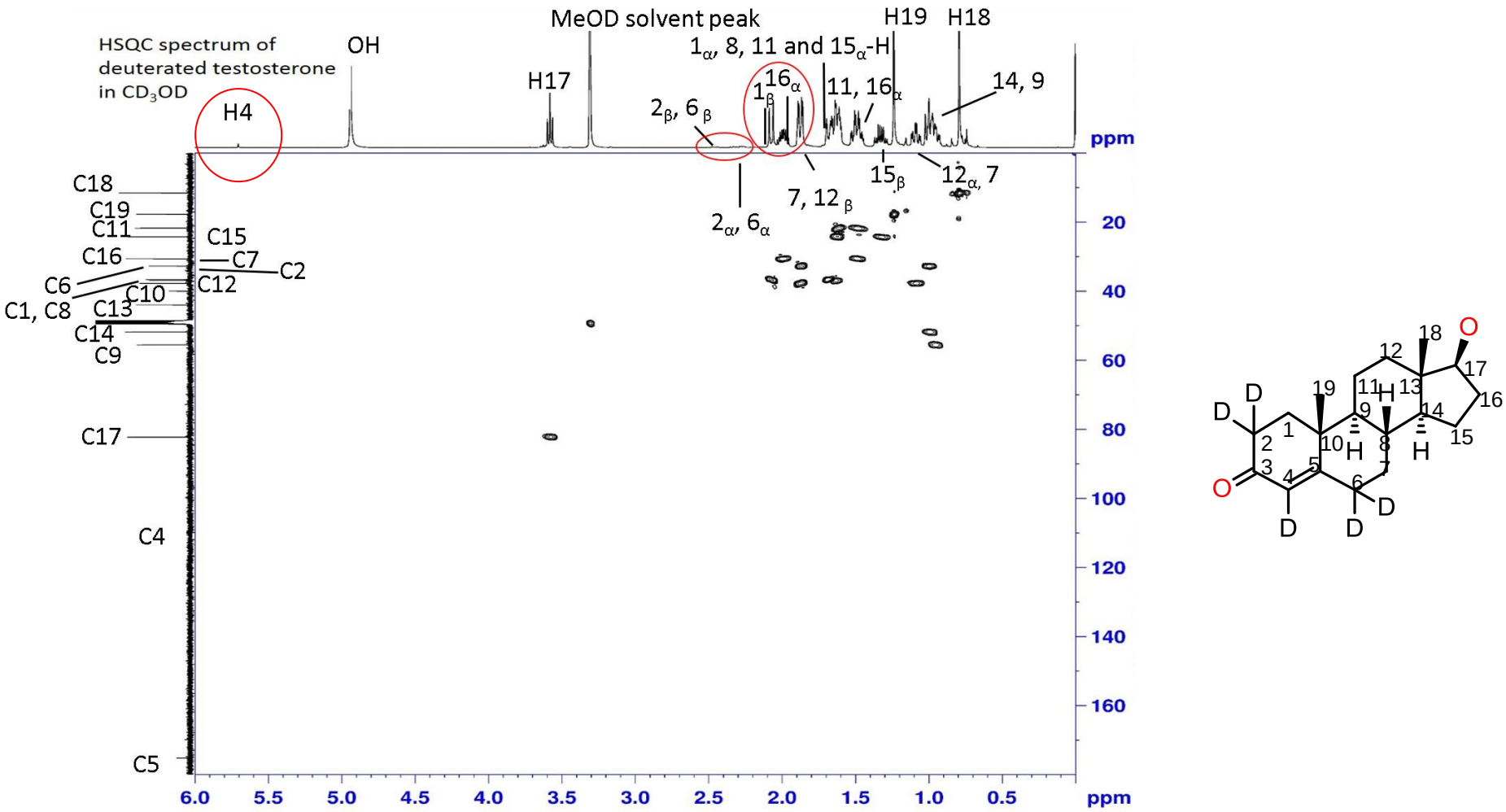

Figure 48. HSQC spectrum with assigned peaks of deuterated testosterone in CD_3OD. HSQC spectrum shows the correlation between a proton coupling to the specific heteronucleus (in this work carbon) it is attached to (one bond). Markings in red show important interactions and differences compared to previous spectrum in figure 47. To the right the chemical structure of deuterated testosterone is shown

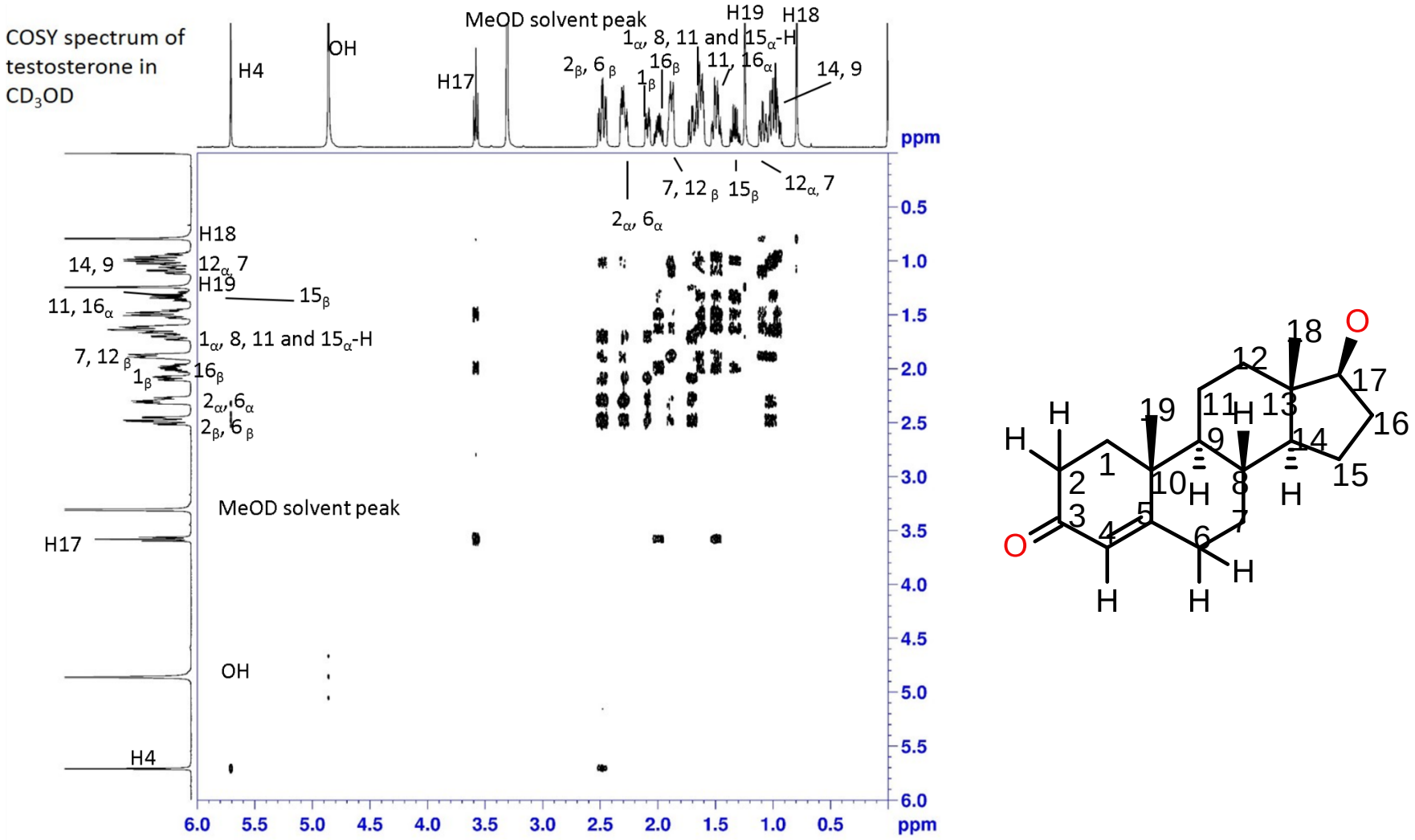

Figure 49. COSY spectrum with assigned peaks of testosterone in CD_3OD. COSY spectrum shows the correlation between a proton coupling to the proton next to it (three bonds). To the right the chemical structure of testosterone is shown.

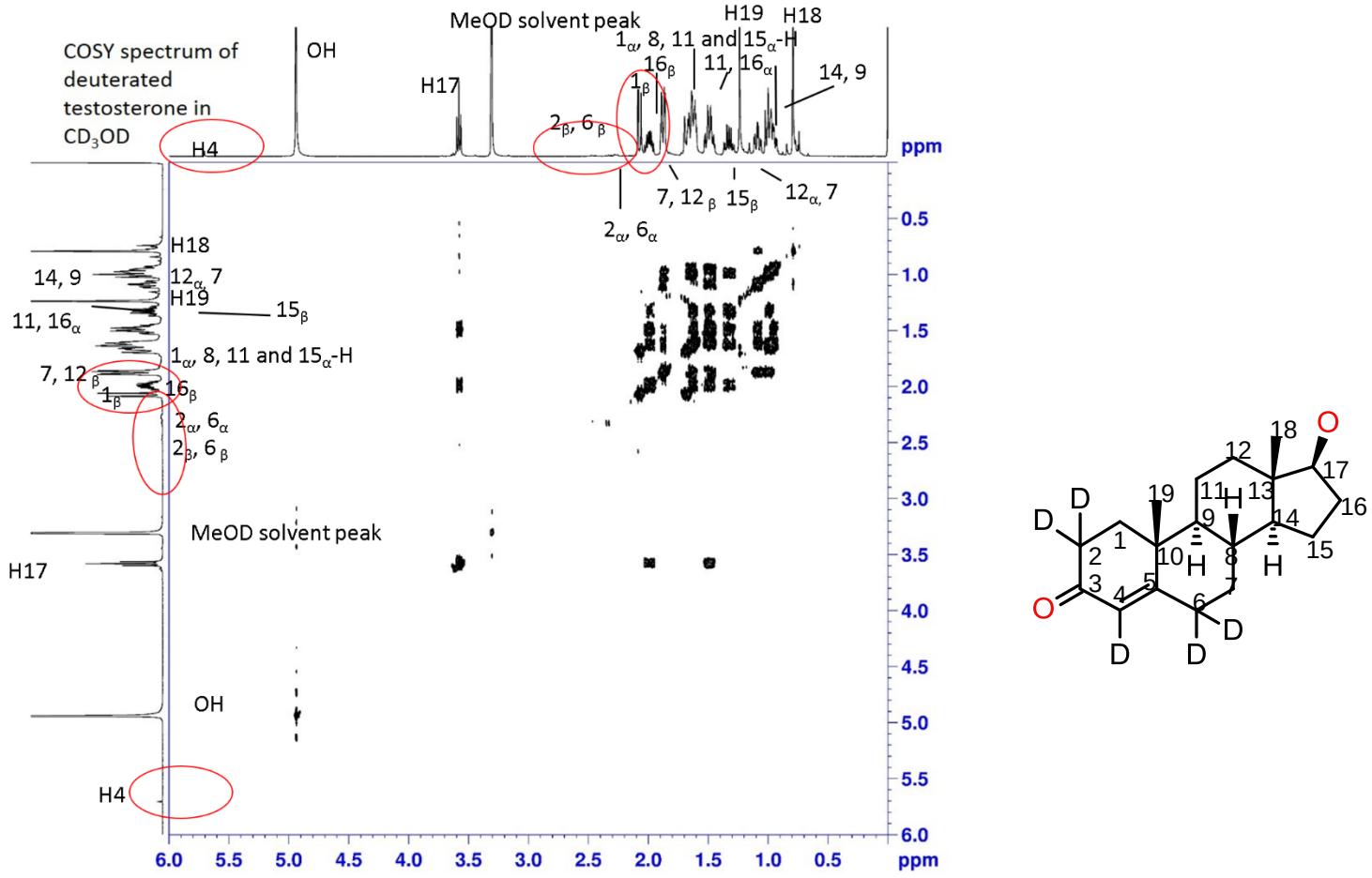

Figure 50. COSY spectrum with assigned peaks of deuterated testosterone in CD_3OD. COSY spectrum shows the correlation between a proton coupling to the proton next to it (three bonds). Red markings show key differential changes compared to testosterone spectrum. To the right the chemical structure of deuterated testosterone is shown.

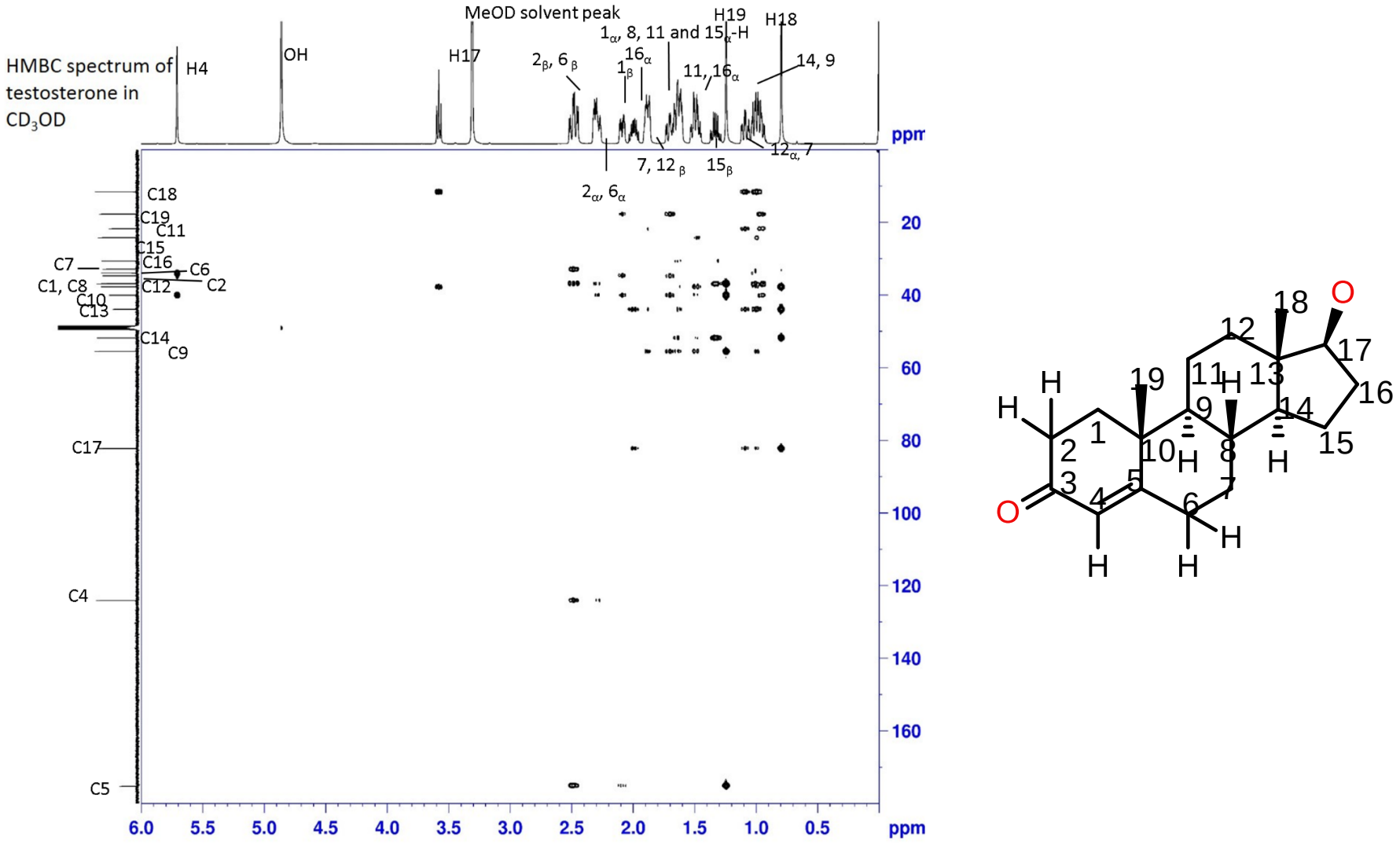

Figure 51. HMBC spectrum with assigned peaks of testosterone in CD_3OD. HMBC spectrum shows the correlation between a heteronucleus (in this case carbon) and a proton coupled to it by 2-4 bonds. To the right the chemical structure of testosterone is shown.

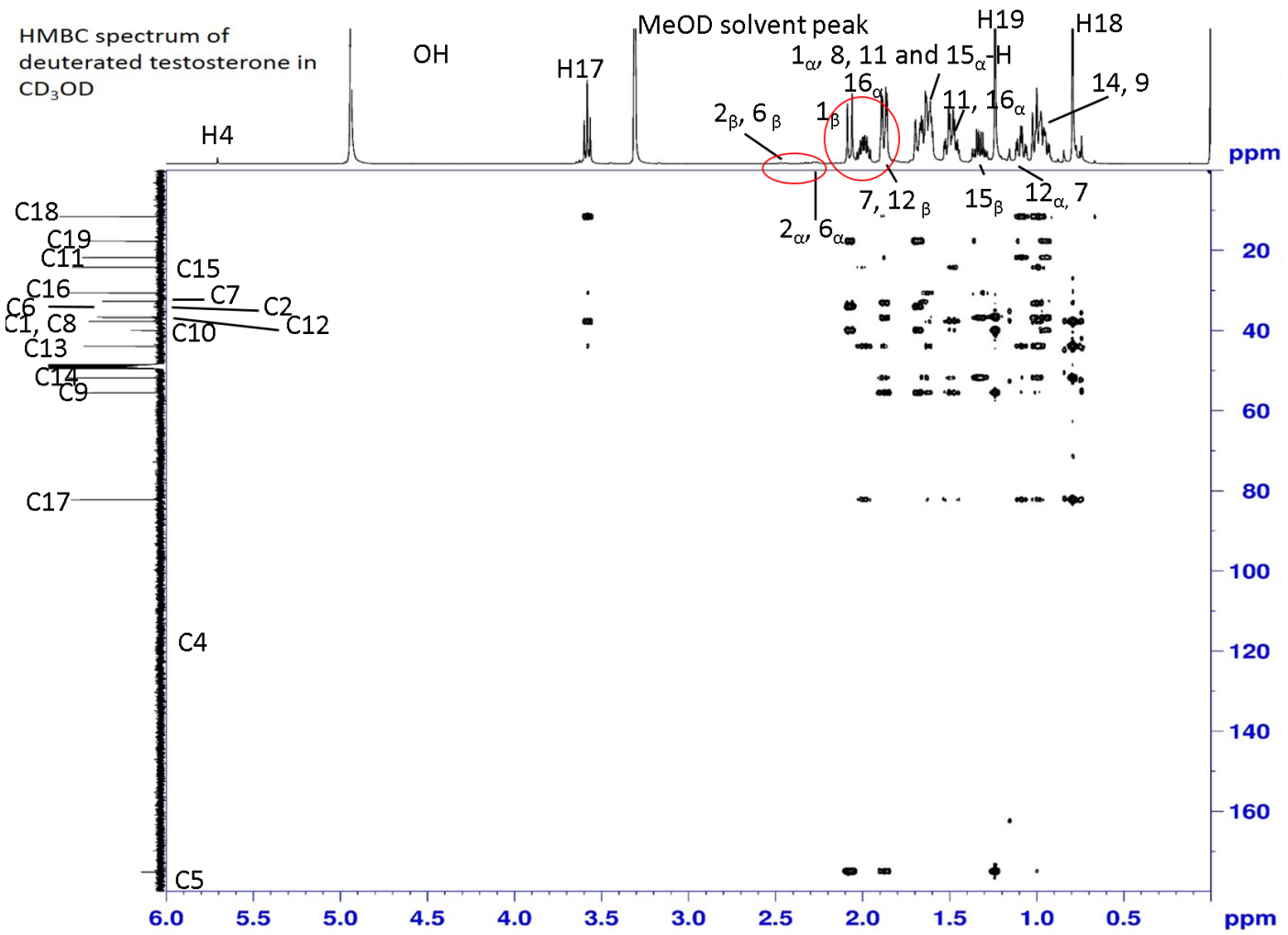

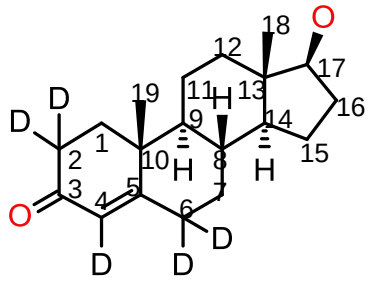

Figure 52. HMBC spectrum with assigned peaks of deuterated testosterone in CD_3OD. HMBC spectrum shows the correlation between a heteronucleus (in this case carbon) and a proton coupled to it by 2-4 bonds. Red markings show key differential changes compared to testosterone spectra. To the right, the chemical structure of deuterated testosterone is shown.

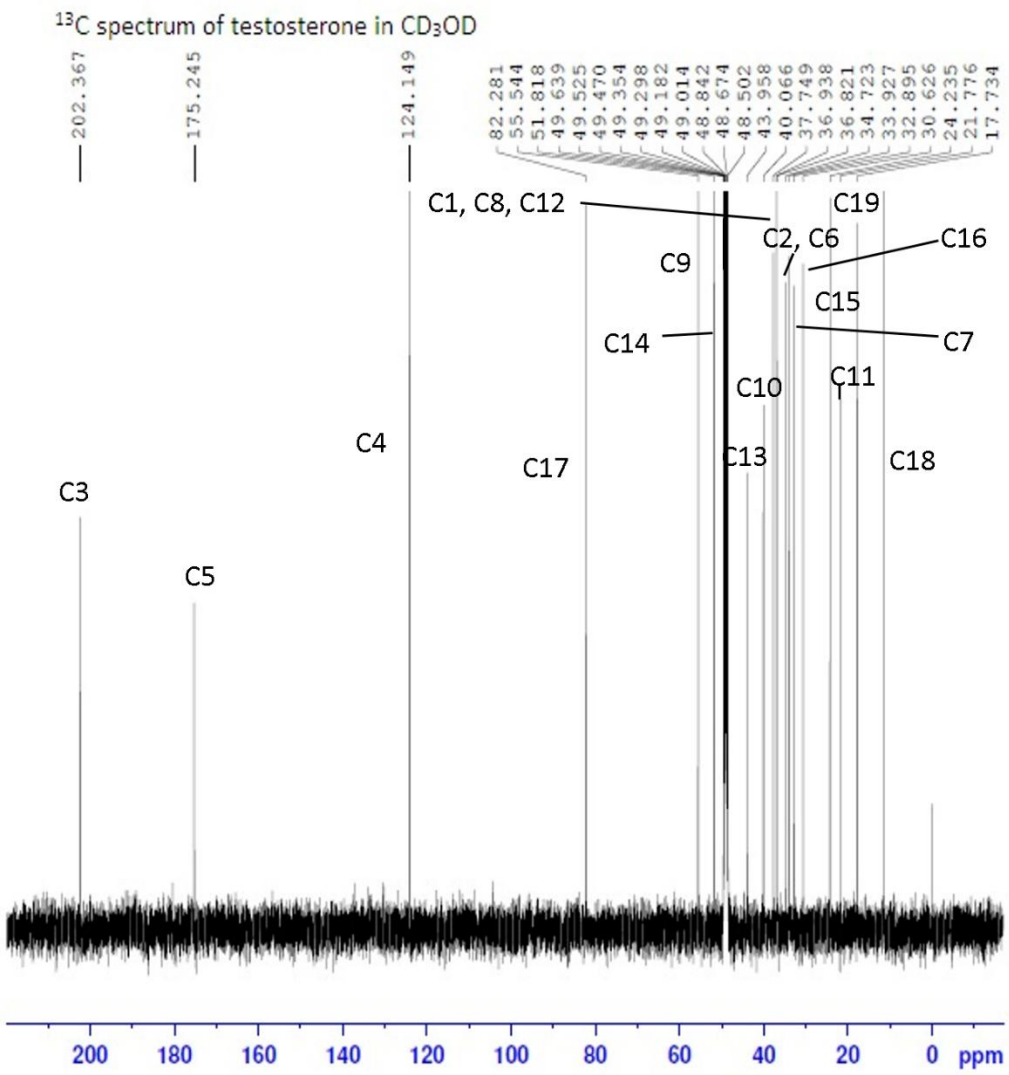

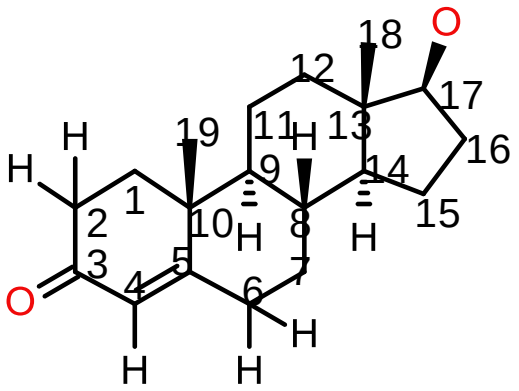

Figure 53. ^{13}C spectrum with assigned peaks of testosterone in CD_3OD. To the right the chemical structure of testosterone is shown.

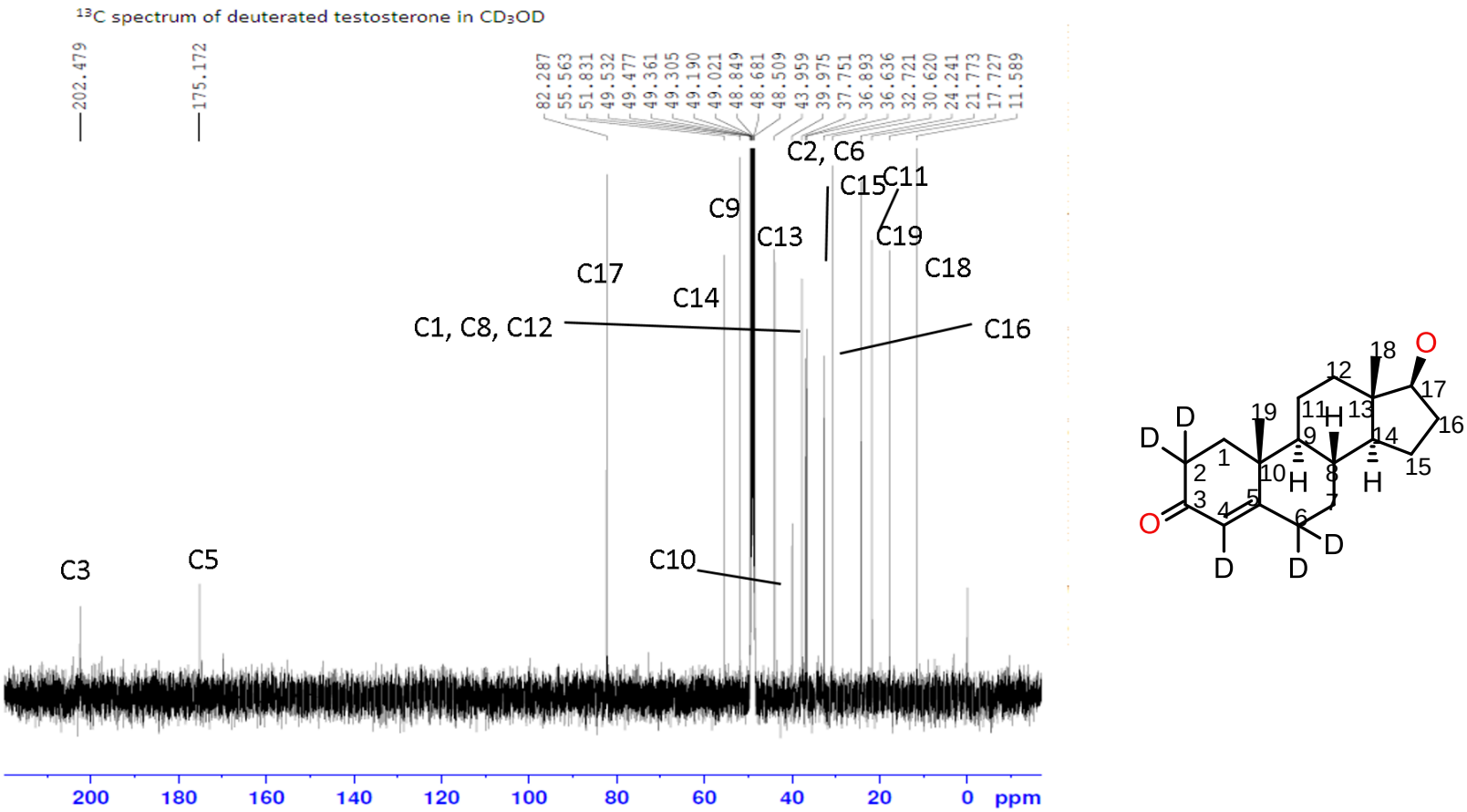

Figure 54. ^{13}C spectrum with assigned peaks of deuterated testosterone in CD_3OD. To the right the chemical structure of deuterated testosterone is shown.

Comparing ^{1}H spectra in deuterated methanol with those performed in deuterated chloroform showed many similarities, however some peaks had switched place (peaks at 2.09 ppm (1_{β}) and 2.00 ppm (16_{α}) and peaks in the cluster at 1.65 ppm). (Kasal *et al.*, 2010; Hayamizu *et al.*, 1990; Atzrodt *et al.*, 2012) The ^{13}C spectra in different solvents overlap better, although there were three peaks that were harder to assign (peaks at 37.7 ppm (12-C) 36.9 ppm (8-C) and 36.8 ppm (1-C) and these have changed order compared to spectra performed in deuterated chloroform. (Harris *et al.*, 2006)

At a first glance on the ^{1}H spectrum of non-deuterated testosterone there are four peaks that clearly stand out. These are three singlets and one triplet.

Two of the singlets, had an integration of three, which then should correspond to methyl groups H18 and H19 were identified in the proton spectrum. In theory H18 should be more upfield than H19, since it only has a hydroxyl group close to it, albeit a very electron withdrawing group, H19 has both a carbonyl group and a double bound nearby pushing it more downfield.

The remaining singlet was found very downfield in the proton spectra, which then should correspond to H4 at 5.71 ppm as it is directly bound to a carbon that is directly bound to a hydroxyl group. In the ^{13}C spectra (figures 53 and 54), and the HSQC spectra (figures 47 and 48), which show the correlation between a proton coupling to the specific heteronucleus (in this work carbon) it is attached to (one bond), the corresponding carbon was found at 124.1 ppm.

The only triplet in the spectra was found at 3.58 ppm and the corresponding carbon at 82.3 ppm (C17) which is the only proton that could give a triplet appearance as it couples to only two other protons belonging to C16.

H16 protons are clearly seen in the COSY spectrum, which shows the correlation between a proton coupling to the proton next to it (three bonds) (figures 49 and 50) as, above mentioned, H17 only can couple with H16 protons, and these are located at 1.49 and 2.00 ppm. The corresponding carbon to these two protons are found in the HSQC spectra (figures 47 and 48), at 30.6 ppm.

In the COSY spectra (figures 49 and 50), the H16 proton at 2.0 ppm clearly couples with itself and the other H16 proton, (and also with H17 which is found very downfield) and a fourth spot (1.65 ppm) which then should belong to one of the H15 protons. The other H16 proton couples faintly with the H15 proton found at 1.65 ppm, and also to one peak at 1.3 ppm and to a cluster of peaks in the 1.0 ppm region. In the HSQC spectra (figures 47 and 48), it is clearly seen that those peaks in the 1.0 ppm region only have one proton, while the protons at 1.65 ppm and 1.33 ppm line up with each other, thus these must belong to H15 protons, and the corresponding carbon can be found in the HSQC spectra at 24.2 ppm. The location of H15 protons was further confirmed by comparing with

spectra (Hayamizu *et al.*, 1990) as one of the H15 protons showed a very characteristic double quartet pattern. This pattern was also seen in the experimental spectra performed during these experiments. Once assigned, the other H15 peak was confirmed as above mentioned, but also with the HSQC to locate the other proton, using C15 position as a final confirmation. In theory, H11 and H7 should also give double quartet patterns, however these peaks were lost in "multiplets".

C10 and C13 carbons are found from the HSQC spectra, as they are the only two carbons left that do not couple with any hydrogens (C3 is easily identified downfield in the spectra as it couples directly to O). These two carbons are very close to each other in the ^{13}C spectra (40.1 and 44 ppm) however it is possible to distinguish them with the HMBC spectra, which shows the correlation between a heteronucleus (in this case carbon) and a proton coupled to it by 2-4 bonds (figures 51 and 52) because H19 protons couple with H1 (3 bonds), H5 (3 bonds), H9 (3 bonds) and H10 (2bonds) while H18 protons can couple with H12 (3 bonds), H13 (2 bonds), H14 (3 bonds) and H17 (3 bonds). This distinguishes H10 carbon (40.1 ppm) from H13 carbon (44 ppm) but also distinguishes H18 (H at 0.79 ppm, and C at 11.6 ppm) and H19 (H at 1.24 ppm and C at 17.7 ppm) peaks from each other.

C9 and C14 are the only carbons that have only one proton attached. (Actually C8 also has only one proton attached, however, C9 and C14 are in a similar surrounding environment *i.e.* shielded by methyl groups). These two carbons can be identified in the HSQC spectra, where two single dots are found at 51.8 and 55.5 ppm. In the HMBC spectra (figures 51 and 52) H18 protons can couple with C12, 13, 14 and 17 carbons, there is only one of these proton peaks that are alone in the HSQC spectra (figures 47 and 48), which then should belong to C14 (51.8 ppm). This leads to the conclusion that the remaining peak belongs to C9. This is further confirmed in the HMBC spectra, where H19 protons can couple to carbon C9 but not C14, and only faintly to C8.

As written earlier, in the HMBC spectra, H18 protons can couple to carbons at C12, 13, 14 and 17, since three peaks already are assigned, it means that the last peak belongs to C12. In the HSQC spectra, the other proton pair peak is easily found and thus the corresponding carbon to C12 is assigned (which lies very close to carbon 8 and 1 though). In the same area, H8 proton is identified because it has only one proton group attached to a carbon, which leaves the other carbon being C1, again confirmed by looking in the HMBC spectra, where H19 can couple with (C1, C5, C9 and C10) and since all those peaks are assigned except C1, it means that the one left should be C1 at 36.8 ppm.

Synthesis on larger scale

The synthesis on a larger scale was monitored by NMR, and as expected from the preliminary results, was successful. The preliminary results confirmed a high deuterium incorporation yield with MS and NMR, and also Raman in the second experiment confirmed a successful deuterium incorporation. The colour change sustained despite evaporating off acetyl chloride at an early stage. In contrast to the more successful recrystallisation of testosterone, recrystallisation using the same co-solvent system for the deuterated compound was a challenge. It was slightly surprising that the recrystallisation attempt on the labelled compound would have such a poor outcome and not at all behave like testosterone. It seemed, using Raman analysis, that the crystals from the recrystallisation attempt was not the desired product, but rather impurities and by-products.

Infrared spectroscopy

The IR spectrum of the deuterated compound and the control only show traces of peaks that have shifted, which is quite surprising, as it was expected that the difference would be more pronounced. However, the shifted peak is in the fingerprint region and thus could be shielded by other peaks. It also seems like the C=O peak might have shifted only a few wavelengths; this is possible as the carbonyl group is surrounded by deuterium in the new compound and these could interact with the carbonyl group.

Mass spectrometry

Masses corresponding to deuterated and non-deuterated testosterone were confirmed in the positive ion mode. Na-adduct products were also observed. As mentioned in the results section, the mass in the deuterated testosterone spectrum does not match with [M+5D+H], as expected. Either one deuterium is lost, and the reason for this can be several (back-exchange with time as the compound is dissolved in methanol rather than deuterated methanol, the hard conditions in the electrospray ionisation (the inlet temperature is 220 °C)) or the compound is not protonated, which is unexpected as the control compound is protonated and it is expected that the new compound would behave in a similar fashion. Also the [M+Na+Deuterium] adduct show a bit surprising results, with m/z 315 [M+Na+ 4D] and 316[M+Na+5D] or [M+Na+4D+H]. It is highly likely that the conditions in the electrospray change the compound. In the literature, back-exchange on deuterated compounds have been investigated with mass spectrometry, and as already mentioned the harsh conditions in the electrospray, albeit a soft ionisation technique, seem to promote back-exchange on deuterated compounds. (Walters *et al.*, 2012; Kostyukevich *et al.*, 2014). The work of (Atzrodt *et al.*,

2012), found m/z which would indicate only D4 incorporation or D3 with ESI-MS, however this pattern was not seen in our experiment and NMR spectra did not change after adding methanol.

Raman spectra

Testosterone itself, and the deuterated analogue are easily detected by Raman in crystalline form, however they do show strong background fluorescing properties. Raman is not a sensitive technique as MS and also fluorescence is easily picked up from the compound itself or the background (in this case from the solvent and any by-products) which interfere with the spectra. The scattering effect which forms the basis of Raman is also a rather weak effect.

Throughout the experiment, the red laser at excitation wavelength 785 nm gave less fluorescence background noise. A slightly surprising discovery was that the two peaks of main interest shifted further apart from each other, and not in the same direction. The left peak could be slightly more visible in skin experiments, while the right peak might be more shadowed by a strong skin peak at 1654 cm^{-1} It is not yet determined how easily deuterated testosterone is detected when in solution or in a pharmaceutical formulation or when applied on the skin.

Part II. In-exchange and back-exchange of [2,2,4,6,6-D_5] testosterone

In-exchange experiment

The synthesis is quick and takes place within an hour after addition of acetyl chloride. Previous synthesis with a control have shown that the acid is the main catalyst for bringing the reaction forward, however if same behaviour (speed of reaction, catalyst effect) is seen with all types of acid is yet to be determined. During these experiments it has been observed that the reaction might be slightly faster using CD_3OD rather than CH_3OD.For cost reasons, CH_3OD is perfectly suitable as a substitute.

The experimental results confirm how much faster the deuterium incorporation occurs for protons at positions 2 and 6. These four hydrogens are exchanged to over 90 % within four minutes, whereas the single proton at position 4 seems to be exchanged to ~60 % before being almost exchanged to 80 % after ~12 minutes. The peaks at 2.09 ppm and 2.0 ppm changed split pattern, following the reaction (see Part I, page 13, Preliminary synthesis reaction section for more information), and thus were not assessed

Back-exchange experiment

After two weeks exposure in different conditions, the product is still deuterated up to ~80%. It was not clearly seen which of the peaks would back-exchange faster, however it can be speculated that the two peaks at 2.2 and 2.4 ppm would back-exchange faster, as the deuterium is incorporated faster at these positions.

By comparing all the figures, it can be seen that both methods show comparable results. The spectra taken in chloroform are slightly more blurry, and the integrals for peaks 2.4-2.2 have to be combined as the two groups cannot be distinguished from each other. Method 1 is more laborious as it entails the extra steps of transferring the sample to a round bottom flasks, removal of the solvent and addition of deuterated chloroform. Chloroform itself is also slightly acidic, and could act as an extra catalysts to the reaction, pushing it slightly forward. Although during the time course of two weeks, the results were comparable to those of Method 2. Regarding the second method, the spectra were more difficult to analyse and interpret towards the end of the experiment. Apart from this disadvantage, the Method 2 approach has an overall advantage in that the same sample is analysed over time, without any external factors affecting the outcome of the analysis. Another clear advantage, is the ease and minimal interference with the sample, the approach offers as it is possible to use normal solvents and analyse them directly with presaturation and diffusional methods.

Conclusion

The proposed synthetic method proved to be very successful in incorporating deuterium with a very high deuterium incorporation yield. The method is very simple and can be carried out in a single step in a round bottom flask.

The NMR spectra of both testosterone and deuterated testosterone in deuterated methanol were fully assigned. The two sets of spectra complemented each other and comparison with literature assignment showed shifting/moving of peaks depending on solvent used.

Although a peak shift was seen for the deuterated compound in Raman (and a small shift in IR) the shift might not be enough of a difference to be distinguished from skin peaks.

The in-exchange of deuterium to the compound is very fast and completed within minutes. The reaction starts as soon as the acid is added.

The deuterated product is still deuterated to 80 % after two weeks of exposure to acidic, mild heat and neutral environments.

The ability to use normal solvents to monitor deuteration and stability of compounds via diffusion or presaturation experiments has a great future potential regarding minimising interference with the sample. Using two methods in combination also minimised the use of deuterated solvents.

Chapter 5

COMBINING RAMAN SPECTROSCOPY AND SKIN DIFFUSION EXPERIMENT

Introduction

Raman is, just like IR, referred to as a vibrational spectroscopic method. However, the difference lies in that where IR measures the light absorbed by a molecule at a specified frequency, Raman depends on scattering of the light. When light is shone upon a sample, different optical phenomena are observed: transmission, absorption and scattering. The latter, albeit a rather weak effect, forms the basis of Raman spectroscopy.

The light to sample interaction can be looked on as a collision, and this collision can be either elastic or inelastic. Raman relies on inelastic collision, where the energy transfer changes after a collision (as opposed to elastic collision, also known as Rayleigh scattering, where the scattered photons are detected at the same frequency as the incident photons). Either the scattered photons lose energy in a process called Stokes scattering, or they can gain energy, known as anti-Stokes scattering. (Franzen and Windbergs, 2015) Raman spectroscopy can be used to study the skin below the surface; it has the advantage of being highly molecule specific and thus the cross-absorption problem is circumvented. (Caspers *et al.*, 2001)

Usually, testosterone topical formulations have a high content of ethanol, which upon application to the skin will evaporate leaving the drug in a transient supersaturated state. This is a desirable effect, however mostly the supersaturated state is too unstable and transient that the drug will crystallise out instead, with an obvious impact on the skin permeation and kinetics of the drug.

The reason for doing skin experiments using Raman is that, in contrast to other techniques such as IR, the surface of the skin can be scanned and analysed. This could inform us about how the drug is distributed over an area and if a correlation to certain anatomical sites (for example hair follicles) could be made, would give information about the penetration pathway of a drug.

Material and methods

The materials used and the preparatory steps for reagents and general methods regarding skin diffusion are all described in chapter 2, unless otherwise specified.

Chemicals and reagents

Fisher

Sodium hydroxide

Fluka

Isopropyl myristate (IPM)

Lubrizol

Carbopol®, 980 NF polymer

Sigma-Aldrich, UK

Poly(ethylene)glycol (average Mn 400), testosterone (T1500 -1 G, ≥98 %)

VWR

Ethanol

Milli-Q water was used for all experiments.

Part I

USING RAMAN SPECTROSCOPY TO EXPLORE THE PHYSICAL STATE OF TESTOSTERONE IN THE SKIN

Experimental methodology

Testosterone solution for skin experiments

Required amount of testosterone was first dissolved in EtOH, next PEG400 was added. The final testosterone concentration was 41.59 mg/ml in 75:25 EtOH:PEG400.

Diffusion and tape stripping experiment

A piece of dermatomed dorsal skin, with a nominal thickness of 750 µm was placed on top of cotton pads soaked in PBS, and then the ensemble was placed on a glass slide. The edges were covered with Parafilm® to minimise evaporation. An additional piece of skin, a smaller sample from the same pig and used as control, was prepared in exactly the same manner. The testosterone solution (0.7 ml) was applied to the larger skin piece (~35 cm^2) only and then both sets were put into a crystallising dish and covered with Parafilm®. The dish was placed in an oven set at 32 °C, for 24 hours.

After 24 hours, the treated skin was cleaned with isopropanol wipe, although a piece of the skin was left uncleaned. The final experimental design after treatment and tape stripping is depicted in figure 55.

Three tapes of each size (4.5 cm x 2.5 cm, 3.0 cm x 2.5 cm and 1.5 cm x 2.5 cm) were cut. The three largest size tapes (4.5 cm x 2.5 cm) were used first, followed by three tapes of size 3.0 cm x 2.5 cm and lastly the tapes of size 1.5 cm x 2.5 cm were used to tape strip the treated skin, as seen in figure 55. The purpose was to generate skin sections of different depths and to observe the physical state of testosterone after application. A map analysis with Raman spectroscopy was performed on each section of the skin in figure 55. Raman spectra were acquired with an inVia Raman Microscope (Renishaw), with an excitation wavelength of 785 nm and a 50x long objective, every two micrometre along lines on the surface of each section of the skin. A sample of Raman map analysis spectra on treated skin without cleaning (*i.e*. the section to the far left in figure 55) is shown in figure 56.

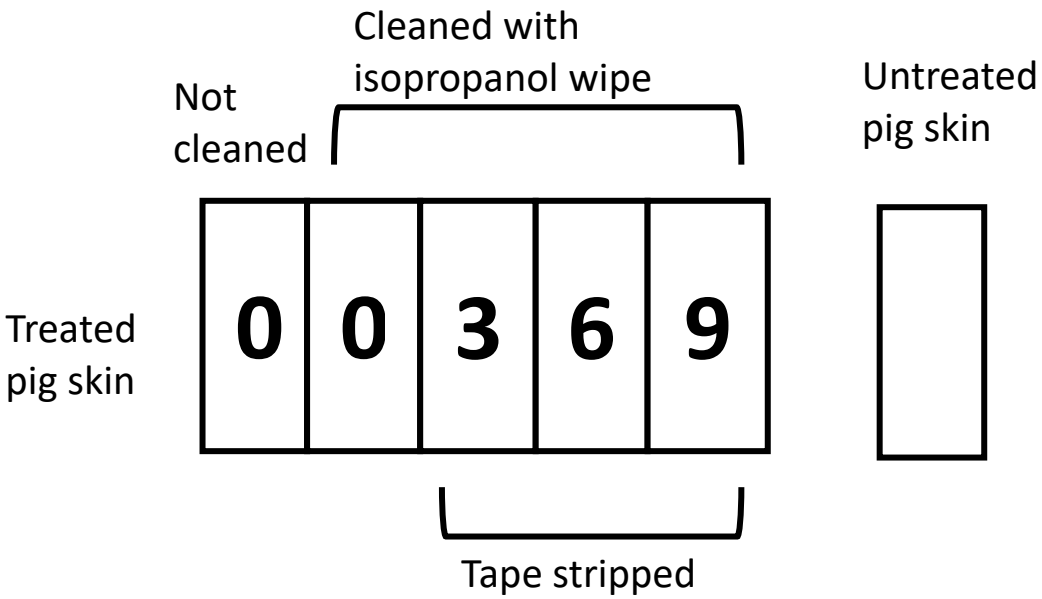

Figure 55. Experimental design followed for Raman spectroscopy experiments. The numbers indicate number of tapes used on each skin section.

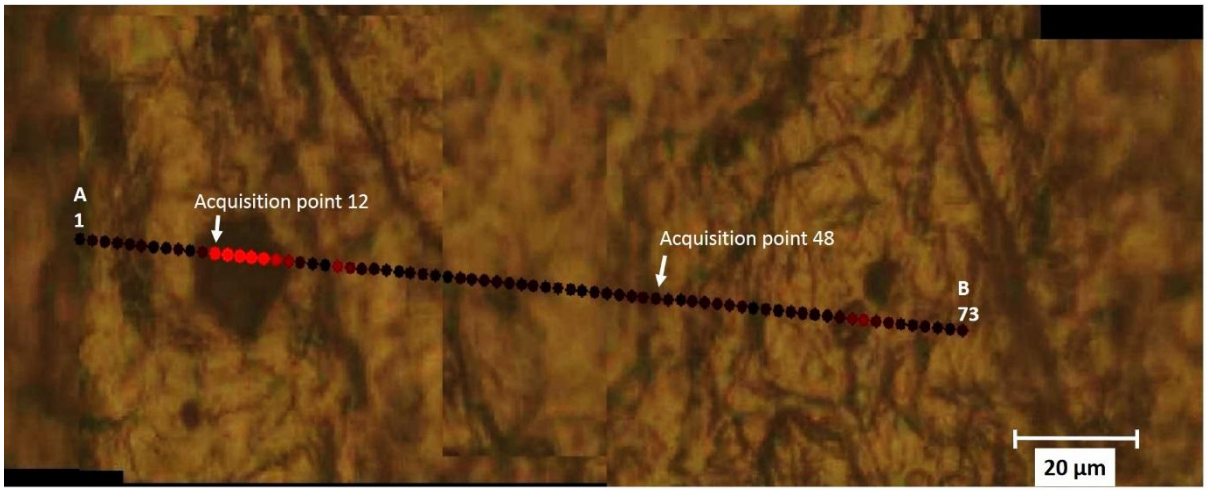

Figure 56. The optical image is a reconstruction of a series of photographs taken along a line along the piece of the treated skin without cleaning, and then merged together. The red dots (moving from A to B) show the locations of where each spectrum (1-73) is taken

As a comparison, a standard diffusion tape stripping experiment was carried out to determine the absorption of testosterone under similar donor conditions as the Raman experiment, but 0.5 ml of testosterone solution was applied on the donor side. The diffusion experiment utilises a Franz cell where a membrane (in this case dermatomed skin, nominal thickness of 750 µm was used) is clamped between a receptor compartment filled with phosphate buffered saline, and a donor

chamber where the compound of interest is applied. The Franz cell is connected to a waterbath set at 37 °C through a water jacket. After 24 hours the Franz cell was dismantled and the skin was cleaned and tape stripped as for the Raman experiment.

Part II

USING RAMAN SPECTROSCOPY ON DEUTERATED TESTOSTERONE AND SKIN DIFFUSION EXPERIMENTS

Introduction

Raman is suitable for skin experiments as it is relatively non-invasive and non-destructive, however the problem lies in that the skin has two broad spectral peaks that can shield the drug peak of interest. Background fluorescing either from the drug or skin is also a problem that affects the results.

Previous tape stripping skin experiments with testosterone involving Raman spectroscopy have shown limited results as skin with its complex structure showed very strong peaks in the Raman spectra and overlap with the testosterone.

Therefore it was hypothesised that labelling testosterone with deuterium could circumvent the low sensitivity seen with Raman and shift the peak of interest away from the skin peaks. The previous chapter describes how testosterone was successfully deuterated at five positions, and also how the Raman signalling peaks from the new compound was distinguished from testosterone.

In this part, using deuterated testosterone, two different protocols were used. The first protocol is different from work in Part I in that deuterated testosterone is used as the drug to study in two different formulations, while the second protocol has a different approach regarding assembly of the experiment, by using a Franz cell.

Experimental methodology

Preparing formulations

Deuterated testosterone solution for skin experiments

See preparatory method in Part I "Testosterone solution for skin experiments" corresponding amount of deuterated testosterone was used.

Gel formulation

The prepared gel was based on the marketed AndroGel ® (distributed under license in Europe as Testogel®) composition, listed in table XXIX, using corresponding amount of deuterated testosterone.

Table XXIX. Composition of AndroGel®, from patent WO 2006/027278 AI (page 44).

Composition of AndroGel®	Amount (g) per 100g gel
Testosterone	1.0
Carbopol 980	0.90
Isopropyl myristate	0.50
0.1 N NaOH	4.72
Ethanol (95 % v/v)	72.5*
Purified water	Up to 100

*corresponding to 67 g of absolute ethanol.

The gel was prepared as described in the patent WO 2006/027278 AI (page 44), although only 10 g were prepared

Preparing for the experiment

The deuterated testosterone was prepared (as described in the previous chapter). Testosterone (0.13 g, 0.44 mmol) was added to a round bottom flask, together with CH_3OD (5 ml) and acetyl chloride (125 µl) under magnetic stirring overnight. CD_3OD (0.5 ml) and acetyl chloride (25 µl) was added. The reaction was monitored by NMR.

Carbopol 980 (0.093 g) was slowly added to water (10 ml) under magnetic stirring. Upon dissolution of Carbopol, the solution was left to stir for another hour. The mixture was stored in the round bottom flask with a rubber septum stopper for 48 h.

Day of experiment

The drug and EtOH (7.79 g) were added to a round bottom flask. When everything was dissolved, IPM (105 µl ~0.05g) was added. The round bottom flask was sealed with a rubber septum and set aside. The Carbopol mixture was added to the EtOH/drug mixture with the help of a syringe and needle. The mixture was under stirring upon addition of 0.1 N NaOH (472 µl *3). The two additional 472 µl was added because the gel did not thicken. However upon addition, the gel still did not set properly, having a more runny appearance.

Skin diffusion experiment

Protocol 1. Diffusion experiment using Franz cell

One Franz cell diffusion cell (with an area of 2 cm^2) was assembled and full thickness pig skin (~0.7 cm) from the dorsal area was used as a membrane. For this experiment deuterated testosterone solution (74.7 µl) of 41.59 mg/ml 75:25 EtOH/PEG400 solution was applied with the use of an Eppendorf pipette. The assembled Franz cell was put into an oven set at 32 °C.

This Franz cell also served as a comparison to the other skin diffusion experiments where big pieces of skin have been exposed to drug formulations.

The experiment was run for 24 hours, a sample was taken out from the cell (which has a total volume of 7.4 ml) towards the end of the experiment. The receptor solution sample was filtered and put into a HPLC vial.

The setup of this experiment differed from previous setups in that Raman spectra were taken alternately with tape stripping.

The piece of skin was carefully transferred to Parafilm® and put under the microscope. Line spectra were taken before cleaning the skin, after cleaning the skin with isopropanol wipes (ten strokes), and after 3, 6, 9 and 12 tape strips. In total, this took ~3 hours.

All the tapes and membranes were then extracted according to the protocol described previously.

Protocol 2. Larger skin piece diffusion experiment with EtOH/PEG400 formulation

The experiment was carried out as previously described in Part I (see “Diffusion and tape stripping experiment”) but using full thickness skin (~0.7 cm) and the deuterated compound instead. The same drug solution as in Protocol 1 (1.344 ml) was applied to the big skin piece (36 cm^2), after which the procedure was the same as previously mentioned.

As a positive control, two Franz cell diffusion cells (with an area of 2 cm^2) were assembled and full thickness pig skin (~0.7 cm) from the dorsal area was used as a membrane. The drug formulation (74.7 µl) was applied with the use of an Eppendorf pipette. The assembled Franz cells were put into an oven set at 32 °C.

The experiment was run for 24 hours, after which a cleaning procedure and tape stripping were carried out as described in previous chapter.

The tape strips taken from the Raman experiment were not extracted nor analysed.

Protocol 3. Larger skin piece diffusion experiment with gel formulation

The diffusion experiment used dorsal skin (32 cm^2) from pig, and the gel (1.066 ml) was applied with a micropipette. The experiment was carried out as previously described in Part I.

As a positive control, two Franz cell diffusion cells (with an area of 2 cm^2) were assembled and full thickness pig skin from the abdominal area was used as a membrane. The deuterated testosterone gel (67 µl) was applied with the use of an Eppendorf pipette. The two Franz cells were placed in an oven set at 32 °C. The following procedure was carried out as previously described.

Raman settings

The spectroscopic parameters for these set of experiments were the same as previously used in Part I.

For each of the experiments (except for the EtOH/PEG400 solution on large skin piece) two line maps were drawn on each section on the skin, one “short step” map where spectra were taken every two micrometres apart, and one “long step” map, where spectra were taken every five micrometres apart.

Data analysis methodology

The Raman spectra data were smoothed using a 19 point second order polynomial Savitzky-Golay filter and the baseline was subtracted using the intelligent background fitting function in Renishaw WiRE 4.2 software. Figure 57 show a stacked spectra plot of the data analysis process. The upper spectrum a) shows an example of a non-processed spectrum of deuterated testosterone gel on skin, before cleaning procedure, the middle spectrum b) shows the same spectrum (a)) after baseline

subtraction and lastly, lower spectrum c)shows the spectrum after baseline subtraction and smoothing.

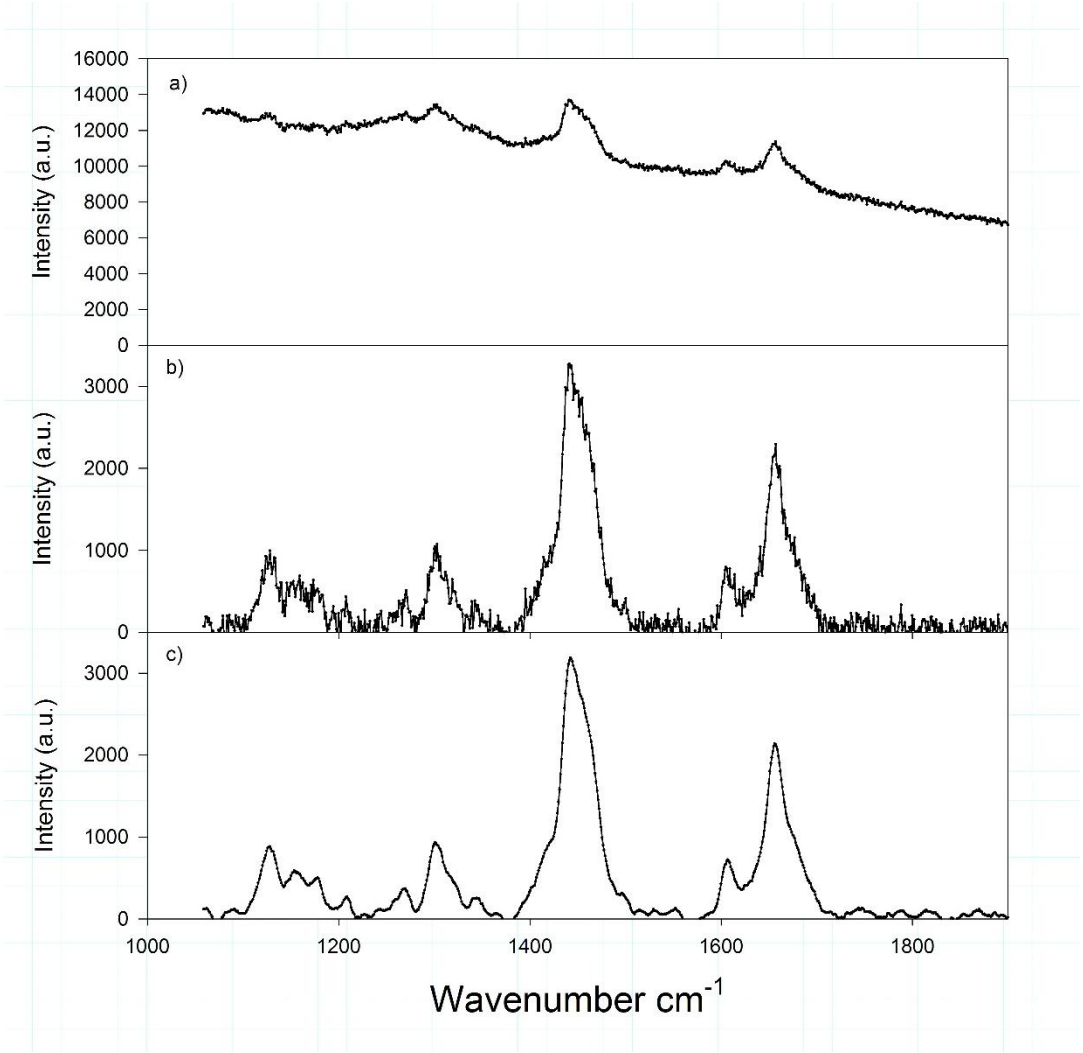

Figure 57. Stack plot of Raman spectra of a) non-processed spectrum of deuterated testosterone gel on the skin, b) same spectrum (a)) after baseline subtraction, and finally c) the same spectrum (a)) after baseline subtraction and smoothing.

Raman spectra

Spectra were acquired from pure skin without treatment, pure testosterone powder on a glass slide and deuterated testosterone on a glass slide. These spectra are shown as a stack plot in figure 58. The upper Raman spectrum a) depicts spectrum of untreated porcine skin which showed strong bands at 1449 and 1654 cm^{-1}, corresponding to the amide I vibration and CH_2 vibration, respectively (Xiao *et al.*, 2004). The middle spectrum b) shows pure testosterone powder on a glass slide. Testosterone showed a strong band at 1610 cm^{-1} (T1) and at 1640 cm^{-1} (T2), however since the latter peak overlaps with the skin peak region, the former peak was used as a marker for testosterone detection.

In the lower spectrum c) deuterated testosterone, showed a strong band at 1600 cm^{-1} (dTST1) and 1650 cm^{-1} (dTST2). The arrow shows the C-D bond, deuterium region. It was anticipated that the new peaks at the deuterium region could be used as references in skin diffusion experiments, as they clearly are separated from the skin peak region. However, due to the low intensity of the peaks and the level of noise (seen more clearly in spectrum a) at 1800-2000 cm^{-1}) it was not feasible, instead the peak dTST1 (spectrum c) in figure 58) was used as reference in skin diffusion experiments. Figure 59 show a stack plot of testosterone and deuterated product, where it is clearly seen that the two main peaks (dTST1 and dTST2) of the deuterated product have shifted from the testosterone main peaks (T1 and T2).

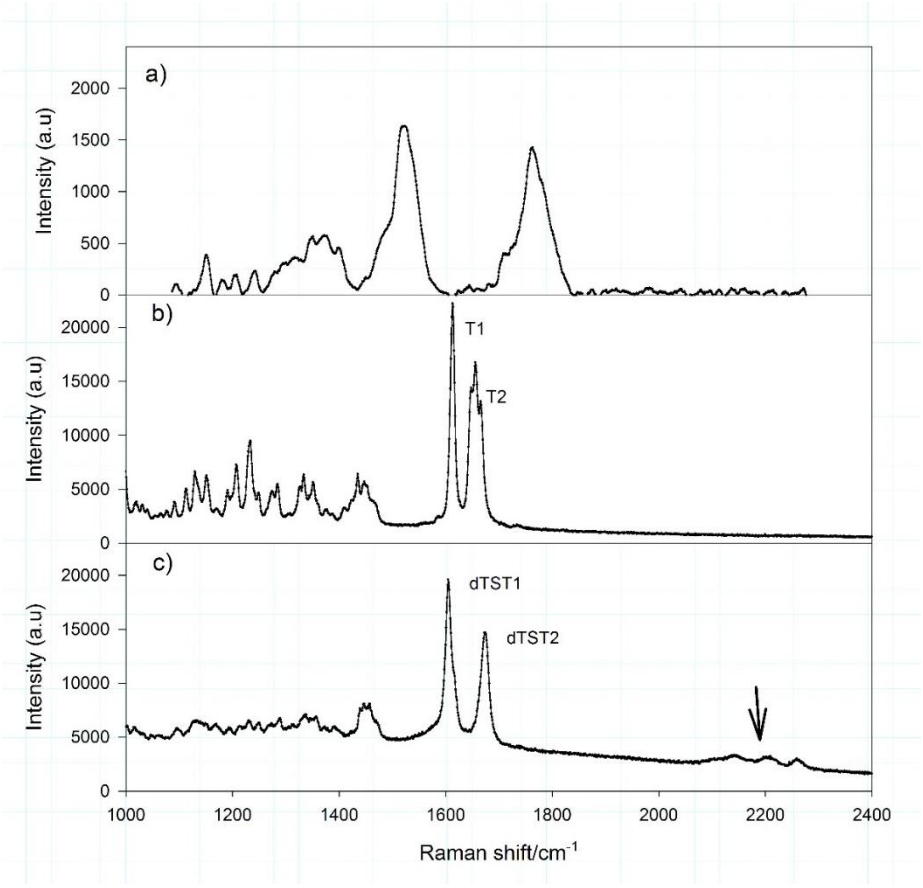

Figure 58. Stack plot of Raman spectra taken with excitation wavelength of 785 nm and a 50x long objective of a) control skin b) pure testosterone on glass slide, and c) deuterated testosterone on glass slide. In spectrum c) the arrow shows the upcoming peaks belonging to C-D bonds.

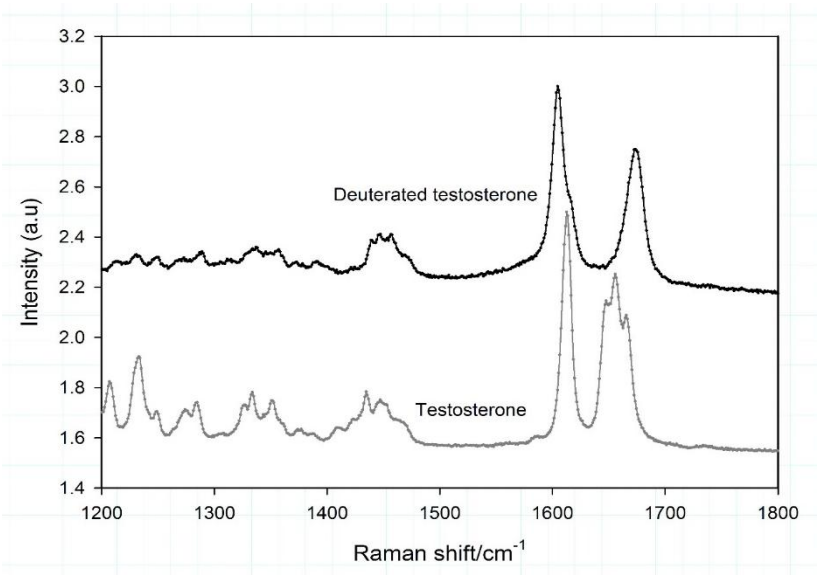

Figure 59. Stack plot of testosterone (lower spectrum) and deuterated testosterone (upper spectrum). Both spectra are normalised to the highest intensity (peak ~1600 cm^{-1}).

Results

Part I. Using Raman spectroscopy to explore the physical state of testosterone in the skin

A series of spectra were taken along a line (see figure 56 for an example of line map analysis) on:

a) untreated skin
b) skin treated with testosterone without cleaning
c) skin treated with testosterone cleaned with isopropanol wipe and
d) skin treated with testosterone and cleaning after 3, 6 (e) and 9 (f) tape strips

The experimental design is shown in figure 55. Figures 60 (taken at point 12) and 61 (taken at point 48) in figure 56, show example of two Raman spectra taken along the map analysis line on skin treated with testosterone without cleaning (b). When comparing figures 60 and 61 with spectra a) and b) in figure 58, it is clear that figure 60 shows a spectrum of a drug crystal, whereas figure 61 shows a spectrum where the skin peaks are more prominent.

In figure 56, each point indicates a skin spectrum being taken and by calculating the signal to baseline intensity of the drug peak (at 1610 cm^{-1}) to that of the skin peak (at 1449 cm^{-1}) an intensity ratio drug peak to skin peak can be plotted as a function of distance (figure 62). The ratio at each spectral point is depicted using different shades of red depending on the intensity ratio. Where the points are very bright and clear red in figure 56, suggests a higher intensity from the drug peak than from the skin peak. For example, the drug peak intensity is clearly higher than skin peak intensity at acquisition points 11-13, at the distance of ~35 µm along the line in figure 62, and at the same distance in figure 56, the colour is very bright red. By analysing the spectra in that region (spectrum number 12 which is shown in figure 60) it is clearly seen that the spectra match well with that of testosterone drug crystal, as previously mentioned. In figure 62 at around 115 µm the corresponding region (~acquisition point 48) for this spectrum in figure 56 is coloured black, meaning that the intensity ratio drug peak to skin peak is low. This is further confirmed by figure 61, which shows spectrum 48, where it is clear that no visible drug peak is seen.

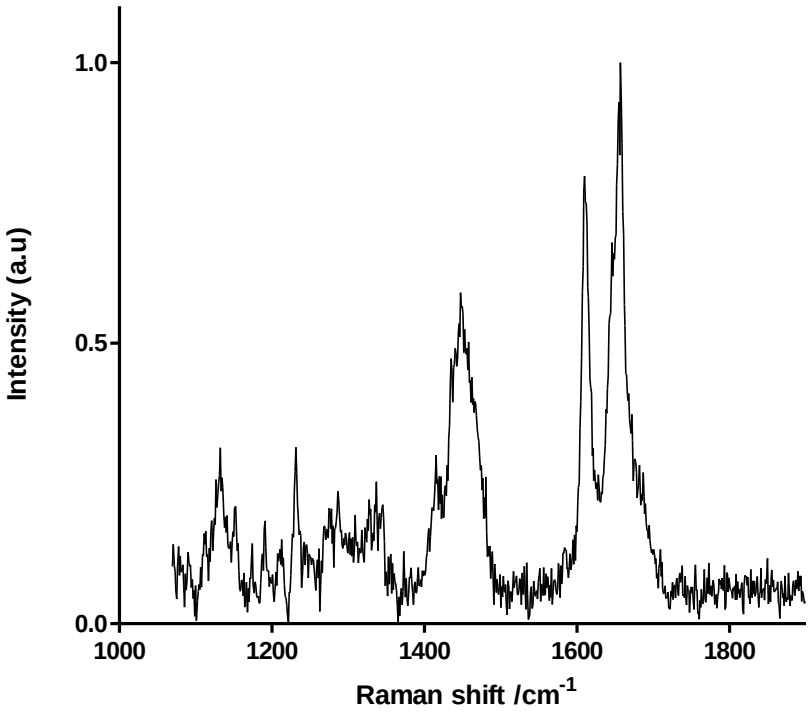

Figure 60. Raman spectrum at acquisition point 12, along the dotted line seen in figure 56.

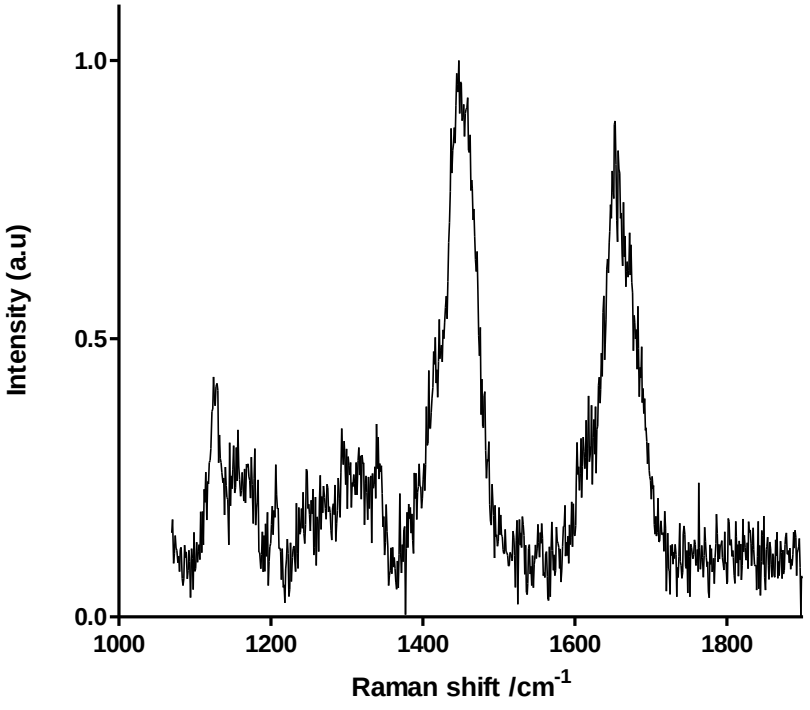

Figure 61. Raman spectrum at acquisition point 48, along the dotted line seen in figure 56.

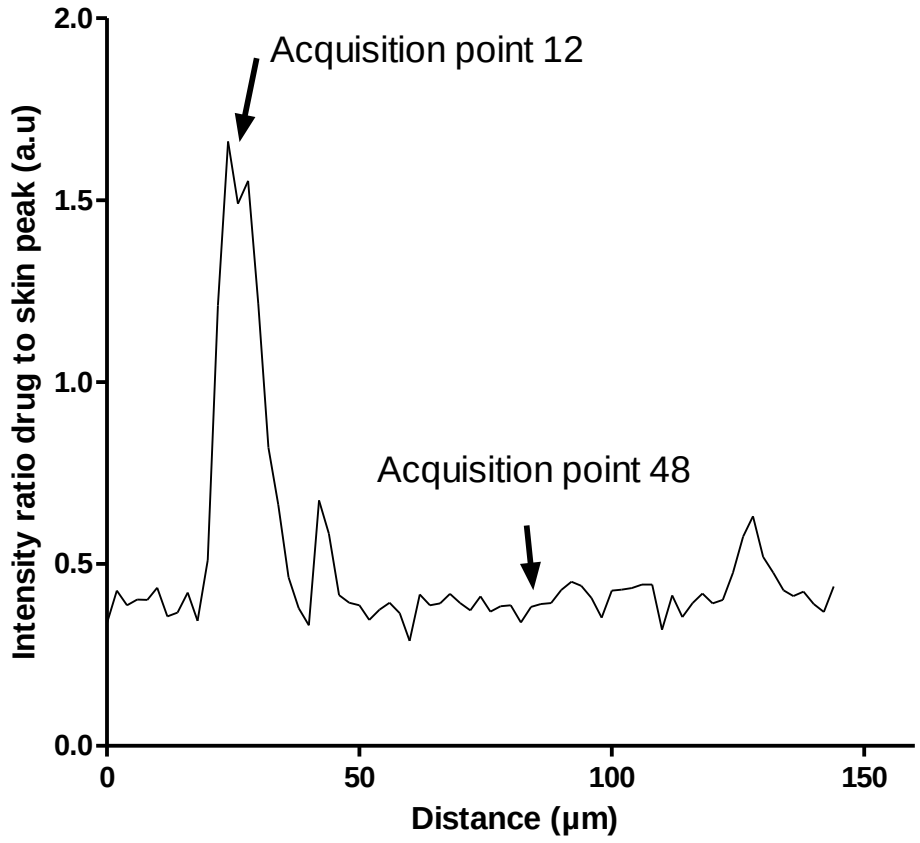

Figure 62. Intensity ratio, $IR_{drug/skin}$, for Raman shift of drug at 1610 cm-1 to skin at 1449 cm-1, along the line shown in figure 56. The arrows denote the intensity ratio for spectral acquisition point 12 and 48, also shown in figure 56.

The intensity ratio (figure 62) from all skin sections are plotted together in one graph in figure 63. From this figure it is evident that higher drug intensity ratios clearly are seen in the first two sections of the layered skin, suggesting the presence of testosterone on the surface of cleaned and uncleaned sample. Figure 64 shows the average intensity ratio drug peak to skin peak for figure 63. Again, it is clearly seen that there is more drug detected in the superficial layers, and that the intensity ratio is higher in these layers, confirming the present of testosterone in the superficial layers of the skin.

The results after 3 tape strips indicate a small hint of drug peak (figure 63), this is further confirmed by the spectrum shown in figure 65, where a small peak of testosterone is seen albeit with a very low intensity. The spectrum was taken at acquisition point number 12, shown by the arrow in figure 63. No drug was detected on skin tape stripped 6 and 9 times.

However, this could be due to limitation of detection of the instrument, rather than the drug not being absorbed since testosterone was detected both in tape 12 and in the receptor solution by HPLC.

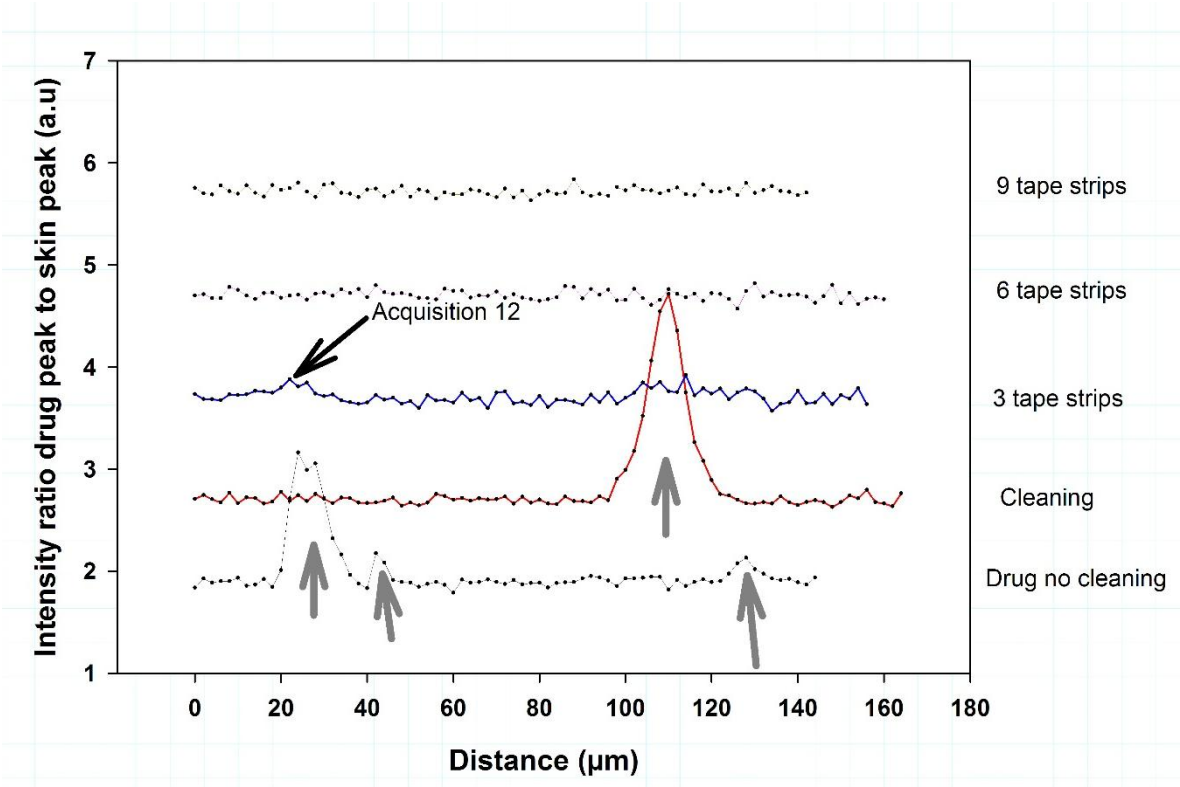

Figure 63. Intensity ratio for each section of the skin in figure 55 plotted together in the same figure. Bottom to top is intensity ratio spectra for skin submitted to no cleaning, cleaning, 3 tape strips, 6 tape strips and 9 tape strip respectively. The black arrow shows a possible intensity peak after 3 tape strip, at spectral acquisition point 12. Grey arrows denote peaks associated with drug.

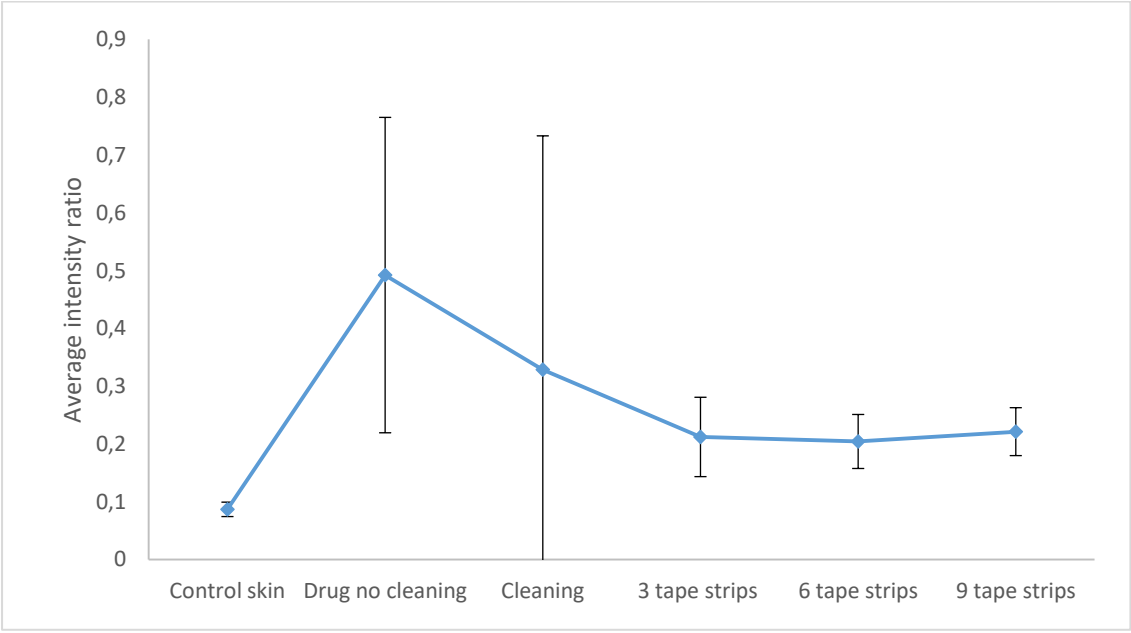

Figure 64. Average intensity of ratio drug peak to skin peak, per depth for Part I experiment. The range of signal to axis intensity was for drug 1600-1620 Raman shift/cm^{-1-} and for the skin 1439-1459 Raman shift/cm^{-1}

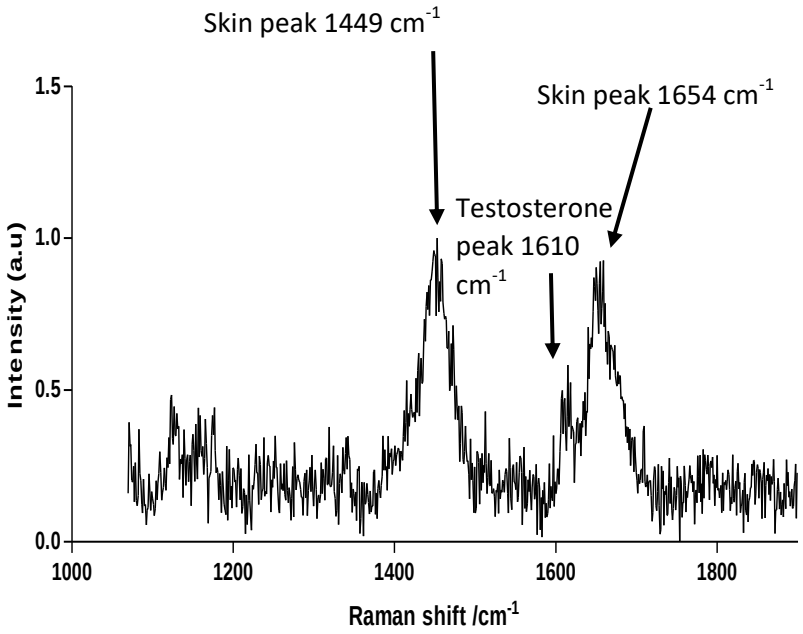

Figure 65. Raman spectrum at acquisition point 12 from the map analysis from a treated skin sample tape stripped 3 times. The two skin peaks at 1449 Raman shift/cm^{-1} and 1654 Raman shift/ cm^{-1} are clearly visible and testosterone peak at 1610 Raman shift/cm^{-1} is also observed.

Part II. Using Raman spectroscopy on deuterated testosterone and skin diffusion experiments

In all experiments, there were no clear drug crystals detected and there were more difficulties with fluorescence in spectra encountered compared to Part I.

Protocol 1. Diffusion experiment using Franz cell

When stacking spectra from each layer, figure 66, it is clearly seen that there is a drug peak seen in the superficial layers which disappears after a few tape strips.

The right hand side skin peak occasionally overlaps with the drug peak, and the spectra are all normalised to intensity and it is therefore not obvious in this spectral presentation that the intensity for all peaks change on each spectrum on the line. Therefore it was proposed that choosing a skin range where the maximum intensity is not affected and thus affect the intensity ratio, while still being apparent and distinguished in the spectra, would increase the sensitivity for ratio calculations. The new range chosen was 1630-1650 Raman shift/cm^{-1}.

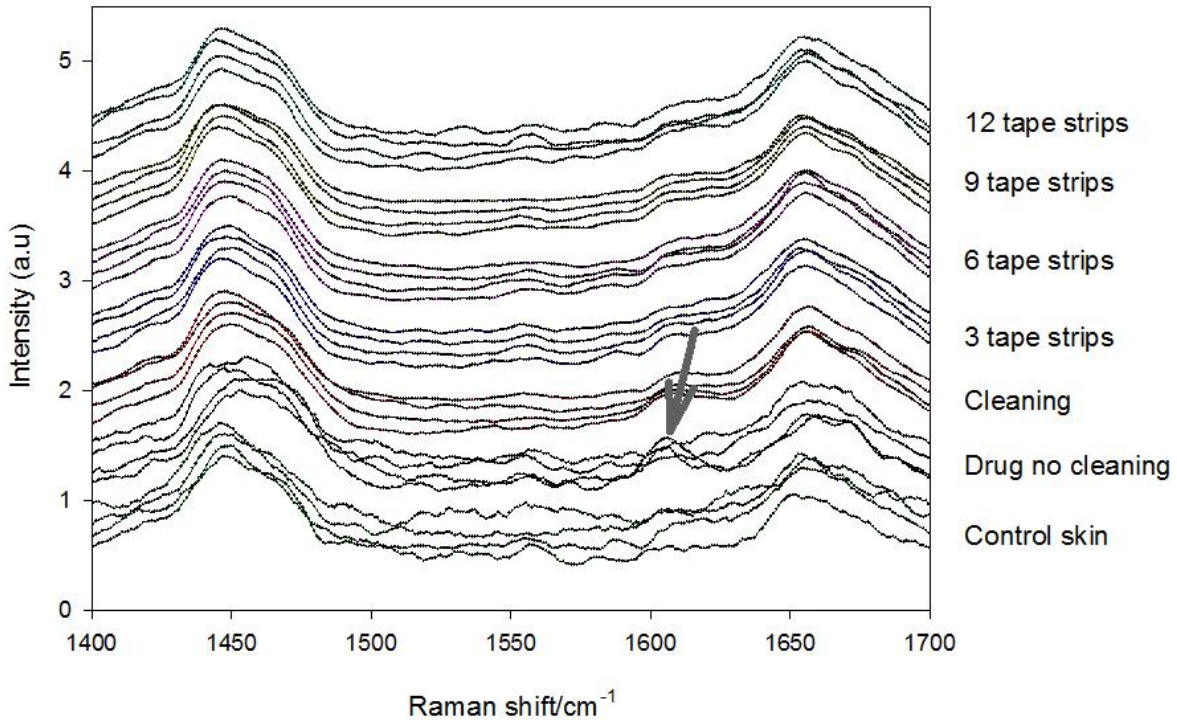

Figure 66. Stacked spectra for Franz cell experiment. Four spectra from each layer stacked together. The first two spectra in each row are spectra which according to the intensity ratio map show a high intensity, while the two latter in each row are spectra with small intensity ratio. The grey arrow in the figure denotes drug peak. All spectra are normalised to intensity.

The experiments were first processed as in Part I, however it was quickly discovered that this would be difficult. In all sets of experiment in Part II, there were no clear crystals detected, hence interpretation of spectra is a challenge. As mentioned in chapter 4, the deuterated product showed a shift in two peaks (1610 Raman shift/cm^{-1} shifted the maximum to 1600 Raman shift/cm^{-1} and

1640 Raman shift/cm^{-1} shifted to 1650 Raman shift/cm^{-1}). Therefore the new range for the drug was set to 1593-1621 Raman shift/cm^{-1}, the skin peak reference range remained the same. Figure 67 shows the intensity ratio for all sections in the Franz cell experiment, there is no clear variation in intensity ratio seen, compared to Part I results. Therefore it was decided to change the skin reference range from 1439-1459 Raman shift/cm^{-1} to 1630-1650 Raman shift/cm^{-1}. This new wavelength range was chosen because it lies in between the maximum of the skin peak (1654 Raman shift/cm^{-1}) and the maximum of the deuterated testosterone reference peak (1600 Raman shift/cm^{-1}).

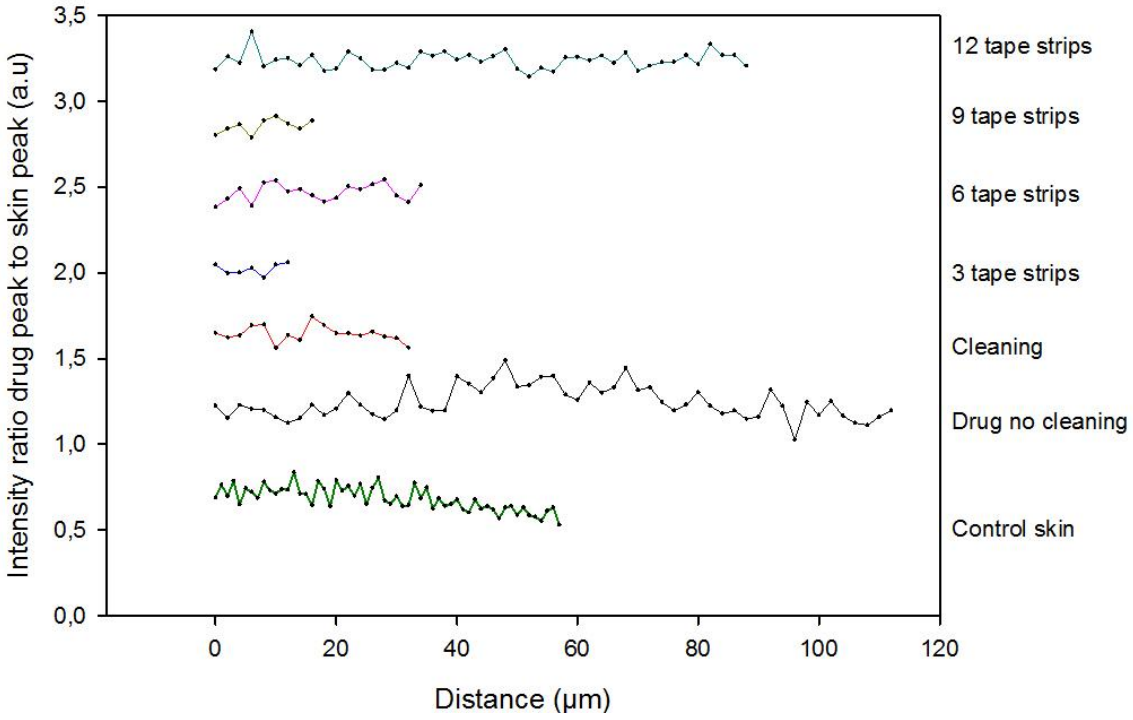

Figure 67. Intensity ratio signal to axis for drug (1593-1621 Raman shift/cm^{-1} to skin peak 1439-1459 Raman shift/cm^{-1} for Franz cell experiment.

In figure 68, depicting the intensity ratio for the drug peak to the new skin reference wavelength range, it is now more apparent that there is a higher variation in drug intensity ratio in the more superficial layers than in the deeper layers. The intensity ratio plot also correspond well with the stacked spectra, and with figure 69, which shows the average intensity ratio per layer. In this figure it is clearly seen that the superficial layers contain drug and have a significant variation in drug concentration, but also an overall higher intensity of the drug peak than in the deeper layers, confirming that the drug is diffusing into the skin.

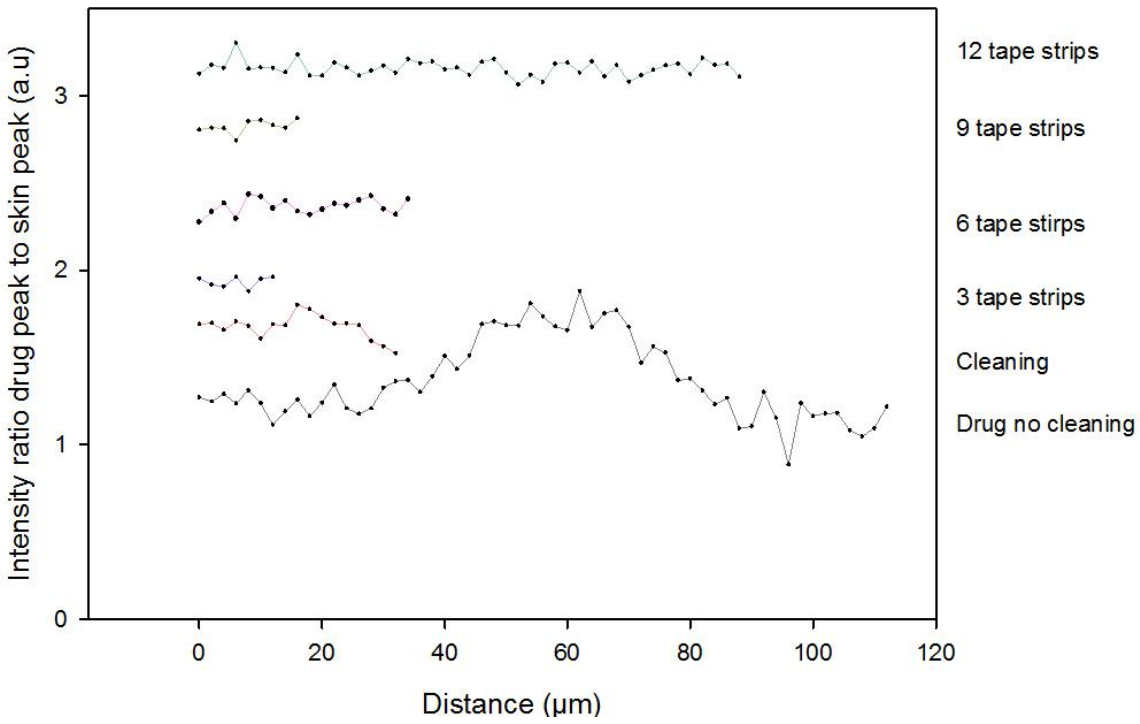

Figure 68. Intensity ratio drug peak (1593-1621 Raman shift/cm^{-1}) to new skin reference wavelength range (1630-1650 Raman shift/cm^{-1}) for Franz cell short step experiment.

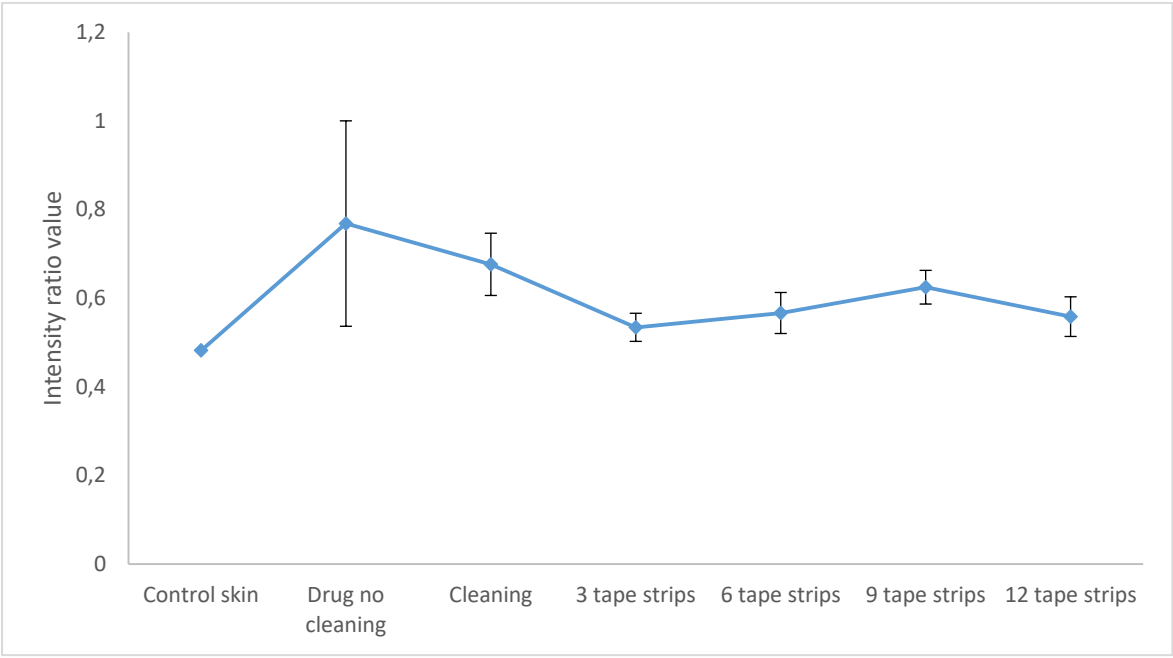

Figure 69. Graph showing the average intensity ratio drug peak (1593-1621 Raman shift/cm^{-1} to skin peak 1630-1650 Raman shift/cm^{-1} per depth for Franz cell experiment.

Protocol 2. Larger skin piece diffusion experiment with EtOH/PEG400 formulation

This particular experiment was a continuation from Part I, but using deuterated drug in the solution applied. Comparing the spectra from this dataset to Part I, there were no clear crystal peaks detected. However, denoted by the arrow in figure 70 below, a clear drug peak was detected in the superficial layers of the skin, which disappears the deeper down in the skin. This is further confirmed in figure 71, where a higher intensity ratio is seen in the superficial layers, and in figure 72 showing the average intensity ratio for the layers of the skin. Again it is clear that a higher drug intensity ratio is seen in the more superficial layers of the skin.

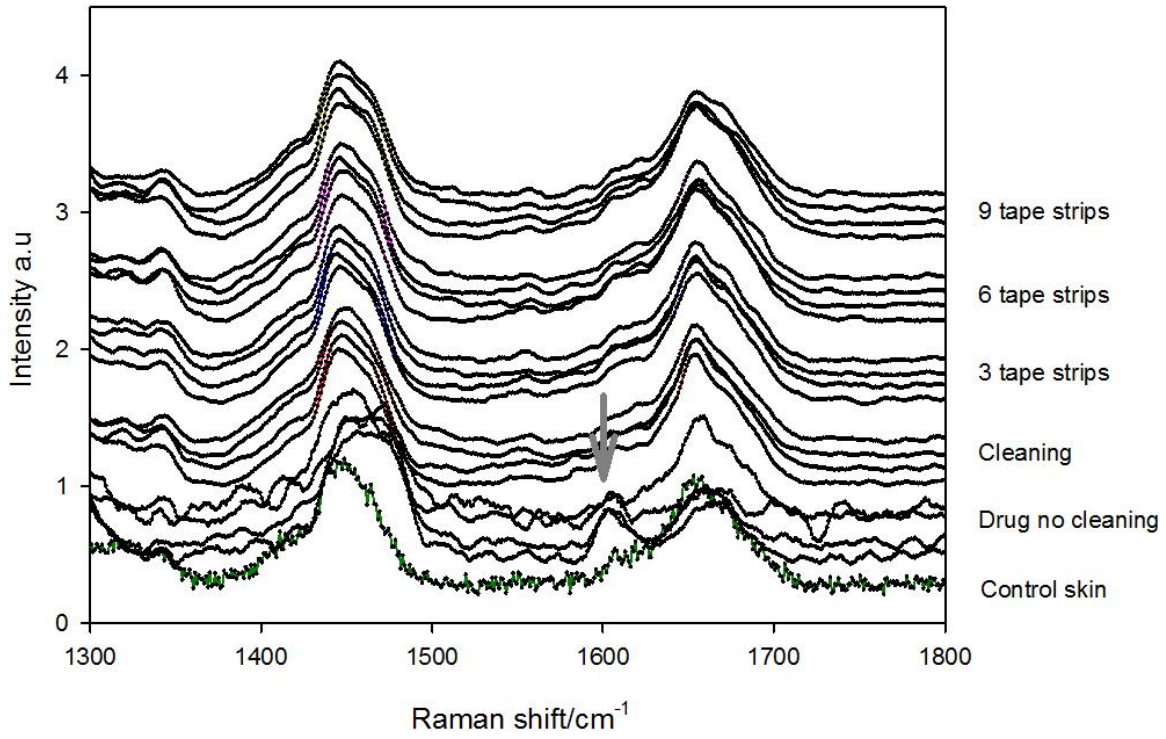

Figure 70. Stacked spectra for deuterated testosterone in EtOH/PEG400 solution. Four spectra from each layer stacked together. The first two spectra in each row are spectra which according to the intensity ratio map show a high intensity, while the two latter in each row are spectra with small intensity ratio. The grey arrow in the figure denotes drug peak. All spectra are normalised to intensity.

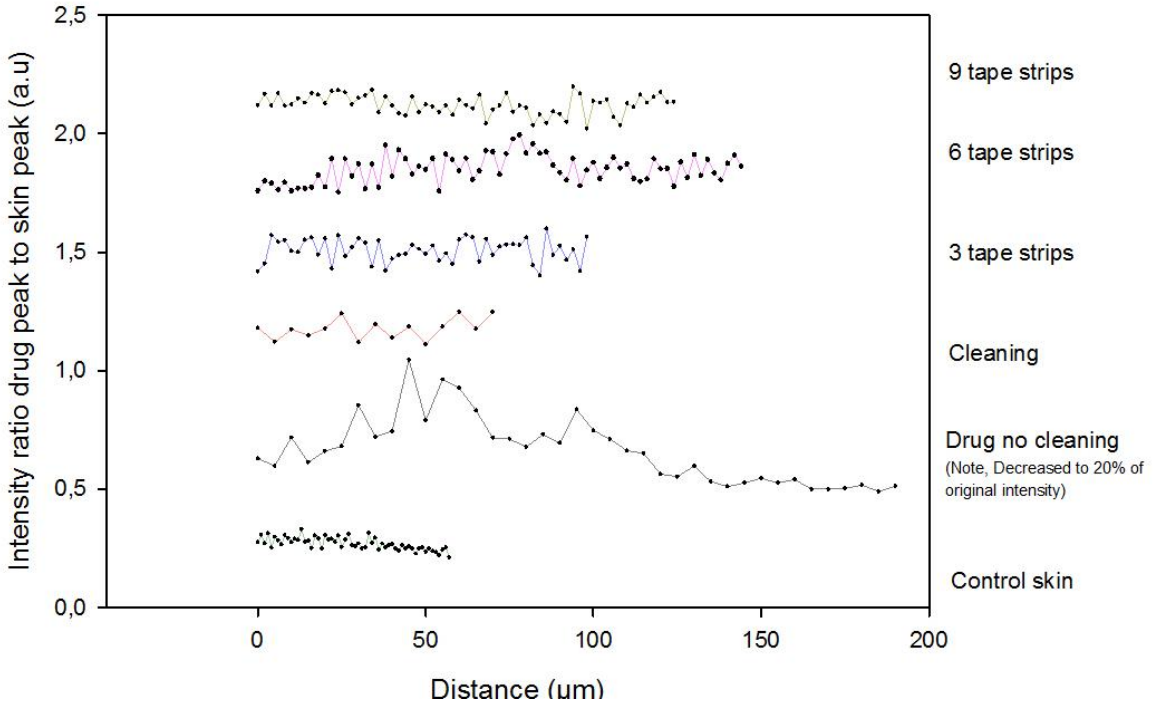

Figure 71. Intensity ratio drug peak (1593-1621 Raman shift/cm^{-1} to skin peak (1630-1650 Raman shift/cm^{-1}) for deuterated testosterone in EtOH/PEG400 75:25 solution.

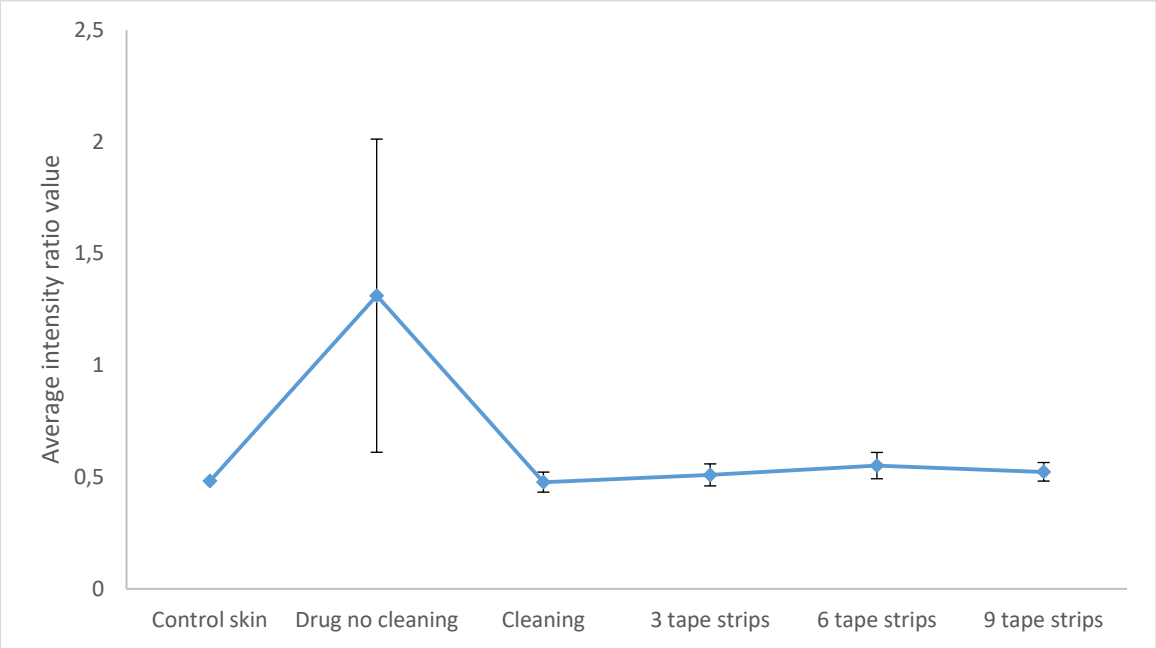

Figure 72. Graph showing the average intensity ratio drug peak (1593-1621 Raman shift/cm^{-1} to skin peak 1630-1650 Raman shift/cm^{-1}) per depth for deuterated testosterone in EtOH/PEG400 75:25 solution.

Protocol 3. Larger skin piece diffusion experiment with gel formulation

This particular experiment was performed in order to investigate how a different formulation than previously used, would behave when applied on the skin. It was proposed that because the product is marketed, and therefore the formulation must be able to deliver the drug through the skin, this experiment might see a different diffusion profile than previous experiments with EtOH/PEG400 solutions.

The encircled area in figure 73, shows no clear diffusion pattern. This is in contrast to previous experiments where a drug peak was detected mostly in the superficial layers and disappeared with depth, while in this experiment, drug was detected in both the superficial layers and after 9 tape strips. In figures 74 and 75 it is seen more clearly that the drug intensity ratio is higher at 3 and 9 tape strips, and in figure 75 also that the average intensity is higher at "drug no cleaning".

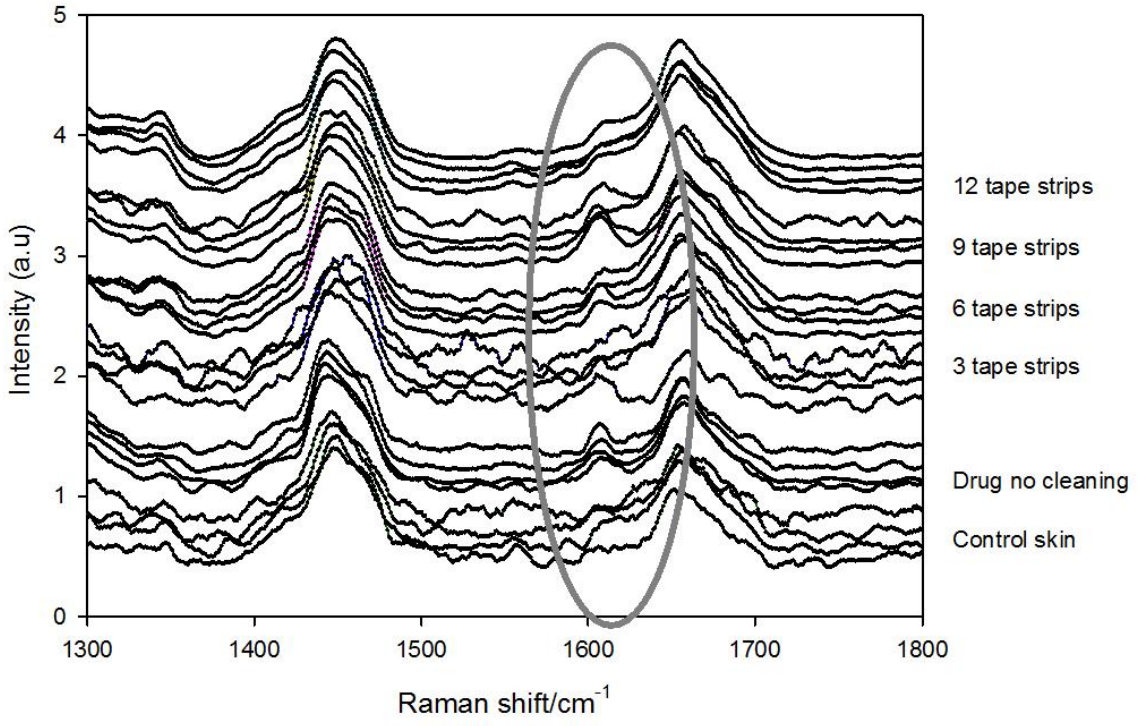

Figure 73. Stacked spectra for deuterated testosterone in gel formulation experiment. Four spectra from each layer stacked together. The first two spectra in each row are spectra which according to the intensity ratio map show a high intensity, while the two latter in each row are spectra with small intensity ratio. The grey circle in the figure denotes drug peak. All spectra are normalised to intensity.

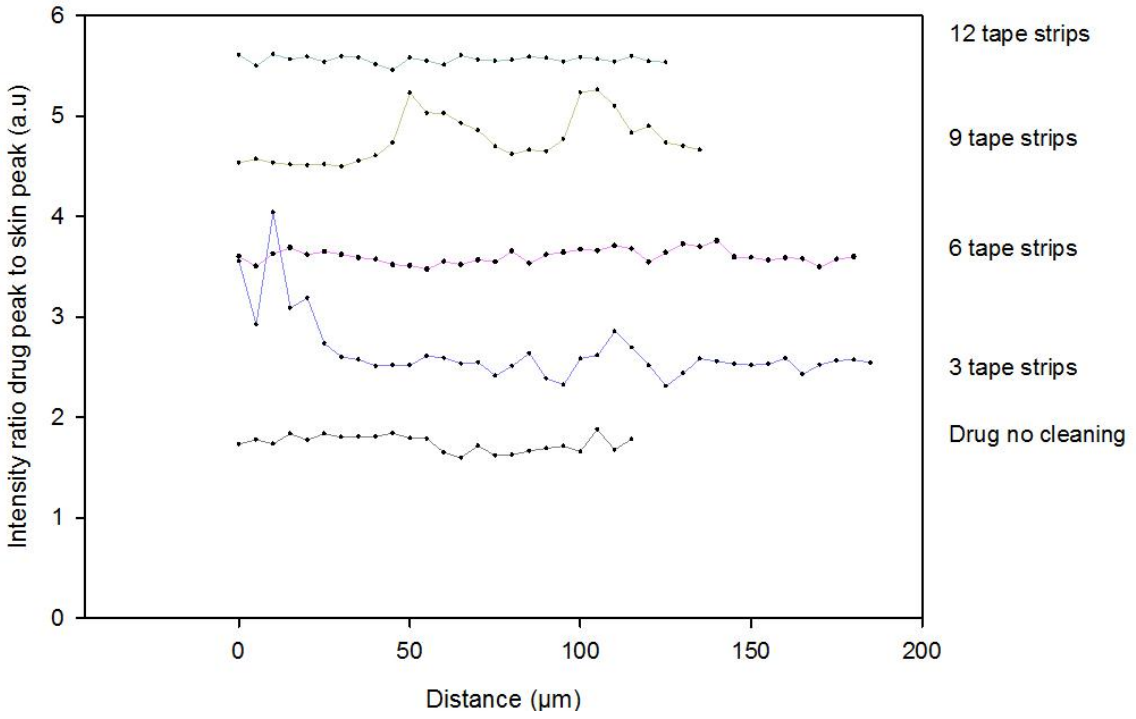

Figure 74. Intensity ratio drug peak (1593-1621 Raman shift/cm^{-1} to skin peak (1630-1650 Raman shift/cm^{-1}) for deuterated testosterone in gel formulation experiment

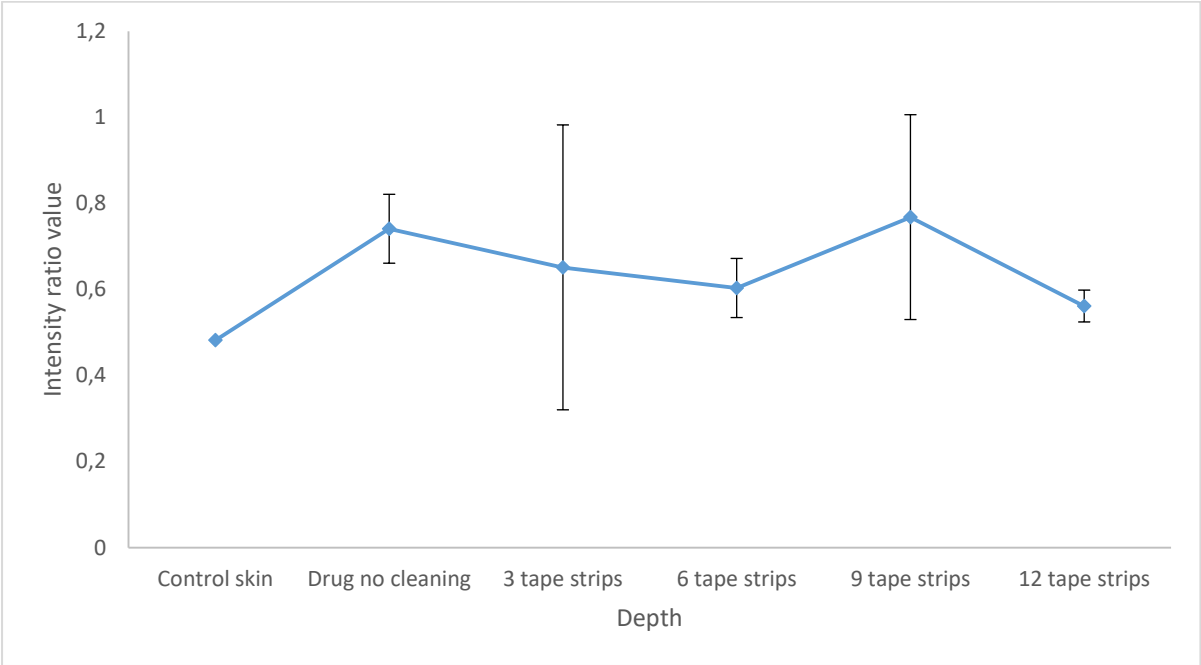

Figure 75. Graph showing the average intensity ratio drug peak (1593-1621 Raman shift/cm^{-1} to skin peak 1630-1650 Raman shift/cm^{-1} per depth for deuterated testosterone in gel formulation.

Discussion

Part I. Using Raman spectroscopy to explore the physical state of testosterone in the skin

Pure testosterone on a glass slide was easily detected with Raman spectroscopy. However when the drug was applied in a formulation on skin, its characteristic peak at 1610 Raman shift/cm^{-1} overlapped with the broad peak at 1654 Raman shift/cm^{-1} from the skin. When the concentration of the drug is small, the intensity of the drug peak drops significantly as well, making it difficult to detect. Both the drug and the skin fluoresce which make it even more difficult to detect. The furthest depth where testosterone was detected was after three tape strips. After six and nine tape strips some diffused drug peaks were detected, however these were not clear crystals and therefore the characteristic high intensity crystal peaks were not observed.

Part II. Using Raman spectroscopy on deuterated testosterone and skin diffusion experiments

The deuteration of testosterone shifted one of the major peaks (at 1610 Raman shift/cm^{-1}) slightly from the skin peak (1654 Raman shift/cm^{-1}) to 1600 Raman shift/cm^{-1} , which made it easier to detect the drug. For these experiments, no crystals were detected.

It was expected that the superficial layers would show an overall higher and more variations regarding intensity ratio due to high drug content, and that the deeper layers would show comparable intensity to the control. Although this was the case for the Franz cell experiment and the EtOH/PEG400 solution, the gel formulation showed a different diffusion profile, where drug was detected both in the superficial and deeper layers of the skin.

It is speculated that due to the nature of the gel, it interferes with the tape stripping in that the stratum corneum does not stick to the tape and therefore is not stripped sufficiently or as uniformly as believed. Using full thickness skin also gives rise to a problem not foreseen; the underlying fatty layer is soft and yields when pressured, making tape stripping difficult, and the uneven layer makes formulations distribute unevenly on the surface.

Because there were no clear drug crystals detected (that would give a strong peak at 1600 Raman shift/cm^{-1}) and because the drug concentration applied is lower (probably due to the full thickness skin being uneven, which may have made the solution and gel distribute unevenly across the surface) than for results in Part I, the intensity ratio is more prone to be affected by changes in the skin peak. The new range for skin peak (1630-1650 Raman shift/cm^{-1}) showed more consistent results that corresponded better with stacked spectra, than when plotting intensity ratio drug peak to skin peak maximum. Also, plotting the average intensity ratio for each layer gives a good overview over the drug diffusion in the layers. Intensity ratio plot gives in conjunction with average intensity ratio and full spectra a more complete information about the drug diffusion in the skin.

Although some problems still remain such as lower sensitivity of detection, and interference of peaks, Raman spectroscopy in conjunction with skin diffusion experiments remains a useful tool to follow the diffusion of a drug. There are still a lot of opportunities in improving the technique, regarding experimental setup and settings. In this particular set of data it obviously would have been useful if the peaks in the deuterium region (~2000 Raman shift/cm^{-1}) had given rise to a high intensity enough to be detected without the drug being in crystalline form, and even if no crystals were detected, which also would have aided the interpretation of spectra. However deuteration of the product was useful in that the peak was shifted, albeit slightly, because this minor difference shifted the drug peak away from the skin peak making it possible to detect smaller amounts of the drug when applied on the skin.

Conclusion

Raman spectroscopy could be used to identify testosterone (crystals) and skin peaks and therefore could be informative about the behaviour of the drug, however fluorescence and sensitivity remains a problem.

Deuteration of the drug shifted the strong drug peak (1600 Raman shift/cm^{-1}) slightly further away from the closest skin peak (1654 Raman shift/cm^{-1}) which increases sensitivity of the Raman detection method. It is demonstrated that the drug can be detected even if it is at a much lower concentration and does not form crystals.

The sensitivity of the Raman detection method can be further increased by increasing the acquisition time in the spectral range of interest. It could be improved even further if methods of reducing the fluorescence background were found.

Although crystals were not detected, spectra can more easily be interpreted regarding intensity ratio if another range of the skin is used, rather than the skin maximum. Stacking full spectra, plotting average intensity ratio and intensity ratio gives useful information about the distribution and diffusion of a drug through the skin layers.

Chapter 6

Discussions and final conclusions

Discussion

This work seeks to understand how testosterone behaves in the skin after application, as this can add to understanding the skin and the stratum corneum better, and the penetration of a drug through this layer. The skin itself presents a challenge in drug delivery, as its purpose is to keep xenobiotic substances out from the body.

Testosterone has been assessed regarding stability and solubility in a range of solvents. Although testosterone is stable in a range of solvents and excipients and in most conditions, it is not easy to predict the behaviour of testosterone in a combination of several excipients.

The drug interacts with the formulation, all the excipients and solvents in the formulation can interact with each other, and also with the skin. In addition, the final product has to be easy to use and accepted by the patient. Transdermal testosterone products have evolved from intramuscular injections giving concentrations in the serum outside the physiological range (Wang and Swerdloff, 1997; Gooren and Bunck, 2004) to gels that give serum concentrations that follow the circadian rhythm of testosterone (Marbury *et al.*, 2003; Wang *et al.*, 2000; McNicholas *et al.*, 2003). However, new challenges arise such as feeling of the gel on skin and cosmetic elegance of the gels, and transfer risk between patients.

Tape stripping and dermatopharmacokinetics are established methods in measuring the concentration of a drug in the stratum corneum after a topical treatment. Previous work with dermatopharmacokinetcs and tape stripping have been able to distinguish between bioequivalent and/or non-bioequivalent topical formulations with a local effect, but not yet for transdermal products. However tape stripping cannot answer all the questions such as the physical state of the drug or the behaviour, or the distribution within an area. The use of skin experiments in conjunction with optical spectroscopy such as IR (Nicoli *et al.*, 2009) or Raman (Adlhart and Baschong, 2011) have been undertaken previously. While the advantages of Raman spectroscopy such as low sensitivity to water content and being molecule specific, have been useful in this project, problems such as overlapping drug peaks and skin peaks, and fluorescence occurred. Crystal peaks were detected on the surface of the skin, but not after a few tape strips.

The overlapping of peaks was circumvented by labelling the drug with deuterium, which shifted two peaks further away from each other and away from the overlapping skin peak. Although the previously clear crystal peaks were not detected, the deuteration allowed lower amounts of the drug to be detected.

These are challenges pharmaceutical formulators face, not only avoiding to combine incompatible excipients, but after combining the right excipients, new unexpected challenges can arise, as seen in

the cases with the gels which circumvented the irritancy problem, to be met by transfer risk to other people.

Combining tape stripping and HPLC can answer questions about quantitative amounts found in each layer of the skin, but not the lateral distribution or the physical state of a drug. Raman spectroscopy can answer the latter, but not the former. NMR is outstanding in determining the structure of a compound, but will be limited when it comes to biological samples.

Conclusions

Testosterone is quickly absorbed into the stratum corneum, and slowly released from there over time.

Testosterone is stable at ambient temperature, ambient light, 70 °C, oxidation and acidic conditions, but less stable in alkaline conditions, indicating stability over the time course used in skin experiments. For all solubility studies, and especially those that are performed in more viscous solvents such as PG and glycerol, measuring solubility for a longer time (72 hours) improved solubility data regarding variation between replicates and relative standard deviation. Testosterone is, in the range investigated, chemically stable in the fifteen solvents assayed.

The proposed synthetic method proved to be very successful in incorporating deuterium with a very high deuterium incorporation yield. The method is very simple and fast, and can be carried out in a single step in the reaction flask. The deuterated product is still deuterated to 80 % after two weeks of exposure to acidic, mild heat and neutral environments.

Raman spectroscopy could be used to identify testosterone (crystals) and skin peaks and therefore could be informative about the behaviour of the drug, however fluorescence and sensitivity remains a problem. Deuteration of the drug shifted the drug peak away from an interfering skin peak slightly, aiding the detection of a smaller amount of drug. Although crystals were not detected, spectra can be interpreted more easily regarding intensity ratio if another range of the skin is used, rather than the skin maximum. Stacking full spectra, plotting average intensity ratio and intensity ratio gives useful information about the distribution and diffusion of a drug through the skin layers.

Future perspective

Dermatopharmacokinetics together with tape stripping gives information about the distribution of drug per mass unit in the skin, but cannot answer all questions about the behaviour of a drug in the skin. The reason for doing skin experiments in conjunction with Raman spectroscopy is that, in

contrast to other techniques such as IR, the surface of the skin can be scanned and analysed. This could inform us about how the drug is distributed over an area and if a correlation to certain anatomical sites (for example hair follicles) could be made, would give information about the penetration pathway of a drug. Also, tracking a diffusing drug's different physical states could give an insight in the interaction between drug and formulation, and drug and skin.

Although there have been problems with sensitivity regarding Raman, it must be remembered that the concentration of drug in the deeper layers of the skin is very low. In addition, the sample matrix, in this case, the skin, shows broad strong bands in a region where probably most of the organic molecules are detected. In this work, the sensitivity issue was circumvented by deuterating the drug of interest, which increased the sensitivity by allowing smaller amounts of drug to be detected. Also, changing parameters such as acquisition time and/or finding a method to reduce fluorescence would increase the sensitivity. There has already been some work using Raman spectroscopy in vivo (Caspers *et al.*, 2001) and measuring drug diffusion in real time (Tfaili *et al.*, 2013). If Raman could be merged together with diffusion experiments and take spectra in real time for longer exposure hours (without damaging the skin), large amount of information concerning how the drug changes physically while diffusing could be generated.

In this work, testosterone was successfully deuterated with a simple method, further the deuterium in-exchange and back-exchange was easily followed in the NMR tube. Although not all molecules might be so easily deuterated using this method, the approach is worthy of consideration if the physicochemical characteristics of the drug allows it, and especially in conjunction with other optical disciplines (for example IR, Raman) where sensitivity might be an issue.

NMR has a great future potential in monitoring experiments over time. It was shown in this work that it was possible to use normal solvents in conjunction with diffusion or presaturation experiments, which open up a wider range of possibilities of experiments, as NMR mainly is performed in deuterated solvents. It was also possible to leave the sample in the NMR tube during the experiment, which minimises interference with the sample.

References

Adlhart, C. & Baschong, W., 2011. Surface distribution and depths profiling of particulate organic UV absorbers by Raman imaging and tape stripping. *International journal of cosmetic science,* 33(6), pp. 527-534.

Ale, I., Lachapelle, J.M. & Maibach, H.I., 2009. Skin tolerability associated with transdermal drug delivery systems: an overview. *Advances in Therapy,* 26(10), pp. 920-935.

Atzrodt, J., Blankenstein, J., Brasseur, D., Calvo-Vicente, S., Denoux, M., Derdau, V., Lavisse, M., Perard, S., Roy, S., Sandvoss, M., Schofield, J. & Zimmermann, J., 2012. Synthesis of stable isotope labelled internal standards for drug-drug interaction (DDI) studies. *Bioorganic & medicinal chemistry,* 20(18), pp. 5658-5667.

Blessy, M., Patel, R.D., Prajapati, P.N. & Agrawal, Y.K., 2014. Development of forced degradation and stability indicating studies of drugs—A review. *Journal of Pharmaceutical Analysis,* 4(3), pp. 159-165.

Bommannan, D., Potts, R.O. & Guy, R.H., 1990. Examination of stratum corneum barrier function in vivo by infrared spectroscopy. *The Journal of investigative dermatology,* 95, pp. 403-408.

Brand, T., Cabrita, E.J. & Berger, S., 2006. Theory and application of NMR diffusion studies. In: G.A. Webb, ed. *Modern Magnetic Resonance.* Dordrecht: Springer Netherlands, pp. 135-143.

Brown, M.B., Traynor, M.J., Martin, G.P. & Akomeah, F.K., 2008. Transdermal Drug Delivery Systems: Skin Perturbation Devices. In: K.K. Jain, ed. *Drug Delivery Systems.* Totowa, NJ: Humana Press, pp. 119-139.

Brümmer, H., 2011. How to approach a forced degradation study. *Life Science Technology Bulletin,* 31, pp. 1-4.

Caspers, P.L., Lucassen, G.W., Carter, E.A., Bruining, H.A. & Puppels, G.J., 2001. In vivo confocal Raman microspectroscopy of the skin: Noninvasive determination of molecular concentration profiles. *The Journal of investigative dermatology,* 116(3), pp. 434-442.

Chang, R.K., Raw, A., Lionberger, R. & Yu, L., 2013. Generic development of topical dermatologic products: formulation development, process development, and testing of topical dermatologic products. *The AAPS journal,* 15(1), pp. 41-52.

Chik, Z., Johnston, A., Tucker, A.T., Chew, S.L., Michaels, L. & Alam, C.A., 2006. Pharmacokinetics of a new testosterone transdermal delivery system, TDS-testosterone in healthy males. *British journal of clinical pharmacology,* 61(3), pp. 275-9.

Claridge, T.D., 2016. *High-resolution NMR techniques in organic chemistry.* Elsevier.

Comstock, G.W., Burke, A.E., Norkus, E.P., Gordon, G.B., Hoffman, S.C. & Helzlsouer, K.J., 2001. Effects of repeated freeze-thaw cycles on concentrations of cholesterol, micronutrients, and hormones in human plasma and serum. *Clinical Chemistry,* 47(1), pp. 139-142.

Elias, P.M. & Feingold, K.R., 2005. *Skin Barrier.* CRC Press.

Farvid, M.S., Ng, T.W., Chan, D.C., Barrett, P.H. & Watts, G.F., 2005. Association of adiponectin and resistin with adipose tissue compartments, insulin resistance and dyslipidaemia. *Diabetes, obesity & metabolism,* 7(4), pp. 406-413.

FDA Draft Guidance, 1998. *Guidance for Industry: topical dermatological drug product NDAs and ANDAs-in vivo bioavailability, bioequivalence, in vitro release, and associated studies. .* US Department of Health and Human Services.

Feldmann, R.J. & Maibach, H.I., 1967. Regional variation in percutaneous penetration of 14C cortisol in man. *The Journal of investigative dermatology,* 48(2), pp. 181-183.

Findlay, J.C., Place, V.A. & Snyder, P.J., 1987. Transdermal delivery of testosterone. *The Journal of Clinical Endocrinology & Metabolism,* 64(2), pp. 266-268.

Franzen, L. & Windbergs, M., 2015. Applications of Raman spectroscopy in skin research - From skin physiology and diagnosis up to risk assessment and dermal drug delivery. *Advanced drug delivery reviews,* 89, pp. 91-104.

Furuta, T., Suzuki, A., Matsuzawa, M., Shibasaki, H. & Kasuya, Y., 2003. Syntheses of stable isotope-labeled 6β-hydroxycortisol, 6β-hydroxycortisone, and 6β-hydroxytestosterone. *Steroids,* 68(7-8), pp. 693-703.

Garson, M.J. & Staunton, J., 1979. Some new N.M.R. methods for tracing the fate of hydrogen in biosynthesis. *Chemical Society Reviews,* 8(4), pp. 539-561.

Goodman, M.P., 2012. Are all estrogens created equal? A review of oral vs. transdermal therapy. *Journal of Women's Health,* 21(2), pp. 161-169.

Gooren, L.J. & Bunck, M.C., 2003. Transdermal testosterone delivery: testosterone patch and gel. *World Journal of Urology,* 21(5), pp. 316-319.

Gooren, L.J. & Bunck, M.C., 2004. Androgen replacement therapy. *Drugs,* 64(17), pp. 1861-1891.

Guy, R.H. & Hadgraft, J., (eds.) 2003. *Transdermal drug delivery systems: revised and expanded.* 2nd ed. New York: Marcel Dekker.

Hadgraft, J. & Lane, M.E., 2015. Transdermal delivery of testosterone. *European Journal of Pharmaceutics and Biopharmaceutics* 92, pp. 42-48.

Harris, R.K., Joyce, S.A., Pickard, C.J., Cadars, S. & Emsley, L., 2006. Assigning carbon-13 NMR spectra to crystal structures by the INADEQUATE pulse sequence and first principles computation: a case study of two forms of testosterone. *Physical Chemistry Chemical Physics,* 8(1), pp. 137-143.

Hathout, R.M., Woodman, T.J., Mansour, S., Mortada, N.D., Geneidi, A.S. & Guy, R.H., 2010. Microemulsion formulations for the transdermal delivery of testosterone. *European Journal of Pharmaceutical Sciences,* 40(3), pp. 188-96.

Hayamizu, K., Ishii, T., Masaru, Y. & Kamo, O., 1990. Complete assignments of the 1H and 13C NMR spectra of testosterone and 17α-methyltestosterone and the 1H parameters obtained from 600 MHz spectra. *Magnetic Resonance in Chemistry,* 28, pp. 250-256.

Hayashi, T., Yamasaki, K., Mimura, M. & Uozumi, Y., 2004. Deuterium-labeling studies establishing stereochemistry at the oxypalladation step in Wacker-type oxidative cyclization of an O-allylphenol. *Journal of the American Chemical Society,* 126(10), pp. 3036-3037.

Herkenne, C., Alberti, I., Naik, A., Kalia, Y.N., Mathy, F.X., Preat, V. & Guy, R.H., 2008. In vivo methods for the assessment of topical drug bioavailability. *Pharmaceutical research,* 25(1), pp. 87-103.

Herkenne, C., Naik, A., Kalia, Y.N., Hadgraft, J. & Guy, R.H., 2007. Dermatopharmacokinetic prediction of topical drug bioavailability in vivo. *The Journal of investigative dermatology,* 127(4), pp. 887-894.

Heyneman, C.A., Lawless-Liday, C. & Wall, G.C., 2000. Oral versus topical NSAIDs in rheumatic diseases. *Drugs,* 60(3), pp. 555-574.

International Council for Harmonisation (ICH). Available from: http://www.ich.org/home.html [Accessed 2 feb 2017].

International Council for Harmonisation (ICH), 1996. *Stability testing: photostability testing of new drug substances and products.* International Council for Harmonisation (ICH), ICH Harmonised tripartite guideline

International Council for Harmonisation (ICH), 2005. *Validation of analytical procedures: text and methodology.* International Council for Harmonisation (ICH), ICH Harmonised tripartite guideline

Jordan Jr, W.P., 1997. Allergy and topical irritation associated with transdermal testosterone administration: a comparison of scrotal and nonscrotal transdermal systems. *American Journal of Contact Dermatitis,* 8(2), pp. 108-113.

Jordan Jr, W.P., Atkinson, L.E. & Lai, C., 1998. Comparison of the skin irritation potential of two testosterone transdermal systems: an investigational system and a marketed product. *Clinical Therapeutics,* 20(1), pp. 80-87.

Kasal, A., Budesinsky, M. & Griffiths, W.J., 2010. Spectroscopic methods of steroid analysis. In: H.L.J. Makin & D.B. Gower, eds. *Steroid analysis.* Second ed.: Springer, pp. 27-161.

Kolet, S.P., Niloferjahan, S., Haldar, S., Gonnade, R. & Thulasiram, H.V., 2013. Biocatalyst mediated production of 6β,11α-dihydroxy derivatives of 4-ene-3-one steroids. *Steroids,* 78(11), pp. 1152-1158.

Kostyukevich, Y., Kononikhin, A., Popov, I. & Nikolaev, E., 2014. In-ESI source hydrogen/deuterium exchange of carbohydrate ions. *Analytical Chemistry,* 86(5), pp. 2595-2600.

Lademann, J., Jacobi, U., Surber, C., Weigmann, H.J. & Fluhr, J.W., 2009. The tape stripping procedure--evaluation of some critical parameters. *European Journal of Pharmaceutics and Biopharmaceutics,* 72(2), pp. 317-23.

Lakshman, K.M. & Basaria, S., 2009. Safety and efficacy of testosterone gel in the treatment of male hypogonadism. *Clinical Interventions in Aging,* 4, pp. 397-412.

Leichtnam, M.L., Rolland, H., Wuthrich, P. & Guy, R.H., 2006a. Enhancement of transdermal testosterone delivery by supersaturation. *Journal of pharmaceutical sciences,* 95(11), pp. 2373-2379.

Leichtnam, M.L., Rolland, H., Wuthrich, P. & Guy, R.H., 2006b. Formulation and evaluation of a testosterone transdermal spray. *Journal of pharmaceutical sciences,* 95(8), pp. 1693-1702.

Leichtnam, M.L., Rolland, H., Wuthrich, P. & Guy, R.H., 2006c. Identification of penetration enhancers for testosterone transdermal delivery from spray formulations. *Journal of Controlled Release,* 113(1), pp. 57-62.

Lu, W., Luo, H., Wu, Y., Zhu, Z. & Wang, H., 2013. Preparation and characterization of a metered dose transdermal spray for testosterone. *Acta Pharmaceutica Sinica B,* 3(6), pp. 392-399.

Marbury, T., Hamill, E., Bachand, R., Sebree, T. & Smith, T., 2003. Evaluation of the pharmacokinetic profiles of the new testosterone topical gel formulation, Testim™, compared to AndroGel®. *Biopharmaceutics & Drug Disposition,* 24(3), pp. 115-120.

Martin, G.J. & Martin, M.L., 1981. Deuterium labelling at the natural abundance level as studied by high field quantitative 2H NMR. *Tetrahedron Letters,* 22(36), pp. 3525-3528.

Mason, L., Moore, R.A., Edwards, J.E., Derry, S. & McQuay, H.J., 2004. Topical NSAIDs for chronic musculoskeletal pain: systematic review and meta-analysis. *BMC Musculoskeletal Disorders,* 5(1).

Mazer, N.A., Heiber, W.E., Moellmer, J.F., Meikle, A.W., Stringham, J.D., Sanders, S.W., Tolman, K.G. & Odell, W.D., 1992. Enhanced transdermal delivery of testosterone: a new physiological approach for androgen replacement in hypogonadal men. *Journal of Controlled Release,* 19(1), pp. 347-361.

McNicholas, T., Dean, J., Mulder, H., Carnegie, C. & Jones, N., 2003. A novel testosterone gel formulation normalizes androgen levels in hypogonadal men, with improvements in body composition and sexual function. *BJU international,* 91(1), pp. 69-74.

The Merck Index Online, 2017. Royal Society of Chemistry. Available from: https://www.rsc.org/merck-index /[Date accessed 1 Feb 2017] CAS 58-22-0, M10594

Moffat, C.A., Osselton, M.D. & Widdop, B., 2004. *Clarke's analysis of drugs and poisons.* 4th ed.: Pharmaceutical Press.

Mohammed, D., Yang, Q., Guy, R.H., Matts, P.J., Hadgraft, J. & Lane, M.E., 2012. Comparison of gravimetric and spectroscopic approaches to quantify stratum corneum removed by tape-stripping. *European Journal of Pharmaceutics and Biopharmaceutics,* 82(1), pp. 171-174.

Møllgaard, B. & Hoelgaard, A., 1983. Permeation of estradiol through the skin — effect of vehicles. *International journal of pharmaceutics,* 15(2), pp. 185-197.

Moser, K., Kriwet, K., Froehlich, C., Kalia, Y.N. & Guy, R.H., 2001a. Supersaturation- Enhancement of skin penetration and permeation of a lipophilic drug. *Pharmaceutical research,* 18(7), pp. 1006-1111.

Moser, K., Kriwet, K., Naik, A., Kalia, Y.N. & Guy, R.H., 2001b. Enhanced skin permeation of a lipophilic drug using supersaturated formulations. *Journal of controlled release : official journal of the Controlled Release Society,* (73), pp. 245-53.

Moser, K., Kriwet, K., Naik, A., Kalia, Y.N. & Guy, R.H., 2001c. Passive skin penetration enhancement and its quantification in vitro. *European Journal of Pharmaceutics and Biopharmaceutics,* (52), pp. 103-112.

N'Dri-Stempfer, B., Navidi, W.C., Guy, R.H. & Bunge, A.L., 2008. Optimizing metrics for the assessment of bioequivalence between topical drug products. *Pharmaceutical research,* 25(7), pp. 1621-1630.

N'Dri-Stempfer, B., Navidi, W.C., Guy, R.H. & Bunge, A.L., 2009. Improved bioequivalence assessment of topical dermatological drug products using dermatopharmacokinetics. *Pharmaceutical research,* 26(2), pp. 316-328.

Naik, A., Kalia, Y.N. & Guy, R.H., 2000. Transdermal drug delivery: overcoming the skin's barrier function. *Pharmaceutical Science & Technology today,* 3(9), pp. 318-326.

Navidi, W., Hutchinson, A., N'Dri-Stempfer, B. & Bunge, A., 2008. Determining bioequivalence of topical dermatological drug products by tape-stripping. *Journal of pharmacokinetics and pharmacodynamics,* 35(3), pp. 337-348.

Nicoli, S., Bunge, A.L., Delgado-Charro, M.B. & Guy, R.H., 2009. Dermatopharmacokinetics: factors influencing drug clearance from the stratum corneum. *Pharmaceutical research,* 26(4), pp. 865-871.

Pellet, M.A., Roberts, M.S. & Hadgraft, J., 1997. Supersaturated solutions evaluated with an in vitro stratum corneum tape stripping technique. *International journal of pharmaceutics,* (151), pp. 91-98.

Pirot, F., Kalia, Y.N., Stinchcomb, A.L., Keating, G., Bunge, A. & Guy, R.H., 1997. Characterization of the permeability barrier of human skin in vivo. *Proceedings of the National Academy of Sciences* 94, pp. 1562-1567.

Prausnitz, M.R., Elias, P.M., Franz, T.J., Schmuth, M., Tsai, J.-C., Menon, G.K., Holleran, W.M. & Feingold, K.R., 2012. Skin barrier and transdermal drug delivery. *Dermatology,* 3, pp. 2065-2073.

Prausnitz, M.R. & Langer, R., 2008. Transdermal drug delivery. *Nature biotechnology,* 26(11), pp. 1261-1268.

Price, W.S., 2006. NMR Diffusometry. In: G.A. Webb, ed. *Modern Magnetic Resonance.* Dordrecht: Springer Netherlands, pp. 109-115.

Rainsford, K., Kean, W. & Ehrlich, G., 2008. Review of the pharmaceutical properties and clinical effects of the topical NSAID formulation, diclofenac epolamine. *Current Medical Research and Opinion,* 24(10), pp. 2967-2992.

Raney, S.G., Franz, T.J., Lehman, P.A., Lionberger, R. & Chen, M.L., 2015. Pharmacokinetics-based approaches for bioequivalence evaluation of topical dermatological drug products. *Clinical pharmacokinetics,* 54(11), pp. 1095-1106.

Rolf, C., Knie, U., Lemmnitz, G. & Nieschlag, E., 2002. Interpersonal testosterone transfer after topical application of a newly developed testosterone gel preparation. *Clinical Endocrinology,* 56(5), pp. 637-641.

Rougier, A., Dupuis, D., Lotte, C., Roguet, R. & Schaefer, H., 1983. In vivo correlation between stratum corneum reservoir function and percutaneous absorption. *The Journal of investigative dermatology,* 81(3), pp. 275-278.

Snyder, L.R., Kirkland, J.J. & Dolan, J.W., 2011. *Introduction to modern liquid chromatography.* John Wiley & Sons.

Tfaili, S., Gobinet, C., Josse, G., Angiboust, J.-F., Baillet, A., Manfait, M. & Piot, O., 2013. Vibrational spectroscopies for the analysis of cutaneous permeation: experimental limiting factors identified in the case of caffeine penetration. *Analytical and bioanalytical chemistry,* 405(4), pp. 1325-1332.

Thomas, B.J. & Finnin, B.C., 2004. The transdermal revolution. *Drug Discovery Today,* 9(16), pp. 697-703.

Thurmond, R.L., Dodd, S.W. & Brown, M.F., 1991. Molecular areas of phospholipids as determined by 2H NMR spectroscopy. Comparison of phosphatidylethanolamines and phosphatidylcholines. *Biophysical Journal,* 59(1), pp. 108-113.

Vulliet, E., Falletta, M., Marote, P., Lomberget, T., Païssé, J.-O. & Grenier-Loustalot, M.-F., 2010. Light induced degradation of testosterone in waters. *Science of the Total Environment,* 408(17), pp. 3554-3559.

Wähälä, K., Väänänen, T., Hase, T. & Leinonen, A., 1995. Synthesis of [2H] 5-epitestosterone. *Journal of Labelled Compounds and Radiopharmaceuticals,* 36(5), pp. 493-496.

Walters, B.T., Ricciuti, A., Mayne, L. & Englander, S.W., 2012. Minimizing back exchange in the hydrogen exchange-mass spectrometry experiment. *Journal of the American Society for Mass Spectrometry,* 23(12), pp. 2132-2139.

Wang, C. & Swerdloff, R.S., 1997. Androgen replacement therapy. *Annals of Medicine,* 29(5), pp. 365-370.

Wang, C., Swerdloff, R.S., Iranmanesh, A., Dobs, A., Snyder, P.J., Cunningham, G., Matsumoto, A.M., Weber, T. & Berman the Testosterone Gel Study Group, N., 2000. Transdermal testosterone gel improves sexual function, mood, muscle strength, and body composition parameters in hypogonadal men. *The Journal of Clinical Endocrinology & Metabolism,* 85(8), pp. 2839-2853.

Wester, R.C. & Maibach, H.I., 1983. Cutaneous pharmacokinetics- 10 steps to percutaneous absorption. *Drug Metabolism Reviews,* 14(2), pp. 169-205.

Wiedersberg, S. & Guy, R.H., 2014. Transdermal drug delivery: 30+ years of war and still fighting! *Journal of Control Release,* 190, pp. 150-6.

Wiedersberg, S., Leopold, C.S. & Guy, R.H., 2009. Dermatopharmacokinetics of betamethasone 17-valerate: influence of formulation viscosity and skin surface cleaning procedure. *European Journal of Pharmaceutics and Biopharmaceutics,* 71(2), pp. 362-6.

Williams, A., 2003. *Transdermal and topical drug delivery from theory to clinical practice.* Pharmaceutical Press.

World health organization (WHO). Geneva: World health organization (WHO). Available from: http://www.who.int/en/ [Accessed 2 feb 2017].

World Health Organization (WHO), 1986. *Accelerated stability studies of widely used pharmaceutical substances under simulated tropical conditions.* WHO/Pharm 86.259 Geneva: World Health Organization, Pharmaceuticals unit

World health organization (WHO), 2006. *Dermal absorption.* 235 Geneva: World health organization,,

Xiao, C.H., Flach, C.R., Marcott, C. & Mendelsohn, R., 2004. Uncertainties in depth determination and comparison of multivariate with univariate analysis in confocal Raman studies of a laminated polymer and skin. *Applied Spectroscopy,* 58(4), pp. 382-389.